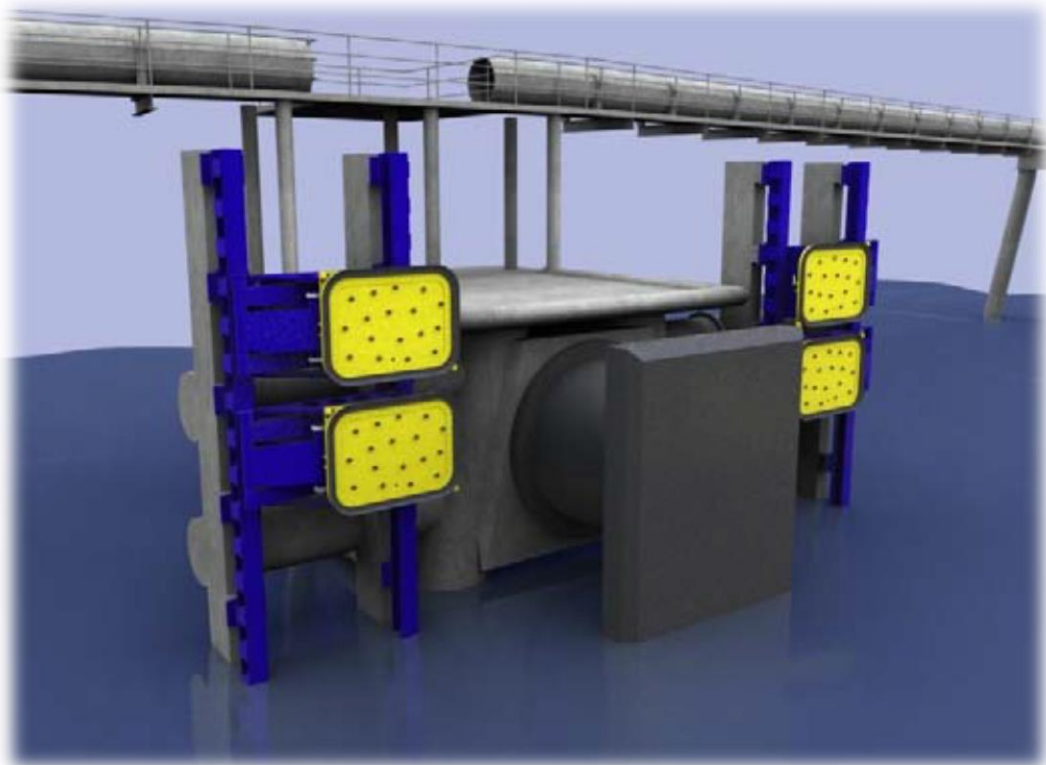


THE SUITABILITY OF THE MOORMASTER™ SYSTEM FOR INLAND SHIPPING

CONSIDERING QUAY SIDE MOORING IN THE AMSTERDAM-RIJNKANAAL
UNDER THE INFLUENCE OF PASSING SHIPS



M.J.J. PENDERS
16-6-2016

THE SUITABILITY OF THE MOORMASTER™ SYSTEM FOR INLAND SHIPPING

CONSIDERING QUAY SIDE MOORING IN THE AMSTERDAM-RIJNKANAAL
UNDER THE INFLUENCE OF PASSING SHIPS

By

M.J.J. Penders

in partial fulfilment of the requirements for the degree of

Master of Science

in Marine Technology – Track Science – Specialisation Ship Hydromechanics

at the Delft University of Technology,

to be defended publicly on July 6th, 2016 at 14:00

Student number	1508326	
Chairman:	Prof. dr. ir. T.J.C. van Terwisga	TU Delft
Thesis committee:	Dr. ir. H.J. De Koning Gans	TU Delft
	Drs. O.C. Koedijk	Rijkswaterstaat, TU Delft
	Ir. E.W.B. Bolt	Rijkswaterstaat
	Dr. Ir. A.F.J. van Deyzen	Royal Haskoning DHV
	Ir. K. Visser	TU Delft

An electronic version of this thesis is available at <http://repository.tudelft.nl/>.

PREFACE

Before you lies my Master thesis, in partial fulfilment of the requirements for the degree of Master of Science in Marine technology. I started the journey of this thesis around April 2015, with a lot of preliminary research. In July I started at Rijkswaterstaat in Rijswijk. Even though I have discovered that a flexible office space is not really my thing, I have certainly enjoyed the company of my colleagues, even if it was only for a short time.

The subject of the project immediately got my attention. Using an innovative mooring system that uses vacuum pads, in inland shipping to solve a logistical problem. Innovation interests me, anything that helps society move forward is worth investigating. Apart from that, inland shipping has caught my attention, simply because it is closer to home and with land, living and industry in the direct vicinity. I have always enjoyed the programming and modelling parts of my education, so the simulating of passing vessels and modelling of the mooring system was something to look forward to.

As I am sure is the case for everybody who has ever had to write a thesis, there were some hiccups along the way. I would like to thank everybody who has helped me, given me feedback, and supported me during this process. I would especially like to thank Henk de Koning Gans, whose help, support, understanding and faith has made every step a bit easier to take. Of course I would also like to thank Rijkswaterstaat, in particular Otto Koedijk, for giving me the opportunity to work on such an interesting subject. Last but certainly not least, I would like to thank Leen den Haan, owner of the 'Shalimar', for giving me information on and insight in inland shipping and Large Rhine vessels.

It has certainly been an adventure, of finding my way and finding myself.

Marijke Penders, Delft, 16-06-2016

ABSTRACT

The demand for mooring facilities directly on the side of busy inland waterways increases. Mooring with conventional ropes would cause a decrease in capacity of the waterway, because passing vessels are legally obliged to reduce speed. A possible solution is the use of the MoorMaster™ 200 system by Cavotec. This research investigates the suitability of this system for inland shipping. A case study is performed on the Amsterdam-Rijnkanaal.

The MoorMaster™ system works with vacuum pads which attach to the ship hull. Active controls react to mooring loads and reduce motions. The system is used successfully in a number of sea ports.

To ensure 90-100% (un)loading efficiency, the amplitude of the surge and sway motion should remain below 400mm. The amplitude of yaw angle should remain below 0.25 degrees. This is based on a literature review of mooring criteria.

The forces on the moored vessel caused by passing vessel are simulated using the panel method. Three vessels are used in the simulations: A Large Rhine vessel, most common on the canal, a Rhinemax vessel and a 4 barge pushed convoy with the maximum allowed dimensions. The simulations are run using the cross section of the Amsterdam-Rijnkanaal, at the maximum allowed speed and for different passing distances and drift angles.

The horizontal ship motions are modelled using $\vec{F} = \vec{M} \cdot \vec{A}$. Damping can be ignored and added mass kept constant. This is justifiable due to the low frequencies. The external forces consist of the force caused by the passing vessels and the forces exerted by the MoorMaster™ units. Two sway correcting MoorMaster™ units and three groups of two surge correcting units are used.

A basic case study construction calculation is done to determine structural integrity.

An increased passing distance decreases the forces on the moored vessel. The larger the passing vessel, the larger the forces, see Figure 0.1. The largest forces encountered are +/- 560 kN in surge direction and 150 kN in sway direction. The motions of the moored vessel stay within the operational criteria, for example see Figure 0.2.

Whether the construction of an inland vessel can withstand the load, is dependent on the stiffener configuration and the other global and local loads on the ship hull.

It is recommended to look into the operational profile and consult with Cavotec to find the optimal configuration. Other waterways and multiple passing vessels should be researched and it is recommended to validate the used model.

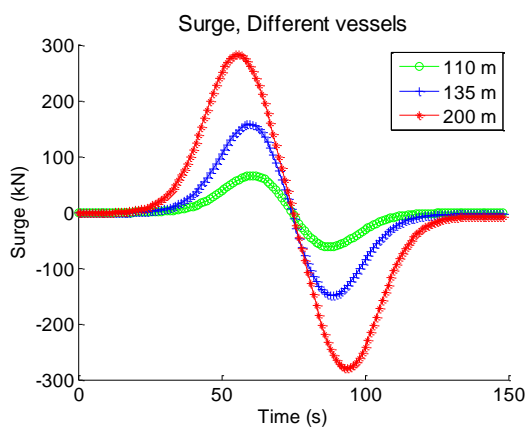


Figure 0.1 Surge force for different passing vessels (88.2 m passing distance)

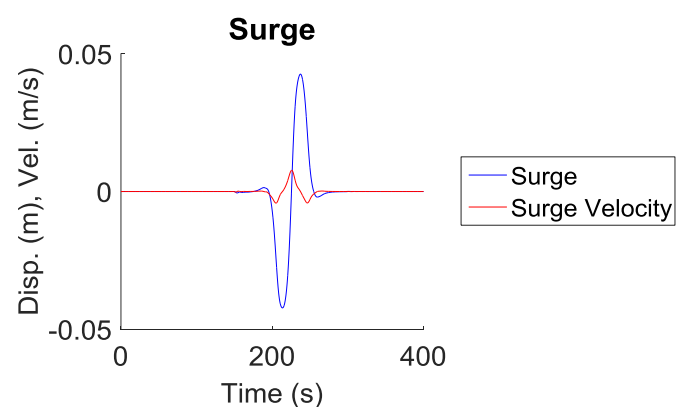


Figure 0.2 Resulting surge motion caused by 110 m Large Rhine vessel at 18 km/h, at a passing distance of 47.40 m

TABLE OF CONTENTS

Preface	I
Abstract	III
List of figures	VI
List of tables	X
List of abbreviations	XI
List of symbols	XII
1. Introduction	1
1.1. Research questions	1
1.2. Research goal	2
1.3. Readers' guide	2
2. Background research	3
2.1. Background information MoorMaster™ system	3
2.2. Literature review Mooring Criteria	5
2.3. Safety criteria	6
2.4. Operational criteria	8
2.5. Characteristics of the Amsterdam-Rijnkanaal and its traffic	9
2.6. Summary Background research	12
3. Simulating passing vessels	15
3.1. Hydromechanics of passing vessels	15
3.2. Ropes; a numerical tool to predict the loads induced by passing vessels	17
3.3. Summary simulating passing vessels	24
4. Modeling moored vessel	27
4.1. Physical model ship motions	27
4.2. Physical model Moormaster™ units	30
4.3. MoorMaster™ units: calculate angle and position error	33
4.4. Verification: One DOF	35
4.5. Verification: Two DOF	39
4.6. Verification: Three DOF	46
4.7. Unit configuration and PD setting	47
4.8. Validation of ship motion model	48
4.9. Summary modeling moored vessel	50
5. Construction calculation	51
5.1. Basic case study calculation load in sway direction	51
5.2. Basic case study calculation load in surge direction	53

6.	Results	55
6.1.	Ropes simulations.....	55
6.2.	Physical model ship motions	58
6.3.	Construction calculation	60
7.	Conclusions	63
8.	Discussion & Recommendations	65
8.1.	Research scope	65
8.2.	Literature	65
8.3.	Modelling improvements	66
8.4.	Results	66
8.5.	Validation.....	66
8.6.	Structural strength.....	66
8.7.	MoorMaster™ system.....	67
9.	References.....	69
Appendix A.	Cross section of Amsterdam-Rijnkanaal	73
Appendix B.	Classification of European inland waterways	77
Appendix C.	Classification of Rijkswaterstaat	78
Appendix D.	Passing locks ARK	81
Appendix E.	Potential flow; Boundary conditions and singularities	83
Appendix F.	Ropes description and sensitivity study.....	87
Appendix G.	Matlab script one DOF model	97
Appendix H.	Matlab script two DOF model: Sway and yaw	103
Appendix I.	Matlab script two DOF model: Surge and yaw	109
Appendix J.	Matlab script two DOF model: Surge and sway.....	115
Appendix K.	Matlab script three DOF model	119
Appendix L.	Matlab script three DOF model with coupling terms, case study input variables and external force	123
Appendix M.	Delfrac Output	129
Appendix N.	Ansys Script File	131
Appendix O.	Ropes simulations results	135
Appendix P.	Reaction forces of MoorMaster™ units	137
Appendix Q.	Results ship motion model	139
Appendix R.	Ship motions	143

LIST OF FIGURES

Figure 0.1 Surge force for different passing vessels (88.2 m passing distance)	III
Figure 0.2 Resulting surge motion caused by 110 m Large Rhine vessel at 18 km/h, at a passing distance of 47.40 m	III
Figure 2.1 A MoorMaster™ unit connected to a ship hull.....	3
Figure 2.2 Schematic overview of MoorMaster™ unit	3
Figure 2.3 Force convention (Cavotec MoorMaster Limited, 2012)	6
Figure 2.4 Cross section of the Amsterdam-Rijnkanaal	9
Figure 2.5 Active inland shipping combinations sailing under the Dutch flag (Rijkswaterstaat, 2009)	10
Figure 2.6 Straight channel with quay	11
Figure 2.7 Quay following RWS guidelines.....	11
Figure 3.1 Panel model of inland vessels	21
Figure 3.2 Schematic overview simulations Ropes	23
Figure 4.1 Free body diagram ship.....	27
Figure 4.2 Mass and damping of a heaving vertical cylinder (Journée & Massie, 2001)	28
Figure 4.3 Free body diagram of MoorMaster™ suction pad.....	30
Figure 4.4 Maximum force MoorMaster unit as a function of angle	31
Figure 4.5 Control diagram MoorMaster™ (Cavotec MoorMaster Limited, 2012)	31
Figure 4.6 Angle of units without yaw	33
Figure 4.7 Angle of units with yaw	34
Figure 4.8 Laplace calculation of one DOF system with $m=1 \cdot 10^6$ kg, $F_{max}=1 \cdot 10^5$ N, $x'(0)=0$ and $x(0) = 1$. $p=d=-0.5$	38
Figure 4.9 Laplace calculation of one DOF system with $m=1 \cdot 10^6$ kg, $F_{max}=1 \cdot 10^5$ N, $x'(0)=0$ and $x(0) = 1$. $p=-0.5$, $d=-1.0$	38
Figure 4.10 Laplace calculation of one DOF system with $m=1 \cdot 10^6$ kg, $F_{max}=1 \cdot 10^5$ N, $x'(0)=0$ and $x(0) = 1$. $p=-1.0$ $d=-0.5$	38
Figure 4.11 Laplace calculation of one DOF system with $m=1 \cdot 10^6$ kg, $F_{max}=1 \cdot 10^5$ N, $x'(0)=0$ and $x(0) = 1$. $p=d=-1.0$	38
Figure 4.12 ODE45 calculation of one DOF system with $m=1 \cdot 10^6$ kg, $F_{max}=1 \cdot 10^5$ N, $x'(0)=0$ and $x(0) = 1$. $p=d=-0.5$	38
Figure 4.13 ODE45 calculation with 0.2 sec time delay of one DOF system with $m=1 \cdot 10^6$ kg, $F_{max}=1 \cdot 10^5$ N, $x'(0)=0$ and $x(0) = 1$. $p=d=-0.5$	38

Figure 4.14 Comparison between exact calculation of y^* , approximation with Eq. 4.40 and further simplification with $\sin(\psi) \approx \psi$	40
Figure 4.15 Sway Laplace calculation of two DOF sway and yaw system with $m=1 \cdot 10^6$ kg, $I=3 \cdot 10^9$ m ⁴ , $F_{max}=1 \cdot 10^5$ N, $y'(0)=N(0)=0$ and $y(0)=-0.5$ and $N(0)=0.001$ rad. $p=d=-0.5$	44
Figure 4.16 Yaw Laplace calculation of two DOF sway and yaw system with $m=1 \cdot 10^6$ kg, $I=3 \cdot 10^9$ m ⁴ , $F_{max}=1 \cdot 10^5$ N, $y'(0)=N(0)=0$ and $y(0)=-0.5$ and $N(0)=0.001$ rad. $p=d=-0.5$	44
Figure 4.17 Sway ODE45 calculation with 0.2 sec time delay of two DOF sway and yaw system with $m=1 \cdot 10^6$ kg, $I=3 \cdot 10^9$ m ⁴ , $F_{max}=1 \cdot 10^5$ N, $y'(0)=N(0)=0$ and $y(0)=-0.5$ and $N(0)=0.001$ rad. $p=d=-0.5$	44
Figure 4.18 Yaw ODE45 calculation with 0.2 sec time delay of two DOF sway and yaw system with $m=1 \cdot 10^6$ kg, $I=3 \cdot 10^9$ m ⁴ , $F_{max}=1 \cdot 10^5$ N, $y'(0)=N(0)=0$ and $y(0) = -0.5$ and $N(0)=0.001$ rad. $p=d=-0.5$	44
Figure 4.19 Test set-up.....	48
Figure 5.1 Cross section of cargo hold of "Damen Riverliner 1145E"	52
Figure 5.2 Estimated cross section of longitudinal stiffeners of "Damen Riverliner 1145E"	52
Figure 6.1 1-d 5th order median filter to filter out peaks	55
Figure 6.2 Simulation at 90 sec.	56
Figure 6.3 Simulation at 109 sec.	56
Figure 6.4 Surge force for different passing distances. (110 m vessel passing). Filtered	56
Figure 6.5 Sway force for different passing distances. (110 m vessel passing).....	56
Figure 6.6 Surge force for different passing vessels (88.2 m passing distance)	57
Figure 6.7 Sway force for different passing vessels (88.2 m passing distance).....	57
Figure 6.8 External forces and moment caused by 200m 4 barge convoy at 18 km/h, at a passing distance of 33.35m, $P=-5$, $D=-3$	58
Figure 6.9 Resulting surge motions caused by 200m 4 barge convoy at 18 km/h, at a passing distance of 33.35m, $P=-5$, $D=-3$	59
Figure 6.10 Resulting sway motions caused by 200m 4 barge convoy at 18 km/h, at a passing distance of 33.35m, $P=-5$, $D=-3$	59
Figure 6.11 Resulting yaw motions caused by 200m 4 barge convoy at 18 km/h, at a passing distance of 33.35m, $P=-5$, $D=-3$	59
Figure 6.12 Resulting sway motions at fore and aft end caused by 200m 4 barge convoy at 18 km/h, at a passing distance of 33.35m, $P=-5$, $D=-3$	59
Figure 6.13 Stress in x direction in side plating due to load of 100 kN/m ² in sway direction	60
Figure 6.14 Stress in y direction in side plating due to load of 100 kN/m ² in sway direction	61
Figure E.1 Visual representation of source (Katz & Plotkin, 1991)	84

Figure E.2 Visual representation of a doublet (Katz & Plotkin, 1991)	85
Figure E.3 Visual representation of a vortex (Katz & Plotkin, 1991)	85
Figure F.1 Simulation input Ropes	87
Figure F.2 Vessel input Ropes	88
Figure F.3 Surge force for varying time step	89
Figure F.4 Sway force for varying time step	89
Figure F.5 Surge force for varying time step, zoom	89
Figure F.6 Sway force for varying time step, zoom	90
Figure F.7 Surge force for varying sailing distance	90
Figure F.8 Sway force for varying sailing distance	91
Figure F.9 Surge force for varying waterway length	91
Figure F.10 Sway force for varying waterway length	92
Figure F.11 Surge force for varying waterway length, zoom	92
Figure F.12 Heave force for varying waterway length	93
Figure F.13 Surge force for varying sailing distances with quay	93
Figure F.14 Sway force for varying sailing distances with quay	94
Figure F.15 Surge force for varying waterway length with quay	94
Figure F.16 Heave force for varying waterway length with quay	95
Figure F.17 Regions panelsizes	95
Figure O.1 Surge force for different drift angles. (110 m vessel passing, 88.2 m passing distance)	135
Figure O.2 Surge force for different loading conditions (110 m vessel passing, 88.2 m passing distance)	135
Figure P.1 Forces of units caused by 200m 4 barge convoy at 18 km/h, at a passing distance of 33.35m, P=-5, D=-3	137
Figure P.2 Forces of units caused by 200m 4 barge convoy at 18 km/h, at a passing distance of 33.35m, P=-2.5, D=-1.5	137
Figure P.3 Forces of units caused by 110m Large Rhine vessel at 18 km/h, at a passing distance of 47.40m, P=-5, D=-3	138
Figure P.4 Forces of units caused by 2 Large Rhine vessels passing 5 seconds after each other, at 18 km/h, at a passing distance of 47.40m, P=-5, D=-3	138
Figure Q.1 Resulting surge motions caused by 200m 4 barge convoy at 18 km/h, at a passing distance of 33.35m, P=-2.5, D=-1.5	139

Figure Q.2 Resulting sway motions caused by 200m 4 barge convoy at 18 km/h, at a passing distance of 33.35m, P=-2.5, D=-1.5.....	139
Figure Q.3 Resulting yaw motions caused by 200m 4 barge convoy at 18 km/h, at a passing distance of 33.35m, P=-2.5, D=-1.5.....	139
Figure Q.4 External forces and moment caused by 110m Large Rhine vessel at 18 km/h, at a passing distance of 47.40m, P=-5, D=-3.....	140
Figure Q.5 Resulting surge motion caused by 110m Large Rhine vessel at 18 km/h, at a passing distance of 47.40m, P=-5, D=-3.....	140
Figure Q.6 Resulting sway motion caused by 110m Large Rhine vessel at 18 km/h, at a passing distance of 47.40m, P=-5, D=-3.....	140
Figure Q.7 Resulting yaw motion caused by 110m Large Rhine vessel at 18 km/h, at a passing distance of 47.40m, P=-5, D=-3.....	140
Figure Q.8 External forces and moment caused by 2 Large Rhine vessels passing 5 seconds after each other, at 18 km/h, at a passing distance of 47.40m, P=-5, D=-3.....	141
Figure Q.9 Resulting surge motion caused by 2 Large Rhine vessels passing 5 seconds after each other, at 18 km/h, at a passing distance of 47.40m, P=-5, D=-3.....	141
Figure Q.10 Resulting sway motion caused by 2 Large Rhine vessels passing 5 seconds after each other, at 18 km/h, at a passing distance of 47.40m, P=-5, D=-3.....	141
Figure Q.11 Resulting yaw motion caused by 2 Large Rhine vessels passing 5 seconds after each other, at 18 km/h, at a passing distance of 47.40m, P=-5, D=-3.....	141
Figure R.1 Ship motions	143

LIST OF TABLES

Table 2.1 Velocity criteria safe mooring (Jensen, et al., 1990)	7
Table 2.2 Safety criteria	7
Table 2.3 Ship motion criteria for container vessels ($L_{oa} = 100-200$ m), maximum amplitude (Jensen, et al., 1990)	8
Table 2.4 Dimensions of vessels according to CEMT class of Amsterdam-Rijnkanaal	9
Table 2.5 Dimensions of most common vessels on Amsterdam-Rijnkanaal	10
Table 2.6 Maximum allowed dimensions of vessels or convoys on Amsterdam-Rijnkanaal by law	10
Table 3.1 Simulated vessels	21
Table 3.2 Correction factors for high velocities	22
Table 6.1 Maximum stress in side shell plating and stiffeners due to force in surge direction	61
Table D.1 Passings in locks in ARK in 2011	81

LIST OF ABBREVIATIONS

ARK	Amsterdam Rijnkanaal
CEMT	Coférence Européenne des Ministres des Transports
CV	Control variable
DOF	Degrees of freedom
PIANC	Permanent International Association of Navigation Congresses
PID	Proportional, Integral, Derivative
PV	Process variable
ROPES	Research on Passing Effects of Ships
RWS	Rijkswaterstaat

LIST OF SYMBOLS

\bar{A}	kg	Added mass matrix of vessel	p	N/m ²	Pressure
\bar{B}	Ns/m	Retardation	p	-	Proportional control value
F_c	-	Correction factor for simulations in Ropes with high depth-based Froude numbers	p	N/m ²	Load
Fr_h	-	Depth based Froude number	Pos	m	Position of MoorMaster™ unit in x direction on hull of vessel
\bar{K}	N/m	Stiffness matrix of moored vessel	r	-	Blocking ratio
\bar{M}	kg	Mass matrix of vessel	s	-	Laplace variable
\bar{X}	m	Motion vector of moored vessel	s	m	Stiffener spacing
U_0	m/s	Velocity of passing vessel	t	s	Time
V_{rel}	m/s	Velocity relative to water	t	mm	Plate thickness
c_0	m/s	Long wave celerity	u	m/s	Velocity in x direction
\bar{u}	m/s	Velocity field	v	m/s	Velocity in y direction
∇	-	Gradient	w	m/s	Velocity in z direction
A	m ²	Area	x	m	Surge displacement
A	m	Amplitude of motion	y	m	Sway displacement
B	m	Breadth of ship	α	degree	Angle of MoorMaster™ unit
C	-	Courant number	Φ	-	Potential
D	m	Draft of ship	ρ	Kg/m ³	Density of water
d	-	Derivative control value	σ	MPa	Stress
e	m	Error in displacement of MoorMaster™ unit	ψ	degree	Yaw displacement
F	N	Force			
g	m/s ²	Gravitational acceleration			
h	m	Water depth			
I	m ⁴	Moment of inertia			
\mathcal{L}	-	Laplace transform			
L_{oa}	m	Length over all of ship			
M	Nm	Moment			
m	kg	Mass of vessel			

1. INTRODUCTION

Rijkswaterstaat (the executive agency of the Dutch Ministry of Infrastructure and the Environment) receives many requests from entrepreneurs in inland shipping container terminals to load and unload at landing quays. A landing quay is defined as a mooring facility directly on the side of the waterway, without an inlet of some kind, see Figure 2.7 on page 11. This is desirable because the cost of building such quays is significantly less than that of constructing an inland port basin.

The issue that Rijkswaterstaat (RWS) has with these requests is that the capacity of the waterway will be decreased. A passing ship is obligated to reduce its speed to prevent damage to, amongst others, moored ships (Binnenvaartpolitiereglement, 2004). When conventional mooring lines are used, the passing ships will have to slow down when they pass other ships which are moored to a landing quay in a canal or river. Therefore for busy waterways, quays directly beside a waterway are advised against.

A potential solution to this problem is an alternative mooring system, the MoorMaster™ system by Cavotec MSL. The desire is that by using this system there is no need for passing vessels to slow down. The MoorMaster™ system works with suction pads that are attached to the ship's hull. These suction pads generate forces in the horizontal plane, reducing the ship motions significantly. Chapter 2 provides some background information on the MoorMaster™. This system is originally designed for mooring seagoing vessels to a quay. The wave forces on a moored sea vessel may be different from the forces caused by a passing ship in a small canal. In addition to this, the size, shape and construction of inland ships is different from seagoing vessels. Therefore the forces of the MoorMaster™ system may have a different result.

1.1. RESEARCH QUESTIONS

It is uncertain whether the MoorMaster™ system is suitable for the application described above.

The main research question of this project is:

- Is the MoorMaster™ 200 system a suitable mooring solution for (un)loading vessels at landing quays in inland waterways in the sense that there is no need for passing vessels to reduce speed?

In order to determine the suitability of the MoorMaster™ system for an inland waterway, the following questions need to be answered:

- 1) What are the forces produced by passing ships at cruising speed on the moored vessel?
- 2) What are the reaction forces of the MoorMaster™ units?
 - a) What configuration of MoorMaster™ units is needed to keep the moored vessel in place?
 - b) What are the forces produced by the MoorMaster™ units on the moored vessel in order to keep it in place?
 - c) How should 'to keep it in place' be defined; what are the tolerances or boundaries for motions from an operational point of view?
- 3) What are the resulting motions of the moored vessel?
- 4) Can the construction of a typical inland vessel withstand these forces?

1.2. RESEARCH GOAL

Not all possible inland waterways can be researched. Therefore, RWS was consulted which waterway would be most beneficial for them to have researched. RWS indicated that the Amsterdam Rijnkanaal would be most beneficial. Thus a case study of the Amsterdam Rijnkanaal (ARK) will be conducted. The goals of this research are:

- Determine the hydrodynamic forces acting on a moored vessel in the ARK as a result of passing vessels
- Determine the reaction forces of the MoorMaster™ system
- Determine the resulting ship motions of the moored vessel and compare these to mooring criteria
- Determine the needed configuration of MoorMaster™ units for this case
- Determine whether the construction of a typical inland vessel can cope with the loads of the MoorMaster™ system

1.3 READERS' GUIDE

To accomplish this, first a literature study into mooring criteria and the characteristics of the ARK and its traffic is conducted in chapter 2. The mooring criteria will be used to compare the resulting ship motions with to ensure suitability. The characteristics of the ARK are important because the waterway needs to be modelled in order to simulate the hydrodynamic forces due to passing vessels. The traffic of the ARK is used to determine what vessels need to be moored and/or passing.

In chapter 3, a literature study of hydrodynamic forces caused by passing vessels and ways to simulate these is performed. A sensitivity study of the chosen model is included in Appendix F. The physical model used to model the MoorMaster™ system and the ship motions is described and verified in chapter 4. The model is programmed in Matlab, the scripts can be found in Appendix G - Appendix L. In this chapter, the configuration and PD setting of the MoorMaster™ units is decided. The chapter concludes with suggestions of validation of the model using model tests.

In chapter 5, the loads on the hull of the vessel and the resulting stress is discussed. An example calculation to determine the stress in a "Damen Riverliner 1145E" is shown.

Chapter 6 shows the results of the passing vessel simulations, the ship motions model and the construction calculations. In chapter 7 conclusions are drawn and finally in chapter 8, the discussion and recommendations are given.

2. BACKGROUND RESEARCH

The goal of this chapter is to provide needed understanding of the MoorMaster™ system, the mooring criteria the system needs to comply with to be deemed suitable and background information on the ARK needed for the simulation of passing vessels.

To provide understanding of the MoorMaster™ system the chapter starts with some background information on the MoorMaster™ system. First, the working mechanism of the system is explained. After that, a literature review of former research on the system is shown.

To determine when a mooring system is suitable, a set of criteria has to be set. Therefore first the criteria a mooring system has to comply with is researched by means of a literature review. The results of the ship motion model will be compared to these criteria.

Next, the characteristics of the Amsterdam Rijnkanaal and its traffic are discussed, in order to establish the situations that need to be simulated in the passing vessel simulations in chapter 3.

2.1. BACKGROUND INFORMATION MOORMASTER™ SYSTEM

First, the working mechanism of the system is explained. After that, a literature review of former research on the system is performed.

2.1.1. MOORMASTER™ SYSTEM

One MoorMaster™ unit consists of a suction pad fastened to the ship hull, connected to an elbow shaped mechanical arm. The arm is movable in the horizontal plane and controlled by a programmable PID controller. The MoorMaster™ has active controls meaning it can react to mooring loads and absorb and reduce mooring energies via the hydraulic cylinders and the associated control system. The arm is mounted on a vertical rail and can move up and down unrestricted. Figure 2.1 shows a unit connected to a ship hull.



Figure 2.1 A MoorMaster™ unit connected to a ship hull

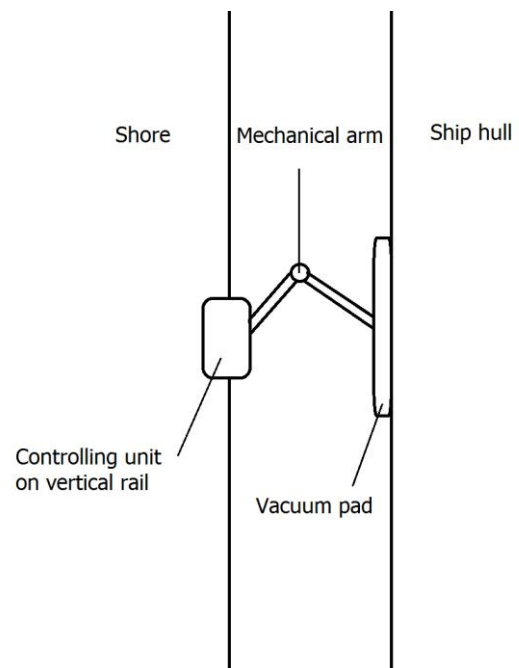


Figure 2.2 Schematic overview of MoorMaster™ unit

Usually, multiple units are installed to moor one ship. When (un)loading the ship, the draft of the vessel can change drastically. When the end of the vertical rail is reached, the units can relocate one by one to a new vertical position on the ship hull. This is called 'stepping'. Considering the little to no freeboard of some inland ships when fully loaded, Cavotec was asked what the possibilities are for this situation. The system can be configured to work under water or partially submerged.

Figure 2.2 shows a schematic representation of a unit. The controlling unit determines the force that is exerted by the mechanical arm on the ship hull in surge and sway direction. This force counteracts horizontal ship motions caused by external forces. When the maximum forces the system is designed for are exceeded, which obviously is not supposed to happen, the vacuum pads will be pried loose. The ship hull or MoorMaster™ system will not be damaged by this.

2.1.2. FORMER RESEARCH TO MOORMASTER™

To create some insight into the background of the MoorMaster™ system, former research on the system is reviewed. Since the system is relatively new, little research has been done, making this research a valuable addition.

(de Bont, et al., 2010) have coupled several numerical models to calculate the motions of moored ships inside a harbour basin, using MoorMaster™ units. They compare the results from the simulations with measurements and conclude that the effect of MoorMaster™ units on motions of moored ships can be simulated well in Quaysim. However, the simulations have not led to accurate results for the frequencies of the ship motions, due to unknown parameters.

(Terblanche & van der Molen, 2013) also model the MoorMaster™ 200 in Quaysim and similarly conclude significant reduction in ship motion.

(Deyzen, et al., 2014) present computer simulations to compare the MoorMaster™ to conventional mooring lines and to the ShoreTension® mooring system. The goal of the research is to see if these mooring systems can decrease the downtime of exposed terminals. A DMA software package is used to simulate a moored container ship. Several different mooring configurations and environmental conditions are simulated. They conclude that the MoorMaster™ significantly reduces the horizontal motions of the moored container vessel, however to assess downtime the modelling should include the probability of occurrence of all relevant environmental conditions.

In 2010, J. de Bont wrote his master thesis called 'Validation of numerical models for motions of ships moored with MoorMaster™ units, in a harbour under influence of ocean waves'. This thesis is however confidential and has not been accessed. (de Bont, 2010)

Cavotec itself provides a document to aid numerical modelling (Cavotec MoorMaster Limited, 2012). It gives the specifications and range of motion and forces. It also describes the system response delay, deadband, possible configurations and a control diagram.

2.2. LITERATURE REVIEW MOORING CRITERIA

To establish whether or not a mooring system is 'suitable', a literature study has been conducted into mooring criteria with respect to (un)loading cargo. First, an overview of the literature will be given, then the chosen criteria will be discussed. In Appendix N an image of the six different ship motions is given.

Mooring criteria can be separated into two categories: safety criteria and operational criteria. Where the safety criteria are mostly concerned with the limits of the mooring system, the operational criteria dictate the limits where (un)loading can still be performed safely and efficiently. The motion criteria found in literature all refer to the operational criteria. Safety criteria are usually mentioned, but not quantified. There are some velocity safety criteria found in literature.

In 1990, a joint research project was undertaken in Scandinavia. The purpose of the project was to establish criteria for acceptable ship movements in harbours for working and safe mooring conditions (Jensen, et al., 1990). Parameters influencing the conditions at berth are discussed and operational motion criteria and safety velocity criteria are set, using field measurements and questionnaires with port masters, crane operators, etc.. The field measurements included ship movements, mooring forces, wind, waves off the port and inside the port and fender deflections in harbours with known ship movement problems.

Upon review of the previously stated study, PIANC (Permanent International Association of Navigation Congresses) decided to set up a research group to study the criteria for ship motions in harbours (Elzinga, et al., 1992). The criteria that followed were slightly different from the ones of (Jensen, et al., 1990). Larger ship motions are allowed, according to (Elzinga, et al., 1992).

Years later, (Goedhart, 2002) wrote a thesis about the criteria for (un)loading containerships. He has developed a model that calculates the reduced handling rates in case of increased ship motion, based on the time it takes a crane driver to put in a container, in such conditions. The thesis concludes that the criteria from PIANC for surge, sway and heave are not strict enough for the 90-100% efficiency.

This conclusion is shared by (Moes & Terblanche, 2010), who also say that the criteria by PIANC are not strict enough and that the ones set by (Jensen, et al., 1990) are more acceptable. (un)Loading efficiencies have been computed using numerical simulations. They also state that surge motion is the principal motion of interest for (un)loading efficiency. They compare several criteria set up over the years. When comparing several criteria, it is noticed that the format of the criteria is critical. Mostly used are peak-to-peak values, although sway is often a zero-to-peak value, considering it is only possible away from the quay. When comparing criteria, it is important to notice these differences.

The Port Designer's Handbook (Thorensen, 2014) also compares the PIANC criteria to those of (Jensen, et al., 1990). However, they do not recommend one above the other.

2.3. SAFETY CRITERIA

Since the safety criteria are not quantified in literature, apart from velocity criteria, these have to be set. They are mainly defined by the limitations of the mooring system, in this case the MoorMaster™ units. The maximum load of the units is determined and safe motions and velocities are discussed.

2.3.1. MAXIMUM LOAD

The forces on the mooring system should not exceed the limits of the mooring system. If the limits of the MoorMaster™ are exceeded, the ship will be detached from the mooring system.

For the MoorMaster™, the maximum forces are given in (Cavotec MoorMaster Limited, 2012). The maximum force is dependent on the angle in which the units are located. Eq. 2.1 gives the maximum force as a function of this angle.

$$F_{max}(\alpha) = \text{greater of: } 100 \text{ kN or } \left(\frac{100 - \left(\frac{100}{\frac{\sin 63.44}{|\sin \alpha|} \cdot |\cos \alpha| + \cos 63.44} \right) \cdot \cos 63.44}{|\cos \alpha|} \right) \text{ kN} \quad \text{Eq. 2.1}$$

Where α is the angle indicated in Figure 2.3 . (Cavotec MoorMaster Limited, 2012)

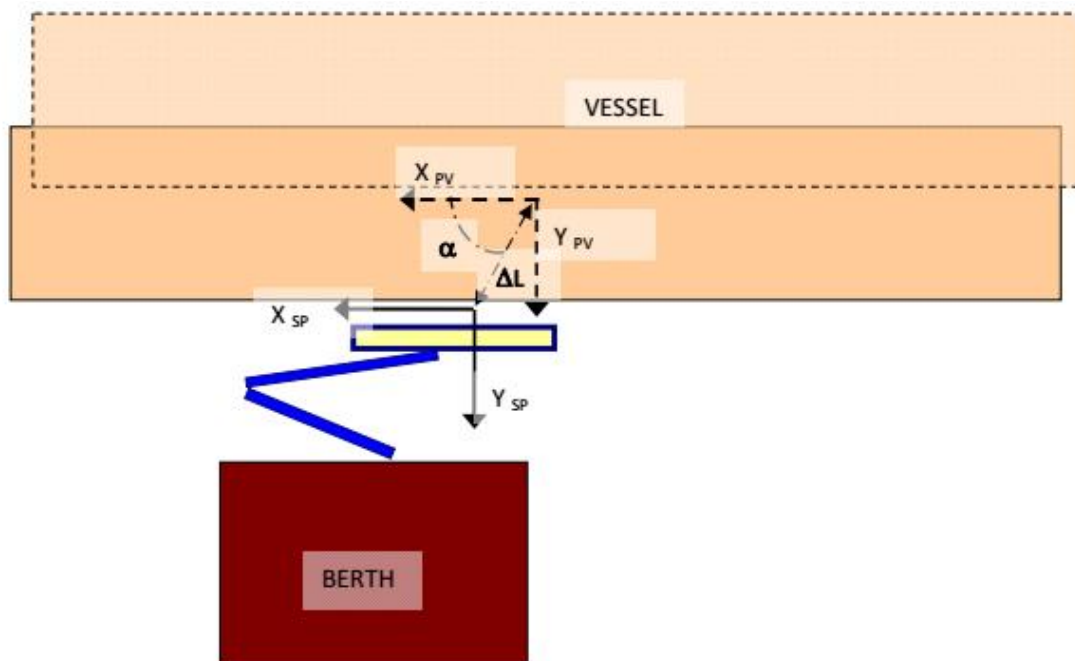


Figure 2.3 Force convention (Cavotec MoorMaster Limited, 2012)

When the units are used purely in one direction, the maximum forces are 100 kN in surge direction or 200 kN in sway direction, per unit.

2.3.2. SAFE MOTIONS

Various types of ship movements can cause different kinds of damage. Large surge motions can cause collisions with other ships aft or fore. Yaw and sway motions can cause damage to quay and fenders, but also the ship itself. (Jensen, et al., 1990). In the context of a restricted canal, not only the surge motion should be limited to prevent collision. The sway motion should be limited as well, to prevent collision with passing ships.

The MoorMaster™ units should prevent excessive horizontal ship motions, thus as long as the maximum forces are not exceeded, the motions should be in a safe range as well. When mooring other ships fore and aft of a ship, one needs to consider the possible range of motion of the MoorMaster™ units to prevent collision.

The range of movement of the MoorMaster™ units is unlimited in heave, within the range of the rail or stepping feature used. In surge, the units can move approximately 400 mm and in sway 2200 mm. These values are subject to change to suit installation location conditions. Therefore, this research will use these values and if they turn out to be insufficient, other possibilities will be looked into. (Cavotec MoorMaster Limited, 2012). Reaching the maximum deflection in sway direction may significantly reduce the passing distance of the passing ship. The increase in forces caused by this event should be taken into account.

2.3.3. SAFE VELOCITY

The velocity and the mass of the vessel are important parameters which determine the dynamic forces. These may cause damage to ship and quay. For this reason, there are also velocity criteria for safe mooring (Jensen, et al., 1990). Table 2.1 shows these velocity criteria, according to (Jensen, et al., 1990).

Table 2.1 Velocity criteria safe mooring (Jensen, et al., 1990)

Size of vessel	Surge (m/s)	Sway (m/s)	Yaw (deg/s)	Roll (deg/s)
1,000 DWT	0.6	0.6	2.0	2.0
2,000 DWT	0.4	0.4	1.5	1.5
5,000 DWT	0.3	0.3	1.0	1.0

A summary of the safety criteria is given in Table 2.2.

Table 2.2 Safety criteria

MoorMaster™	
Forces	Not exceed Eq. 2.1
Motions	Not exceed 400 mm surge (peak to peak) or 2200 mm sway (zero to peak)
Velocity	Not exceed Table 2.1

2.4. OPERATIONAL CRITERIA

Operational criteria involve (un)loading efficiency. The criteria are set to determine efficient operational conditions.

2.4.1. OPERATIONAL MOTIONS

In order to maintain efficient operational conditions, the ship motions should be kept within limits. There are several other parameters to be considered when looking into operational conditions, such as the loading equipment, skill level of the personnel, type of goods and type of vessel. (Jensen, et al., 1990). However, in this research only the ship motions of container vessels will be looked into. The other parameters are independent of the mooring system. Container vessels are chosen because the literature study indicates that for (un)loading this type of vessels, the ship motions are most critical.

The motion criteria recommended by (Jensen, et al., 1990) will be used, these can be found in Table 2.3. The frequency of exceedance of these movements should be less than 2%.

Table 2.3 Ship motion criteria for container vessels (L_{oa} = 100-200 m), maximum amplitude (Jensen, et al., 1990)

	Surge (m)	Sway (m)	Heave (m)	Yaw (deg)	Pitch (deg)	Roll (deg)
90-100% efficiency	0.50	0.40	0.45	0.25	0.75	1.50
50% efficiency	1.00	1.00	0.60	0.75	1.25	3.00

2.5. CHARACTERISTICS OF THE AMSTERDAM-RIJNKANAAL AND ITS TRAFFIC

The circumstances in which these criteria have to be met have to be established. For this research a case study is executed on a virtual quay side mooring site in the Amsterdam-Rijnkanaal. Therefore, the waterway and its traffic is reviewed.

2.5.1. THE WATERWAY

The Amsterdam-Rijnkanaal (ARK) has a draught of approximately 6 m and is 70 to 120 m wide. The cross section of the ARK is shown in Figure 2.4. This is based on a situation sketch of RWS in 1979, see Appendix A. (Lieveense, 2010) and (Verheij, et al., 2012) also use the same cross section, in more recent publications.



Figure 2.4 Cross section of the Amsterdam-Rijnkanaal

This is the cross section this research will use.

2.5.2. TRAFFIC

All European waterways can be classified using the resolution of the European Conference of Ministers of Transport (Coférence Européenne des Ministres des Transports, 1992), or the CEMT classification. An overview of different classes can be found in Appendix B. This classification expresses the type of ships the waterway is suitable for. The ARK is a class VIb canal, suitable for Rhinemax vessels and 4-barge pushed convoy (Dienst Verkeer en Scheepvaart, 2008). Rijkswaterstaat also has a further specified classification of its own, which can be found in Appendix C. The approximate dimensions of the vessels and convoys for which the ARK is deemed suitable can be found in Table 2.4.

Table 2.4 Dimensions of vessels according to CEMT class of Amsterdam-Rijnkanaal

Class VIb	Rhinemax vessel	4 barge pushed convoy
Length	135 m	185-195 m
Beam	17.0 m	22.8 m
Draught (laden)	4.0 m	3.5-4.0 m

Figure 2.5 shows the active inland shipping combinations sailing under the Dutch flag in 2007 and 2008 (Rijkswaterstaat, 2009). This only entails the ships sailing under the Dutch flag. When looking at the number of vessels that have passed certain locks in the ARK (Rijkswaterstaat, 2009), it is found that about 65% of all ships sailing in the ARK have a Dutch origin. Therefore the distribution of classes shown in Figure 2.5 is presumed representative of the total number of ships sailing in the ARK. They are divided by the classification of RWS, as

found in Appendix C. Even though the canal is suitable for 4-barge pushed convoy, the most common vessel on the ARK is a class Va M8 motor vessel, of which the dimensions can be found in Table 2.5.

Table 2.5 Dimensions of most common vessels on Amsterdam-Rijnkanaal

Class Va	Large Rhine vessel (M8)
Length	110 m
Beam	11.4 m
Draught (laden)	3.5 m

Furthermore, the maximum allowed dimensions of a vessel on the ARK, according to law (Binnenvaartpolitiereglement, 2004), are displayed in Table 2.6.

Table 2.6 Maximum allowed dimensions of vessels or convoys on Amsterdam-Rijnkanaal by law

BPR	Maximum allowed dimension of vessel or convoy on ARK
Length	200 m
Beam	23.5 m
Draught (laden)	4.0 m

Appendix D shows some statistics of class VI vessels passing two locks in the ARK in 2011. These statistics show that a four barge pushed convoy will pass once or twice a day.

Based on this information, this research focusses on three vessel types. The large Rhine vessel, Rhinemax vessel and a 4-barge pushed convoy with the maximum allowed dimension on the ARK.

Actieve binnenvaartcombinaties varend onder Nederlandse vlag, 2007 - 2008

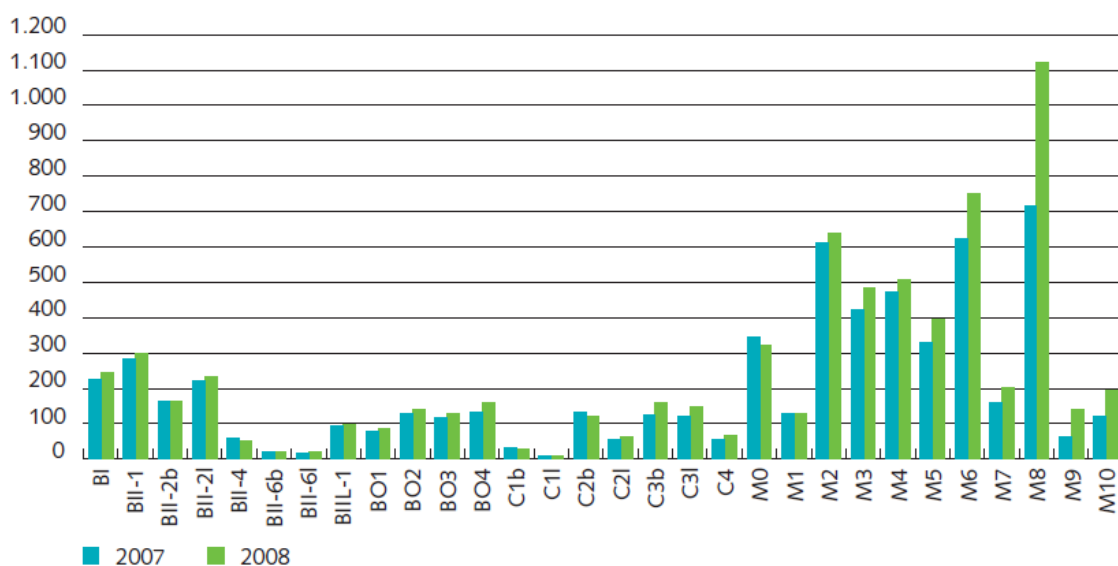


Figure 2.5 Active inland shipping combinations sailing under the Dutch flag (Rijkswaterstaat, 2009)

The maximum speed on the ARK is 18 km/h. In practice, the speed vessels sail at strongly depends on the type of vessel, installed power and the loading condition. For instance, a large Rhine vessel owner says to sail at 12 km/h when it's fully loaded and 15 km/h when empty.

2.5.3. QUAY

Considering the waterway and its traffic, the quay can be defined. The quay needs to be deep enough to accommodate the mooring vessels. The configuration that would still maintain a straight channel, would be to dig out the slope over the length of the quay, as in Figure 2.6. The downside to this configuration is the narrowness of the canal. If two 4 barge convoys were to pass each other, with a moderate drift angle of 6 degrees, there would be no room left for a moored vessel.

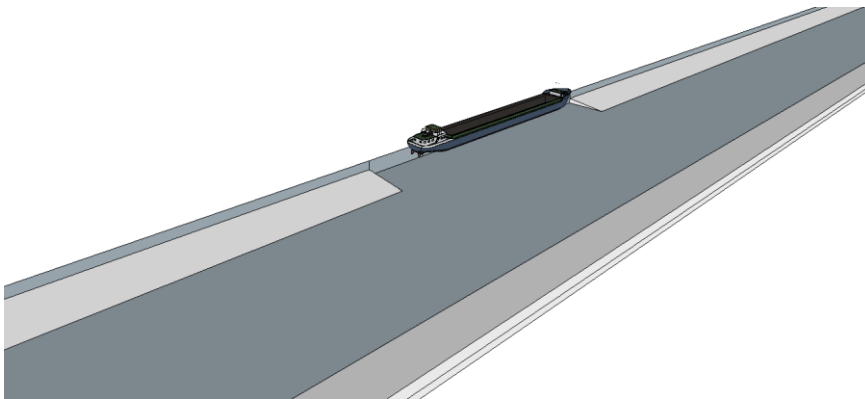


Figure 2.6 Straight channel with quay

For busy waterways, defined as a waterway class V or higher where more than 30,000 commercial vessels pass per year, quays directly beside a waterway are advised against by RWS. This is the case in the ARK. However, RWS does give guidelines for quays directly beside a normal or quiet waterway (Rijkswaterstaat, 2011). Figure 2.7 shows the advised configuration. The length of the quay should be at least 1.1 times the length of the moored vessel. The width should be the width of the vessel plus a safety zone which is 7.0 m for a class Vb vessel. The transition from the quay to the waterway should go smooth, at an gradient of at least 1:2. (Rijkswaterstaat, 2011)

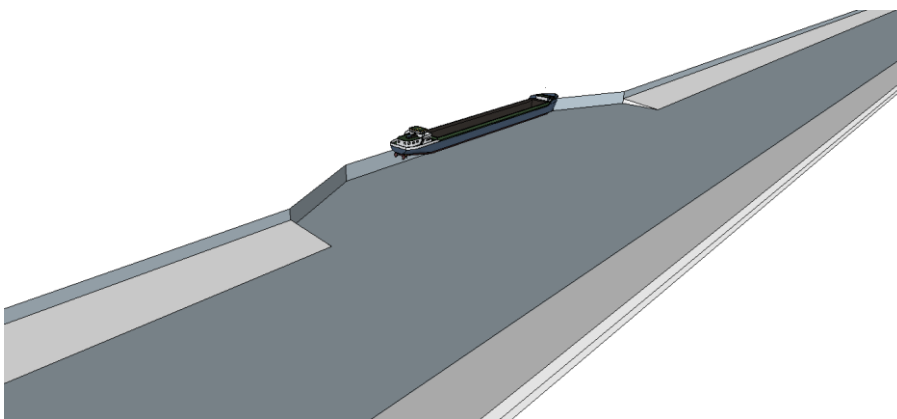


Figure 2.7 Quay following RWS guidelines

The length and width of the class Vb Rhinemax vessel are used to determine the dimensions of the quay. This is chosen because it is desirable for container terminal entrepreneurs to be able to moor a Rhinemax vessel at the quay. This results in a length of 150 m and a width of 24 m. A 1:2 slope is used for the transition to the canal.

2.6. SUMMARY BACKGROUND RESEARCH

In this chapter background research is conducted to support the main research questions. Mooring criteria are researched to establish when a mooring system can be deemed suitable. The characteristic of the ARK are studied for the purpose of modelling the waterway to simulate hydrodynamic forces. The traffic of the ARK is studied to ensure the right vessel types are used in the simulations.

2.6.1. MOORING CRITERIA

A summary of the chosen mooring criteria is given below. The criteria are separated in basic criteria for safety, these have to be met at all times. Then there is an set of extra criteria to accomplish 50% (un)loading efficiency. These criteria are additional to the basic criteria for safety. The last set of criteria are for 90-100% (un)loading criteria. These are also additional to the former sets of criteria. This is the desired level of efficiency.

2.6.1.1. BASIC CRITERIA FOR SAFETY

These criteria have to be met at all times, to ensure structural integrity of the mooring system and the moored vessel:

- The maximum force on each MoorMaster™ unit is less than or equal to Eq. 2.1, when used in surge and sway direction.
- The maximum forces on each MoorMaster™ are less than or equal to 200 kN in surge or 100 kN in sway, when used in one direction only.
- The amplitudes of the ship motions of the moored vessel will not exceed the following:
 - $A_{Surge} \leq 0.40 \text{ m}$
 - $A_{Sway} \leq 1.10 \text{ m}$
- The velocity of the moored vessel will not exceed the values in Table 2.1

2.6.1.2. EXTRA CRITERIA FOR 50% (UN)LOADING EFFICIENCY

To ensure 50% (un)loading efficiency, these extra criteria have to be met, on top of the safety criteria.

The amplitudes of the ship motions of the moored vessel will not exceed the following:

- $A_{Sway} \leq 1.00 \text{ m}$
- $A_{Heave} \leq 0.60 \text{ m}$
- $A_{Yaw} \leq 0.75^\circ$
- $A_{Pitch} \leq 1.25^\circ$
- $A_{Roll} \leq 3.00^\circ$

2.6.1.3. EXTRA CRITERIA FOR 90-100% (UN)LOADING EFFICIENCY

These criteria have to be met for most passing events, to ensure efficient (un)loading of the moored vessel, on top of the safety criteria and extra criteria for 50% (un)loading efficiency.

The amplitudes of the ship motions of the moored vessel will not exceed the following:

- $A_{Sway} \leq 0.40 \text{ m}$
- $A_{Heave} \leq 0.45 \text{ m}$
- $A_{Yaw} \leq 0.25^\circ$

- $A_{Pitch} \leq 0.75^\circ$
- $A_{Roll} \leq 1.50^\circ$

2.6.2. CASE STUDY

The case study is about a virtual quay in the ARK. The criteria mentioned above need to be satisfied in the following harbour geometry and passing situations for the case study.

2.6.2.1. HARBOUR GEOMETRY

The ARK has a draught of approximately 6 m and is 70-120 m wide. The cross section of the ARK is shown in Figure 2.4. Figure 2.7 shows the quay following RWS guidelines. The length and width of the class VIb Rhinemax vessel are used to determine the dimensions of the quay. This results in a length of 150 m and a width of 24 m. A 1:2 slope is used for the transition to the canal.

2.6.2.2. PASSING AND MOORED VESSELS

Based on the traffic sailing the ARK, this research focusses on three vessel types. The large Rhine vessel and Rhinemax vessel and a 4-barge pushed convoy with the maximum allowed dimension on the ARK. The dimensions of these vessels can be found in Table 2.4 - Table 2.6.

3. SIMULATING PASSING VESSELS

In the previous chapter, background information on the MoorMaster™ system is provided, as well as mooring criteria and characteristics of the ARK and its traffic. In this chapter the method to determine the forces acting on the moored vessel is explained. The hydromechanics of passing ships are studied in 3.1. A numerical tool to predict these forces, Ropes, is evaluated and the theoretical background is discussed in 3.2. The characteristics of the ARK and its traffic from the previous chapter is used as input for the Ropes simulations.

The output of the simulations is displayed in the results, chapter 6.

3.1. HYDROMECHANICS OF PASSING VESSELS

The hydromechanics of passing vessels is too complex to be estimated with rules of thumb or empirical methods. Model tests are a common method to predict loads on moored vessels caused by passing vessels. These give a good prediction of forces and motions, however these can be expensive and time consuming. That is why over the last decades, numerical methods have been developed to predict the forces on moored ships caused by passing ships. Another advantage of numerical methods is that the velocities and pressures can be calculated at each point of the wet surface of the ship hull and of the free surface. This gives more insight in the behaviour of the flow.

3.1.1. CONTRIBUTING FACTORS IN LOAD

In restricted waterways, the main contributor to the forces acting on the moored ship is the pressure wave. The passing ship pushes the water forward, creating this wave. The water level ahead of the vessel raises, while a draw down can be observed to the side and aft. Current itself does not have a great direct influence on the total load on the moored vessel, only a small static offset, however it can significantly influence the contribution of the pressure waves on the load because the current has a strong influence the water level drop (van der Hout & de Jong, 2014). At low depth-based Froude numbers (<0.3) the generation of waves by the sailing ship can be ignored (Remery, 1974). The depth-base Froude number is defined by Eq. 3.1.

$$Fr_h = \frac{V_{rel}}{\sqrt{g \cdot h}} \quad \text{Eq. 3.1}$$

Where V_{rel} is the velocity of the ship relative to the water, g is the gravitational acceleration and h the water depth. Other possible contributors to the load on the moored vessels are propeller action and viscous effects, however these do not seem to have a significant contribution to the loads (Talstra & Bliet, 2014).

3.1.2. RELATIONS BETWEEN PARAMETERS AND LOAD

Early on in the research on the effects of passing ships, a relation between the speed of the passing vessel and the forces on the moored vessel was already concluded (Remery, 1974). The loads induced by a passing ship on a moored vessel are proportional to the square of the speed of the passing vessel. They are also related to the relative position between both vessels. The same research also concludes that although the size and distance of the passing vessel is of course of influence on the load, the character of the curves is similar for the various sizes and passing distances of the sailing ship that were investigated. These relations are confirmed in later research and elaborated on (Talstra & Bliet, 2014). For depth-based Froude numbers <0.3, the normalized shape of the curve of the mooring loads as a function of longitudinal vessel-vessel distance is practically only determined by the passing distance and the moored vessels hull form. All mooring loads are roughly proportional to the inverse of the lateral passing distance and proportional to a negative power of K of the

under keel clearance. The power K is strongly dependent on the force/moment type (surge, yaw, sway, etc.) and some vessel specific properties. Some relation between displacement of the moored vessel and some forces/moments is also found. The drift angle of the passing vessel can have a large influence on the interaction effects. An increasing drift angle, bow towards the moored ship, increases the loads on the moored vessel (de Koning Gans, et al., 2007). The lift effects of the vortices in the wake flow caused by sailing under a drift angle have so far not been successfully implemented in a numerical model (de Koning Gans, et al., 2007). However, in moderate drift angles (<6 degrees) the flow separation can be assumed insignificant (Talstra & Bliet, 2014).

3.2. ROPES; A NUMERICAL TOOL TO PREDICT THE LOADS INDUCED BY PASSING VESSELS

A joint industry project researching the effects of passing ships on moored vessels named ROPES (Research on Passing Effects of Ships) was presented at the PIANC World Congress in San Francisco 2014 (van den Boom, et al., 2014). The numerical methods that Ropes uses are based on a 3D flow model which uses two simplifications: double-body flow and potential flow.

The first simplification is double-body flow, i.e. no free-surface effects can take place. This implies that only the primary ship wave is used for the solution and secondary wave effects are ignored. Using a double-body flow model means that as soon as free-surface effects start to dominate, Ropes underestimates the loads on the moored ship. This is where most deviations of the Ropes model from measurements come from. In complex harbour geometries, Ropes does not provide a good estimate of the hydrodynamic forces, because the free surface shock wave propagation will dominate. A non-uniform bottom is however no problem for Ropes, as well as an ambient current in a straight channel. (van der Hout & de Jong, 2014). For more details on the theoretical background on the double-body flow model, see (Pinkster & Pinkster, 2014). The second simplification, potential flow, will be further explained in 3.2.1 Panel method.

The reason of these simplifications is the fact that it greatly simplifies the prediction method and thus decreases computing time (Pinkster & Pinkster, 2014). The numerical method used is the panel method. This method will be elaborated on. Then the validity of the results for this research is discussed.

3.2.1. PANEL METHOD

The panel method is a numerical method to calculate flow velocity fields. The velocity field can be used to calculate pressures, forces and more. The theoretical background of the method will now be explained. The panel method uses potential flow, which will first be explained. Then the boundary conditions that can be applied to potential flow are discussed. After that, the solving method of the panel method is elaborated on.

3.2.1.1. POTENTIAL FLOW

When using potential flow, one assumes a inviscid, irrotational and incompressible flow. In case of passing vessels, the inertia forces are large compared to the viscous forces, which justifies the inviscid flow.

The irrotational flow assumption is justified when the passing vessel does not cause significant flow separation. As stated before, this can be assumed when drift angles are moderate. A flow is irrotational when the water particles do not rotate.

Apart from that, viscous effects are significant only in the very thin boundary layer around an object in the water. As with viscous effects, rotational flow is bound to the boundary layer around an object. Therefore it is appropriate to assume irrotational as well as inviscid flow outside of these regions. (Katz & Plotkin, 1991)

Though compressible flow is possible, assuming a constant density greatly simplifies the analysis. The assumption of incompressible flow is generally accepted when studying ships, since the velocities are of such a nature that compressibility can be neglected.

With these assumptions, the potential Φ can be defined as in Eq. 3.2:

$$\bar{u} = \nabla\Phi \quad \text{Eq. 3.2}$$

Where u is the velocity field of the flow and ∇ represents the gradient. Eq. 3.3 shows Eq. 3.2 in Cartesian coordinates.

$$u = \frac{\partial \Phi}{\partial x} \quad v = \frac{\partial \Phi}{\partial y} \quad w = \frac{\partial \Phi}{\partial z} \quad \text{Eq. 3.3}$$

Considering the conservation of mass in incompressible flow, the continuity Eq. 3.4 can be set up.

$$\bar{u} \cdot \nabla = 0 \Leftrightarrow \frac{\partial u}{\partial x} + \frac{\partial v}{\partial y} + \frac{\partial w}{\partial z} = 0 \quad \text{Eq. 3.4}$$

Combining Eq. 3.2 and Eq. 3.4 gives the Laplace equation, Eq. 3.5.

$$\nabla^2 \cdot \Phi = 0 \quad \text{Eq. 3.5}$$

In order to analyse the potential flow, the Laplace equation needs to be solved for Φ using the appropriate boundary conditions. These boundary conditions can be found in Appendix E.

(Katz & Plotkin, 1991)

3.2.1.2. SOLVING PANEL METHOD

Since the Laplace equation is a linear differential equation, the superposition principle applies. If A and B are both solutions to the equation, any linear combination of A and B is also a combination. Using Green's theorem and the boundary conditions, a series of elementary solutions of the Laplace equation can be computed. Examples of these singularities, sources/sinks, doublets and vortices, are discussed in Appendix E. Any linear combination of these singularities will satisfy the Laplace equation. With the right combination, complex flow fields can be simulated.

To solve a potential flow around a complex body, the geometry of the body is divided into panels. Each panel consists of a number of vertices (corner points) and has a collocation point. Each collocation point is the location of a singularity and the boundary conditions are specified at each collocation point. This way, a distribution of N singularities over the surface of the body is obtained. The total potential is the sum of the potentials of all singularities, Eq. 3.6.

$$\Phi = \sum_{k=1}^n c_k \Phi_k \quad \text{Eq. 3.6}$$

For example a source distribution is used and the boundary conditions are specified at each collocation point. Filling in the Laplace equation Eq. 3.5 for each panel, N equations with N unknown source strengths can be acquired. By solving this set of equations for the source strengths, the velocity field is obtained.

Filling in Bernoulli's equation and solving for the pressure gives the pressure field, Eq. 3.7. (Pinkster & Pinkster, 2014)

$$p = -\rho \cdot \frac{\partial \Phi}{\partial t} - \frac{1}{2} \cdot \rho \cdot \bar{\nabla} \cdot \Phi^2 \quad \text{Eq. 3.7}$$

With ρ the density of the water.

Next, by integrating the pressure distribution over the surface of the body, the forces and moments on the body can be obtained, Eq. 3.18. (Pinkster & Pinkster, 2014)

$$\bar{F} = - \iint_S p \bar{n} dS \quad \text{Eq. 3.8}$$

Filling in Eq. 3.7 in Eq. 3.8 gives Eq. 3.9.

$$\bar{F} = -\rho \iint_S \left(-\frac{\partial \Phi}{\partial t} - \frac{1}{2} \cdot \bar{\nabla} \Phi^2 \right) \bar{n} dS \quad \text{Eq. 3.9}$$

Considering the difficulties with evaluating partial time derivatives of the local value of the potential, the following relationship between the total derivative and the partial derivative is used, Eq. 3.10. (Pinkster Marine Hydrodynamics BV, 2013)

$$\frac{d\Phi}{dt} = \frac{\partial \Phi}{\partial t} + \bar{\nabla} \Phi \cdot \bar{U} \quad \text{Eq. 3.10}$$

Filling this in in Eq. 3.9 gives Eq. 3.11.

$$\bar{F} = -\rho \iint_S \left(-\frac{d\Phi}{dt} + \bar{\nabla} \Phi \cdot \bar{U} - \frac{1}{2} \cdot \bar{\nabla} \Phi^2 \right) \bar{n} dS \quad \text{Eq. 3.11}$$

Separating the contributions due to the velocities gives Eq. 3.12:

$$\bar{F} = \rho \frac{d}{dt} \iint_S \Phi \bar{n} dS - \rho \iint_S \left(\bar{\nabla} \Phi \cdot \bar{U} - \frac{1}{2} \cdot \bar{\nabla} \Phi^2 \right) \bar{n} dS \quad \text{Eq. 3.12}$$

The first term in Eq. 3.12 is concerned with the added mass and added mass coupling coefficients between the various bodies. The second term contains the earth-fixed velocities $\bar{\nabla} \Phi$ and the ship velocity \bar{U} . In some cases it is preferred to use the fluid velocities related to the body-fixed axes to evaluate this term. Eq. 3.13 gives the relation between the fluid velocity in the earth-fixed system, $\bar{\nabla} \Phi$, and the fluid velocity in the ship-bound system, $\bar{\nabla} \Phi'$. (Pinkster Marine Hydrodynamics BV, 2013)

$$\bar{\nabla} \Phi' = \bar{\nabla} \Phi - \bar{U} \quad \text{Eq. 3.13}$$

Substituting the ship-bound velocity in Eq. 3.12 gives Eq. 3.14, which can be rewritten as Eq. 3.15.

$$\bar{F} = \rho \frac{d}{dt} \iint_S \Phi \bar{n} dS - \rho \iint_S \left((\bar{\nabla} \Phi' + \bar{U}) \cdot \bar{U} - \frac{1}{2} \cdot (\bar{\nabla} \Phi' + \bar{U})^2 \right) \bar{n} dS \quad \text{Eq. 3.14}$$

$$\bar{F} = \rho \frac{d}{dt} \iint_S \Phi \bar{n} dS - \rho \iint_S \left(\frac{1}{2} \bar{U}^2 - \frac{1}{2} \cdot \bar{\nabla} \Phi'^2 \right) \bar{n} dS \quad \text{Eq. 3.15}$$

The corresponding equation for the moments acting on the vessels is given in Eq. 3.16.

$$\bar{M} = \rho \frac{d}{dt} \iint_S \Phi (\bar{r} \times \bar{n}) dS - \rho \iint_S \left(\frac{1}{2} \bar{U}^2 - \frac{1}{2} \cdot \bar{\nabla} \Phi'^2 \right) (\bar{r} \times \bar{n}) dS \quad \text{Eq. 3.16}$$

(Pinkster Marine Hydrodynamics BV, 2013)

The Ropes software includes several panel models of parent hull forms which can be scaled to size. The panel models of the harbour geometry are defined by the user.

An important parameter when using the panel method in a time simulation is the Courant number. The Courant number is a dimensionless transport per time step as defined by Eq. 3.17.

$$C = \frac{u \cdot \Delta t}{\Delta x} \quad \text{Eq. 3.17}$$

In case of a sailing ship, it is the velocity of the ship relatively to the water multiplied with the time step of the simulation, divided by the panel size. It can be described by the number of panels that are passed in one time step. It is desirable to have a Courant number below 1. A Courant number higher than 1 can affect convergence negatively. (Schär, 2015)

3.2.2. VALIDITY

The validation of the Ropes software took place making use of the hull definitions included within the software tool, scaled to the right measurements of the experiments, because the validation of the model should not be dependent on very specific custom-made hull forms. For a straight channel, a generally good match is found between model tests and computational results, for lower speeds. For larger depth-based Froude numbers, up to about 0.80-0.90, a correction factor F_c can effectively compensate for the deviation (Talstra & Bliiek, 2014). In (Wictor & van den Boom, 2014) the results of the full scale measurements, used to validate the results of the Ropes prediction software, are presented.

The output of Ropes is a time trace of the captive forces and moments in six degrees of freedom (DOF) on the moored vessel, ready to be used in non-linear mooring simulation software (Pinkster & Pinkster, 2014).

In this research, the maximum velocity that needs to be researched is 18 km/h, or 5 m/s (excluding current), since this is the maximum allowed speed at the ARK. The water depth is 6 m. This results in a maximum depth based Froude number of 0.65. Since this research is about a straight channel, Ropes is a suitable tool to use in this research, given that the correction factor proposed by (Talstra & Bliiek, 2014) is used to correct the results of the higher Froude numbers.

3.2.3. INPUT

The program Ropes is used to simulate different events of passing ships in the ARK, in order to obtain the hydrodynamic forces on the moored vessel. The input and run simulations are discussed in this paragraph.

Before the exact input is defined, a sensitivity study of the model is done. The sensitivity study and a presentation of the input interface of Ropes can be found in Appendix F.

Based on the sensitivity study, the chosen time step is 1 sec, the length of the modelled canal 1500 m, the distance the passing vessel will sail is 750 m and the panel size will be kept at 5 m/panel, the standard setting in Ropes. The passing ships will be sailing at a speed of 5 m/s, the maximum velocity in the ARK, which results in a Courant number of 1, which should be sufficient. A Courant number higher than 1 could cause an instable solution.

3.2.3.1. VESSELS

Table 3.1 shows the particulars of the ships that are used in the simulation, as mentioned before in paragraph 2.5. The Large Rhine vessel is always used as the moored vessel. Since it is the smallest, it is assumed that the passing events will be most critical when this vessel is moored. All three vessels will be used as passing vessels.

Table 3.1 Simulated vessels

Vessels	Large Rhine vessel	Rhinemax vessel	4 barge pushed convoy
L_{oa}	109.95 m	135.00 m	200.00 m
B	11.42 m	17.00 m	23.50 m
D (fully laden)	3.45 m	4.00 m	4.00 m
Cargo capacity	3,300 t	4,000 t	12,000 t

Ropes provides several parent hull form panel models. Figure 3.1 shows the panel model used for the Large Rhine vessel and, scaled to size, the Rhinemax vessel. For the barge, a panel model of a rectangular barge is used.

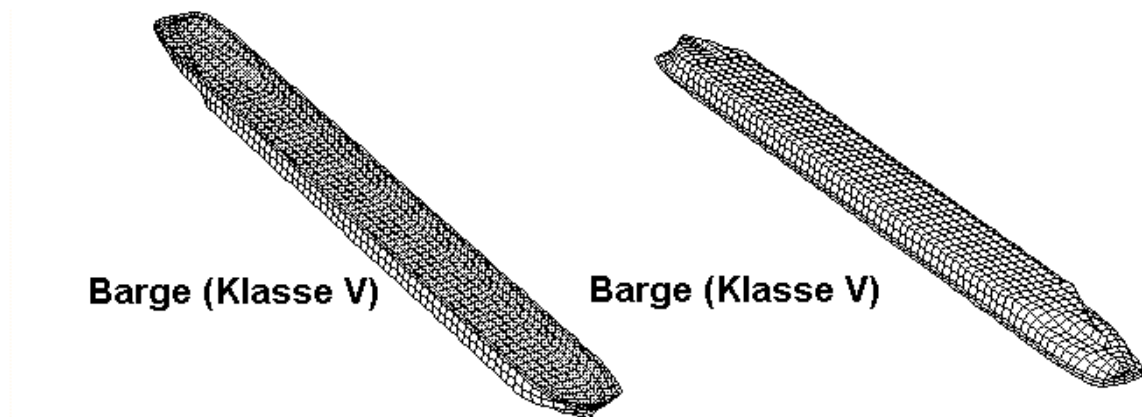


Figure 3.1 Panel model of inland vessels

3.2.3.2. LOADING CONDITIONS

The passing vessel is always loaded full, since this gives the largest forces on the moored vessel. The moored vessel is simulated both full and empty. For the empty vessel, a draft of 0.825m and a trim of -0.5 degrees is selected. This is based on information provided by a ship owner. Corresponding to this draft and trim, Ropes

calculates a displacement of 812m³. The fully loaded ship has a draft of 3.45m, 0 trim and a displacement of 3849m³.

3.2.3.3. PASSING SPEEDS

The passing speed has a quadratic influence in Ropes. Therefore it is sufficient to run the simulations at one single velocity. In order to obtain results for other passing speeds, the results simply have to be corrected quadratic for the speed. All simulations are run at 5 m/s, or 18 km/h, the maximum allowed speed in the ARK. Off course at higher speeds, the correction factor mentioned in 3.2 has to be taken into account. The factor, F_c , is given in Eq. 3.18 and is based on the depth-based Froude number and the blocking ratio of the canal. These are embedded in the constant c , which is given in Eq. 3.19. (Talstra & Bliet, 2014)

$$F_c = 1 + \left(\frac{U_0}{c}\right)^2 \quad \text{Eq. 3.18}$$

Where U_0 is the speed of the passing vessel and c is given by Eq. 3.19:

$$\frac{c}{c_0} = \left(\frac{2}{3}\right)^{1.5} \cdot \left(1 - r + 1/2 \cdot \frac{c^2}{c_0^2}\right)^{1.5} \quad \text{Eq. 3.19}$$

Where c_0 is the standard long wave celerity $c_0 = \sqrt{g \cdot h}$, h being the depth of the canal. r represents the blockage of the canal, defined by A_s/A_c , the area of the cross section of the ship divided by the area of the cross section of the canal.

The correction factor is calculated for each passing vessel, these can be found in Table 3.2.

Table 3.2 Correction factors for high velocities

Passing vessel	Correction factor F_c
Large Rhine vessel	1.918
Rhinemax vessel	2.247
4 barge pushed convoy	2.609

The results from Ropes will be multiplied with these factors. The results presented in the sensitivity study are not multiplied with the factor, since this has no added value when looking at the relationships between and accuracy of the solutions.

3.2.3.4. PASSING DISTANCES

The simulations where a single ship is passing are performed at three passing distances. The first route is as close to the moored vessel as practically possible, i.e. as close to the side that the depth of the canal is 0.5 m more than the draft of the sailing vessel. The second route is in the middle of the right hand side of the canal, given that the moored vessel is on the right hand side. The third route is in the middle of the left hand side of the canal, sailing in the opposite direction.

3.2.3.5. DRIFT ANGLE

In general, each simulation is run with 0, 7 and 15 degrees drift angle. Exceptions are routes where these drift angles are not practically possible, for example because the vessel would run aground.

Figure 3.2 gives a schematic overview of the simulations in Ropes.

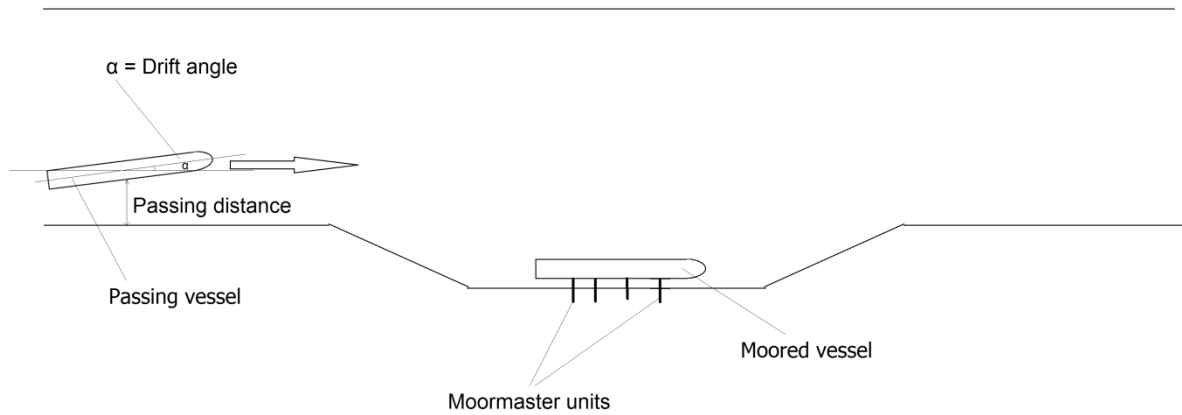


Figure 3.2 Schematic overview simulations Ropes

3.3. SUMMARY SIMULATING PASSING VESSELS

In this chapter the method to determine the forces acting on the moored vessel is explained. Hydromechanics of passing vessels in restricted water are discussed as well as the numerical tool used to simulate the scenarios of the case study.

3.3.1. HYDROMECHANICS OF PASSING VESSELS

Because of the complexity of the hydromechanics of passing vessels, numerical methods are used to predict forces caused by the passing vessels. In restricted waterways, the main contributor to the forces acting on the moored ship is the pressure wave. There is a quadratic relation between the velocity of the passing vessels and the loads induced on the moored vessel. Although the size and distance of the passing vessel is of course of influence on the load, the character of the curves is similar for the various sizes and passing distances. The drift angle of the passing vessel can have a large influence on the interaction effects. However, in moderate drift angles (<6 degrees) the flow separation can be assumed insignificant.

3.3.2. SIMULATION OF PASSING VESSELS

To simulate forces on the moored vessel caused by the passing vessels, ROPES (Research on Passing Effects of Ships) is used. Ropes is a joint industry project researching the effects of passing ships on moored vessels. The numerical methods that Ropes uses are based on a 3D flow model which uses two simplifications: double-body flow and potential flow. The reason of these simplifications is the fact that it greatly simplifies the prediction method and thus decreases computing time. The numerical method used is the panel method.

The output of Ropes is a time trace of the captive forces and moments in six degrees of freedom (DOF) on the moored vessel, ready to be used in non-linear mooring simulation software.

(Wictor & van den Boom, 2014), describes the validation of the Ropes software. For a straight channel, which is the case in this study, a generally good match is found between model tests and computational results, for lower speeds. The maximum depth based Froude number in this case study is 0.65. Ropes is a suitable tool to use in this research, given that the correction factor proposed by (Talstra & Bliet, 2014) is used to correct the results of the higher Froude numbers.

3.3.2.1. INPUT

Before the exact input is defined, a sensitivity study of the model is done. The sensitivity study and a presentation of the input interface of Ropes can be found in Appendix F.

Based on the sensitivity study the following parameters are selected:

- Time step: 1 sec
- Length modelled canal: 1500 m
- Sailing distance passing vessel: 750 m
- Panel size: 5 m

The passing ships will be sailing at a speed of 5 m/s, the maximum velocity in the ARK, which results in a Courant number of 1, which should be sufficient.

Three different passing vessels are simulated:

- 110 m Large Rhine vessel
- 135 m Rhinemax vessel
- 200 m 4-barge pushed convoy

For detailed characteristics, see Table 3.1. The moored vessel is always a 110 m Large Rhine vessel. Considering the 5 m/s passing speed, a correction factor for high depth-based Froude numbers is calculated for each vessel, see Table 3.2.

Three different passing distances are simulated:

- As close to the moored vessel as possible
- Middle of the right of the waterway
- Middle of the left of the waterway

Three different drift angles are simulated, 0, 7 and 15 degrees.

4. MODELING MOORED VESSEL

Previous chapters describe background information on the MoorMaster™ system, mooring criteria, characteristics of the ARK and its traffic and the simulation of the forces acting on the moored vessel caused by passing vessels. The goal of this chapter is to determine the reaction forces of the MoorMaster™ units and the resulting ship motions. To this end, a physical model of the resulting ship motions is shown in 4.1. The physical model to predict the reaction forces of the MoorMaster™ units is set up in 4.2. 4.3 shows some calculations necessary for the models. Paragraphs 4.4 - 4.6 display the verification of the models, starting with a simple one DOF scenario and working to a three DOF fully functioning model. In 4.7 the definitive configuration of MoorMaster™ units and their PD settings are discussed. Lastly, 4.8 shows methods to validate the models. All Matlab scripts of the models can be found in Appendix G-Appendix L. The results of the models are displayed in the results chapter, where they will be compared to the set criteria.

4.1. PHYSICAL MODEL SHIP MOTIONS

A physical model is proposed to model the ship motions of the vessel moored with MoorMaster™ units. Figure 4.1 shows a free body diagram of a ship moored with a number of equispaced MoorMaster™ units. F_y , F_x and M_h are the external hydrodynamic forces and moments on the ship caused by the passing vessels. F_{mm} is the sum of the reaction forces of all the units, as modelled in 4.2. Since the units are not placed at the centre of gravity of the ship, these forces also cause a moment around the centre of gravity of the ship M_{mm} , as is modelled in the function.

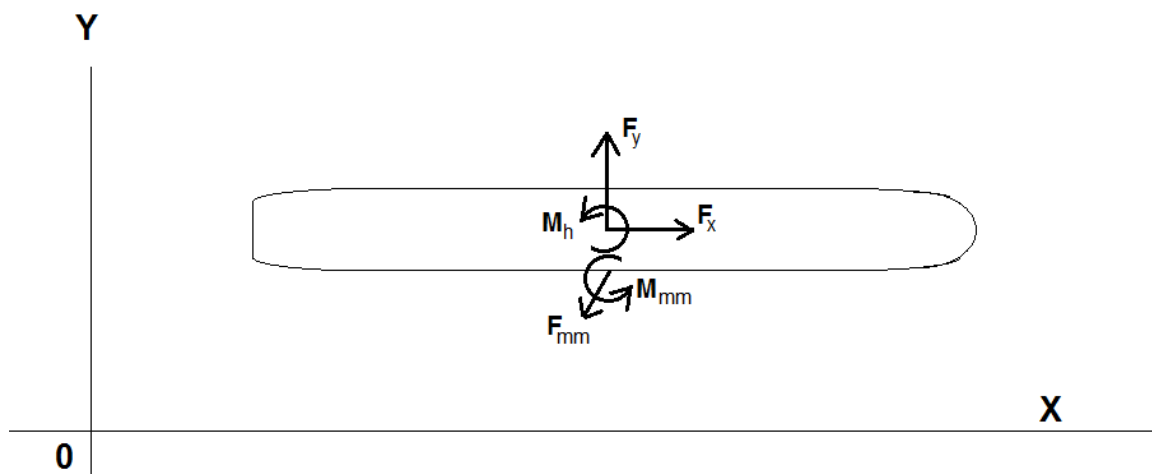


Figure 4.1 Free body diagram ship

The equation of motion of a vessel theoretically consists of four parts:

- The mass and added mass times the acceleration
- The retardation function, representing damping, times the velocity
- The hydrostatic spring coefficient times the displacement
- The external forces

See Eq. 4.1 (Journée, 2000).

$$(\bar{M} + \bar{A}) \cdot \ddot{\bar{X}}(t) + \int_0^{\infty} \bar{B}(t - \tau) \cdot \dot{\bar{X}}(\tau) \cdot d\tau + \bar{K} \cdot \bar{X}(t) = \bar{F}_{ext}(t) \quad \text{Eq. 4.1}$$

Where \bar{M} is the mass matrix, \bar{A} the added mass, \bar{B} the retardation functions and \bar{K} the stiffness matrix. \bar{X} is the motion vector.

The retardation and added mass are dependent on the frequency of the motions. At low frequencies, the damping is close to zero and can thus be neglected (Journée & Massie, 2001). For example see Figure 4.2, where the mass and damping of a heaving cylinder is displayed. The studied situation in this thesis consists of very low frequency motions. Therefore the damping of the ship will be neglected. The added mass can be considered constant at these low frequencies. Of course the MoorMasterTM units do introduce damping to the system, as is explained in 4.2.

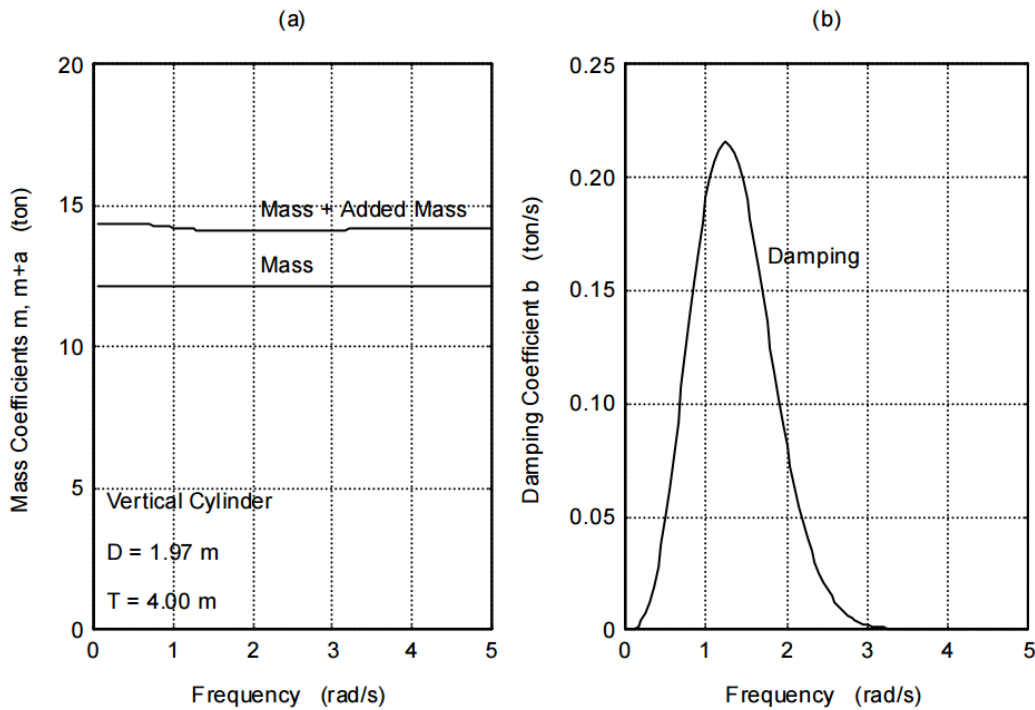


Figure 4.2 Mass and damping of a heaving vertical cylinder (Journée & Massie, 2001)

Since the MoorMasterTM units only produce forces in the horizontal plane and the horizontal motions are expected to be the most critical, only the motions in the horizontal plane will be considered: surge, sway and yaw. The hydrostatic spring coefficient is only relevant for vertical motions and zero for non-vertical motions.

Considering the added mass constant, the damping neglected and only the horizontal plane motions, the equation of motion reduces to the manoeuvring model, Eq. 4.2 (Pinkster, 2006).

$$\begin{bmatrix} m - A_{11} & -A_{12} & -A_{16} \\ -A_{21} & m - A_{22} & -A_{26} \\ -A_{61} & -A_{62} & I_{zz} - A_{66} \end{bmatrix} \cdot \begin{bmatrix} \ddot{x} \\ \ddot{y} \\ \ddot{\psi} \end{bmatrix} = F_{ext} \quad \text{Eq. 4.2}$$

Where m is the mass of the vessel, A_{ij} the entries of the added mass matrix, I_{zz} is the mass moment of inertia around the z axis, x is the surge motion, y the sway motion, ψ the yaw motion.

To determine the added mass, the vessel is run through Delfrac, a 3-D diffraction program developed at the Delft University of Technology by means of which the hydrodynamic interaction effects between several free-floating or fixed or interconnected bodies can be calculated. The vessel is excited by a series of low frequency waves. The output of Delfrac is given in Appendix M. Theoretically, $A_{ij} = A_{ji}$. However, in the results from Delfrac this is not always the case. Therefore, the average of A_{ij} and A_{ji} is taken. For more background information on Delfrac, see (Pinkster, 1995). Eq. 4.4 shows the added mass.

$$A = \begin{bmatrix} 3.374 \cdot 10^2 & -2.360 \cdot 10^0 & 2.049 \cdot 10^2 & -1.448 \cdot 10^1 & 8.759 \cdot 10^4 & -1.565 \cdot 10^3 \\ -2.360 \cdot 10^0 & 6.176 \cdot 10^3 & 9.074 \cdot 10^2 & -1.464 \cdot 10^4 & -1.517 \cdot 10^3 & 4.415 \cdot 10^3 \\ 2.049 \cdot 10^2 & 9.074 \cdot 10^2 & 5.647 \cdot 10^4 & -1.576 \cdot 10^3 & 9.429 \cdot 10^4 & 1.054 \cdot 10^3 \\ -1.448 \cdot 10^1 & -1.464 \cdot 10^4 & -1.576 \cdot 10^3 & 5.976 \cdot 10^4 & -2.320 \cdot 10^3 & 1.834 \cdot 10^4 \\ 8.759 \cdot 10^4 & -1.517 \cdot 10^3 & 9.429 \cdot 10^4 & -2.320 \cdot 10^3 & 3.515 \cdot 10^7 & -9.096 \cdot 10^5 \\ -1.565 \cdot 10^3 & 4.415 \cdot 10^3 & 1.054 \cdot 10^3 & 1.834 \cdot 10^4 & -9.096 \cdot 10^5 & 3.633 \cdot 10^6 \end{bmatrix} \quad \text{Eq. 4.3}$$

The mass moment of inertia of the vessel is estimated using a radius of inertia of 25% of the vessels length.

F_{ext} is the external force acting on the ship, consisting of the hydrodynamic force caused by the passing vessel and the applied force by the MoorMaster™ units, see Eq. 4.4.

$$\bar{F}_{ext} = \bar{F}_{Passing\ vessel} + \bar{F}_{MoorMaster} \quad \text{Eq. 4.4}$$

The external hydrodynamic force is modelled with the output from the Ropes simulations. The output from Ropes is the force on the centre of gravity of the vessel when it is in the original position. During the simulation, the ship will however move. Considering the passing force on the centre of gravity during the entire simulation, will result in a slight time shift from reality. The motions are assumed small enough to neglect this effect of the moving vessel, since only the time is shifted slightly, not the magnitude of the force.

4.2. PHYSICAL MODEL MOORMASTER™ UNITS

The previous paragraph show the equation of motion of the ship, where the external forces consist of the hydrodynamic force caused by the passing vessel and the applied force by the MoorMaster™ units. In this paragraph the physical model of the MoorMaster™ units is explained, in order to determine the second part of the external forces. Details about the system can be found in Chapter 2. Figure 4.3 shows a free body diagram of the suction pad of a unit. The forces acting on the ship result in a certain offset from the neutral position of the unit. This offset is translated into an error in x direction and an error in y direction. The MoorMaster™ unit responds to the error in displacement with a reaction force, with the aim of getting the unit, and thus ship, back in the neutral position. The model of the MoorMaster™ units is written to calculate the angle and magnitude of this reaction force.

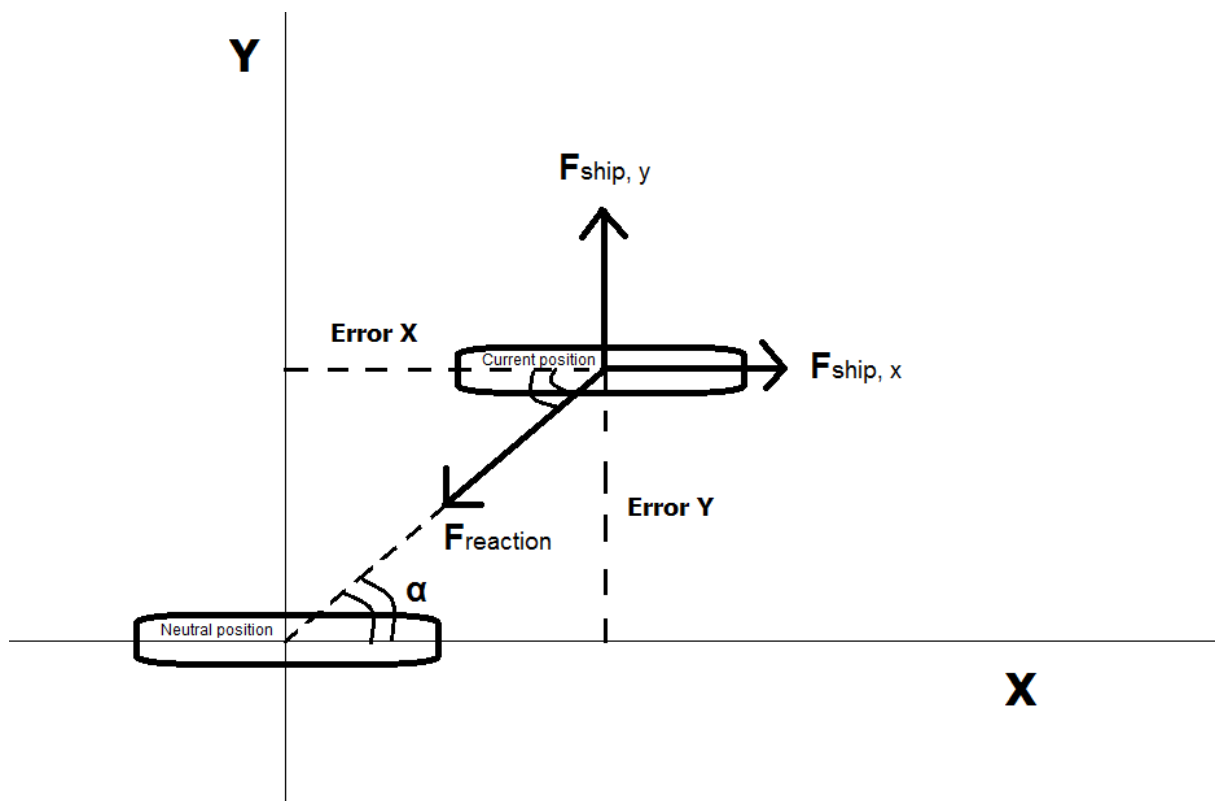


Figure 4.3 Free body diagram of MoorMaster™ suction pad

The control diagram used to model the force applied by the MoorMaster™ units is shown in Figure 4.5. The error in x and y direction are run through a PID controller. The control value from the PID controller and the angle α , defining the maximum force, are used to determine the applied force.

The maximum forces of the MoorMaster™ units are given before in 2.3. For convenience, it will be repeated here. The maximum force is dependent on the angle in which the units are located. Eq. 4.5 gives the maximum force as a function of this angle.

$$F_{max}(\alpha) = \text{greater of: } 100 \text{ kN or } \left(\frac{100 - \left(\frac{\sin 63.44}{|\sin \alpha|} \cdot |\cos \alpha| + \cos 63.44 \right) \cdot \cos 63.44}{|\cos \alpha|} \right) \text{ kN} \quad \text{Eq. 4.5}$$

Where α is the angle indicated in Figure 4.3. (Cavotec MoorMaster Limited, 2012) When the units are used purely in one direction, the maximum forces are 100 kN in surge or 200kN in sway, per unit.

Figure 4.4 shows the maximum force of a MoorMaster™ unit as a function of the angle α .

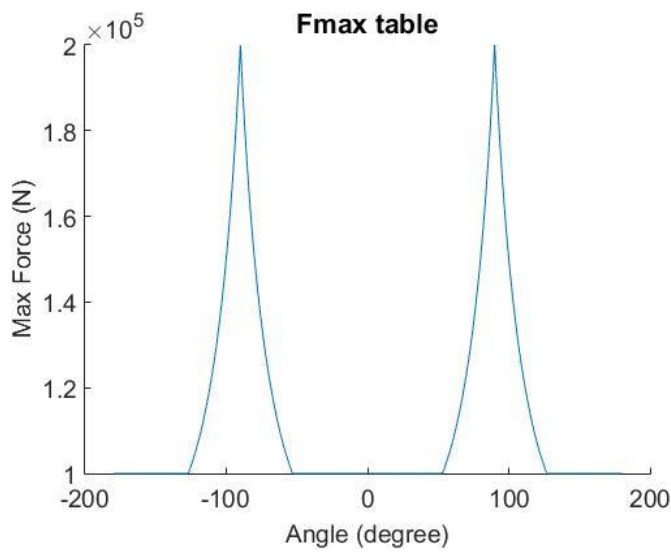


Figure 4.4 Maximum force MoorMaster unit as a function of angle

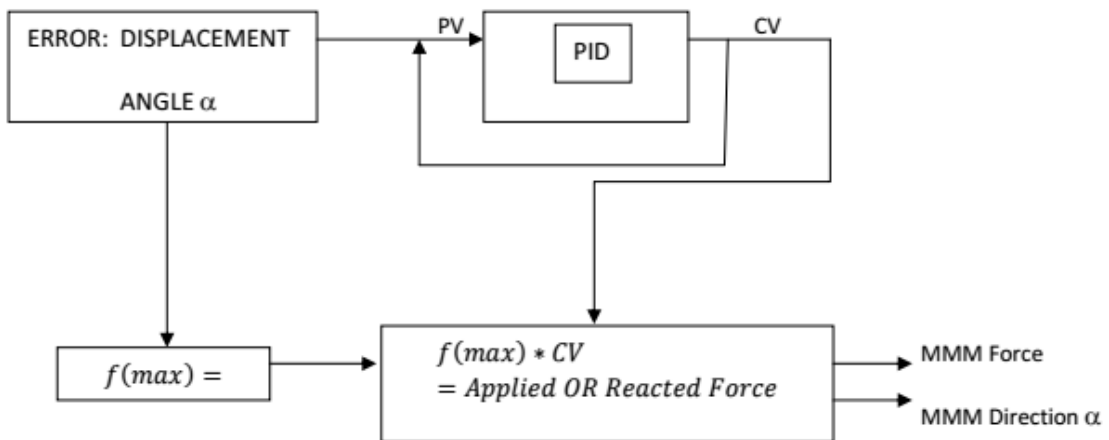


Figure 4.5 Control diagram MoorMaster™ (Cavotec MoorMaster Limited, 2012)

The error in displacement is the process variable, PV. It is run through a PID regulator, resulting in a control variable, CV. The definition of CV is given in Eq. 4.6.

$$CV = P \cdot error + I \cdot \int error dt + D \cdot \dot{error} \quad \text{Eq. 4.6}$$

P stands for proportional and is in a way the spring coefficient of the system. The proportional part of the control value ensures that as the error gets larger, the reaction force also gets larger and vice versa.

The I represents the integrate part and it is considered with the inertia of the system. The longer an error occurs, the larger the reaction force to make it disappear. The integrator is necessary to eliminate steady state error, which would occur in cases such as a current or strong wind forces. In this thesis, the correction of a steady state error is not of concern. If without a steady state force the P and D controller are able to control the system, an integral controller can always be added to solve a steady state force. Therefore, the integral control will be left out in the model.

The damping of the system is determined by D, which stands for differentiate. If the change in error is large, i.e. if the ship is moving fast, the reaction force will be larger than when the speed of change in error is only small.

The maximum force multiplied by the control variable is applied in the direction of α , see Eq. 4.7. To prevent forces larger than the maximum force, the control variable has a maximum of 1. If Eq. 4.6 results in a higher number than 1, the CV is set to 1.

$$F = CV \cdot F_{max}(\alpha) \quad \text{Eq. 4.7}$$

4.3. MOORMASTER™ UNITS: CALCULATE ANGLE AND POSITION ERROR

The maximum force a MoorMaster™ unit can exert is dependent on the angle it is in. Therefore, this angle needs to be calculated. A yaw angle of the vessel will result in an extra surge and sway displacement for a unit placed on a certain position on the hull of the vessel. Thus, the error in displacement of a single unit is not only dependent on the surge and sway position of the vessel, but also on the yaw angle and position of the vessel. This paragraph shows the calculations to determine the angle and displacement error of any MoorMaster™ unit.

Without yaw, the angle α and position errors e_x and e_y of the MoorMaster™ units can be defined by Eq. 4.8 - Eq. 4.10. Also see Figure 4.6.

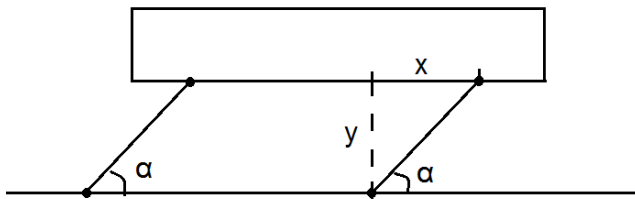


Figure 4.6 Angle of units without yaw

$$e_x = x \quad \text{Eq. 4.8}$$

$$e_y = y \quad \text{Eq. 4.9}$$

$$\angle \alpha = \tan^{-1} \left(\frac{y}{x} \right) \quad \text{Eq. 4.10}$$

Where y is the sway position of the vessel and x the surge position of the vessel. If x is 0, α is 90 degrees.

When introducing yaw, the angle and error of a single unit is dependent on the position it holds on the ship. Starting from a certain surge and sway position, adding yaw adds an additional x and y displacement to each unit, see Eq. 4.11, Eq. 4.12 and Figure 4.7.

$$e_x = x + x^* \quad \text{Eq. 4.11}$$

$$e_y = y + y^* \quad \text{Eq. 4.12}$$

Where x^* the extra surge displacement caused by yaw and y^* the extra sway displacement caused by yaw. x^* and y^* are defined by Eq. 4.13 and Eq. 4.14.

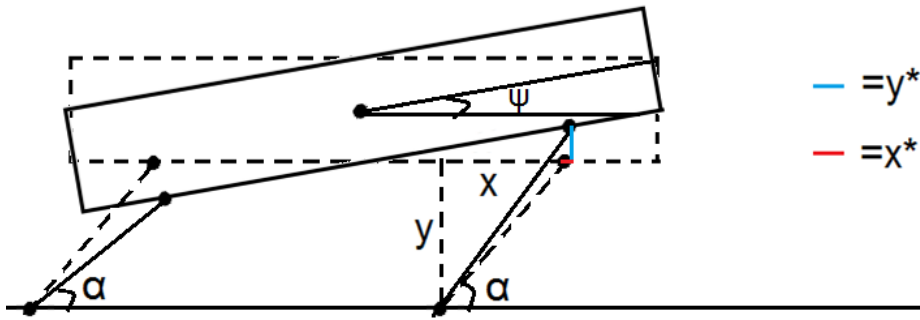


Figure 4.7 Angle of units with yaw

$$x^* = Pos \cdot (\cos(\psi) - 1) + \frac{1}{2}B \cdot \sin(\psi) \quad \text{Eq. 4.13}$$

$$y^* = Pos \cdot \sin(\psi) + \frac{1}{2}B \cdot (1 - \cos(\psi)) \quad \text{Eq. 4.14}$$

Where Pos is the position of the MoorMaster™ unit in x direction, measured from amidships and N is the yaw angle in degrees. Now the angle of a unit, measured in degrees, can be defined with surge, sway and yaw, Eq. 4.15.

$$\angle \alpha = \tan^{-1} \left(\frac{y + y^*}{x + x^*} \right) \quad \text{Eq. 4.15}$$

4.4. VERIFICATION: ONE DOF

In order to verify the model, first a simplified one DOF system, only surge, with one MoorMaster™ unit is looked at. The saturation of the control value, dependency of F_{max} on the angle, the external hydrodynamic force, added mass and the time delay are left out at this point. The equation of motion of a mass held with one MoorMaster™ unit would be:

$$m \cdot \ddot{x} - d \cdot F_{max} \cdot \dot{x} - p \cdot F_{max} \cdot x = 0 \quad \text{Eq. 4.16}$$

To solve this equation, Laplace transforms are used. The Laplace transform of the derivative of a function is given in Eq. 4.17.

$$\mathcal{L}\{f^{(n)}(t)\} = s^n \mathcal{L}\{f\} - \sum_{i=1}^n s^{n-i} f^{(i-1)}(0) \quad \text{Eq. 4.17}$$

Transforming the equation of motion gives Eq. 4.18 - Eq. 4.21:

$$\mathcal{L}\{x\} = X \quad \text{Eq. 4.18}$$

$$m \cdot (s^2 X - s \cdot x(0) - \dot{x}(0)) - d \cdot F_{max} \cdot (sX - x(0)) - p \cdot F_{max} \cdot X = 0 \quad \text{Eq. 4.19}$$

$$(m \cdot s^2 - d \cdot F_{max} \cdot s - p \cdot F_{max}) \cdot X = m \cdot s \cdot x(0) + m \cdot \dot{x}(0) - d \cdot F_{max} \cdot x(0) \quad \text{Eq. 4.20}$$

$$X = \frac{(m \cdot s - d \cdot F_{max}) \cdot x(0) + m \cdot \dot{x}(0)}{m \cdot s^2 - d \cdot F_{max} \cdot s - p \cdot F_{max}} \quad \text{Eq. 4.21}$$

This is solved in two separate parts, Eq. 4.22 and Eq. 4.23.

Part 1

$$\frac{x(0) \cdot (m \cdot s - d \cdot F_{max})}{m \cdot s^2 - d \cdot F_{max} \cdot s - p \cdot F_{max}} \quad \text{Eq. 4.22}$$

Part 2

$$\frac{m \cdot \dot{x}(0)}{m \cdot s^2 - d \cdot F_{max} \cdot s - p \cdot F_{max}} \quad \text{Eq. 4.23}$$

First part 1 is solved, Eq. 4.24 - Eq. 4.32:

$$x(0) \cdot \frac{s - \frac{d \cdot F_{max}}{m}}{s^2 - \frac{d \cdot F_{max}}{m} \cdot s - \frac{p \cdot F_{max}}{m}} \quad \text{Eq. 4.24}$$

This can be rewritten, Eq. 4.27 - Eq. 4.31, to fit the Laplace transforms of Eq. 4.25 and Eq. 4.26:

$$\mathcal{L}\{e^{\alpha t} \cdot \cos(bt)\} = \frac{s - \alpha}{(s - \alpha)^2 + \beta^2} = \frac{s - a}{s^2 - 2\alpha \cdot s + \alpha^2 + \beta^2} \quad \text{Eq. 4.25}$$

$$\mathcal{L}\{e^{\alpha t} \cdot \sin(bt)\} = \frac{\beta}{(s - \alpha)^2 + \beta^2} = \frac{\beta}{s^2 - 2\alpha \cdot s + \alpha^2 + \beta^2} \quad \text{Eq. 4.26}$$

$$-2\alpha = -\frac{d \cdot F_{max}}{m} \quad \text{Eq. 4.27}$$

$$\alpha = \frac{d \cdot F_{max}}{2 \cdot m} \quad \text{Eq. 4.28}$$

$$\alpha^2 + \beta^2 = -\frac{p \cdot F_{max}}{m} \quad \text{Eq. 4.29}$$

$$\beta = \sqrt{-\frac{p \cdot F_{max}}{m} - \frac{d^2 \cdot F_{max}^2}{4 \cdot m^2}} \quad \text{Eq. 4.30}$$

$$x(0) \cdot \frac{s - \frac{d \cdot F_{max}}{m}}{s^2 - \frac{d \cdot F_{max}}{m} \cdot s - \frac{p \cdot F_{max}}{m}} = x(0) \cdot \frac{s - 2\alpha}{(s - \alpha)^2 + \beta^2} \quad \text{Eq. 4.31}$$

The solution of part 1 is given by Eq. 4.32:

$$x_{part1} = x(0) \cdot e^{\alpha t} \cdot \cos(\beta t) - x(0) \cdot \frac{\alpha}{\beta} \cdot e^{\alpha t} \cdot \sin(\beta t) \quad \text{Eq. 4.32}$$

With α and β as in Eq. 4.28 and Eq. 4.30.

Then part 2, Eq. 4.33, is solved:

$$\frac{\dot{x}(0)}{s^2 - \frac{d \cdot F_{max}}{m} \cdot s - \frac{p \cdot F_{max}}{m}} \quad \text{Eq. 4.33}$$

This can be rewritten to fit Laplace transform of Eq. 4.34:

$$\frac{\dot{x}(0)}{s^2 - \frac{d \cdot F_{max}}{m} \cdot s - \frac{p \cdot F_{max}}{m}} = \frac{\dot{x}(0)}{b} \cdot \frac{\beta}{(s - \alpha)^2 + \beta^2} \quad \text{Eq. 4.34}$$

The solution of part 2 is given by Eq. 4.35:

$$x_{part2} = \frac{\dot{x}(0)}{\beta} \cdot e^{\alpha t} \cdot \sin(\beta t) \quad \text{Eq. 4.35}$$

With α and β as in Eq. 4.28 and Eq. 4.30

The total solution of the equation of motion is written in Eq. 4.36 and Eq. 4.37:

$$x(t) = x(0) \cdot e^{\alpha t} \cdot \cos(\beta t) - x(0) \cdot \frac{\alpha}{\beta} \cdot e^{\alpha t} \cdot \sin(\beta t) + \frac{\dot{x}(0)}{\beta} \cdot e^{\alpha t} \cdot \sin(\beta t) \quad \text{Eq. 4.36}$$

$$x(t) = x(0) \cdot e^{\alpha t} \cdot \cos(bt) + \left(\frac{\dot{x}(0)}{b} - x(0) \cdot \frac{\alpha}{b} \right) \cdot e^{\alpha t} \cdot \sin(bt) \quad \text{Eq. 4.37}$$

With α and β as in Eq. 4.28 and Eq. 4.30.

The solution consist of a cosine and a sine element, dampened by a natural exponential function. To guaranty a stable system, α has to be negative, meaning d has to be negative. To prevent an imaginary frequency, the number under the square root in β should be positive, thus p should also be negative.

The frequency of the system is equal to $\frac{\beta}{2\pi}$. This means an increase in the absolute value of p means an increase in frequency and an increase in the absolute value of d will result in a decrease of frequency. The damping of the system is reliant on α . A larger negative number will result in more dampened system. An increase in the absolute value of d should result in a more dampened system.

A simple scenario is chosen to verify the model: a mass of $1 \cdot 10^6 kg$, a maximum force of $1 \cdot 10^5 N$. Figure 4.8 shows a calculation with $p=d=-0.5$. Doubling the d value, should result in a more dampened system. Figure 4.9 confirms this. Doubling p should result in an increased frequency, which Figure 4.10 shows. Doubling of both p and d is shown in Figure 4.11.

Even though Laplace is very convenient for simple differential equation systems, as the model increases in size and complexity this method will not be practical anymore. Therefore the ODE45 function of Matlab is used to solve the differential equation. As can be seen in Figure 4.12, the ODE45 function gives the exact same results as the Laplace method.

Since the external force on the system will be different for each time step and the MoorMaster™ units have a 0.2 second time delay, for each time step a new system of equations is solved. The next step of the verification is to do an ODE45 calculation for each time step separately. This still gives the exact same results.

The final step is to calculate the force of each time step separately, instead of incorporating it in the differential equation. In this step, the 0.2 second time delay can also be introduced. The 0.2 second time delay results in slightly higher amplitudes, as can be expected, see Figure 4.13.

The verified Matlab script of the one DOF model can be found in Appendix G.

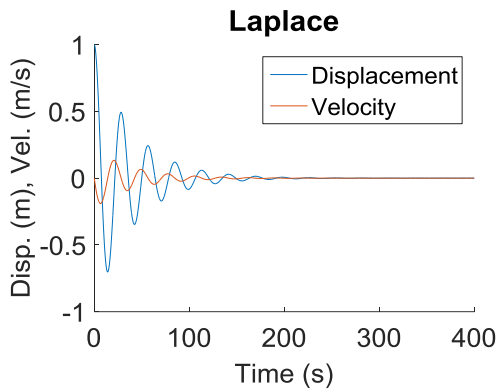


Figure 4.8 Laplace calculation of one DOF system with $m=1 \cdot 10^6$ kg, $F_{max}=1 \cdot 10^5$ N, $x'(0)=0$ and $x(0) = 1$. $p=d=-0.5$

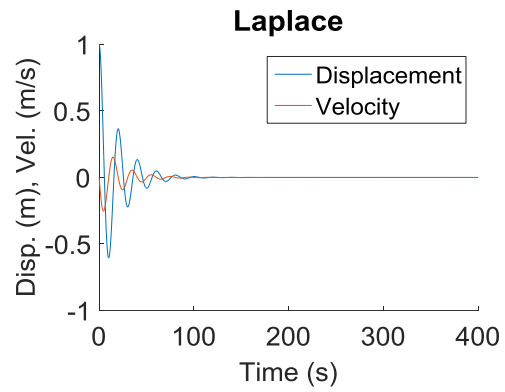


Figure 4.11 Laplace calculation of one DOF system with $m=1 \cdot 10^6$ kg, $F_{max}=1 \cdot 10^5$ N, $x'(0)=0$ and $x(0) = 1$. $p=d=-1.0$

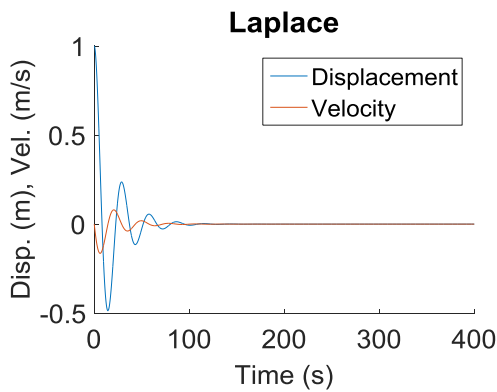


Figure 4.9 Laplace calculation of one DOF system with $m=1 \cdot 10^6$ kg, $F_{max}=1 \cdot 10^5$ N, $x'(0)=0$ and $x(0) = 1$. $p=-0.5$, $d=-1.0$

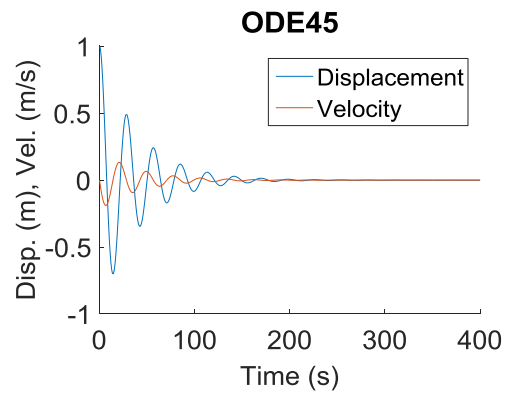


Figure 4.12 ODE45 calculation of one DOF system with $m=1 \cdot 10^6$ kg, $F_{max}=1 \cdot 10^5$ N, $x'(0)=0$ and $x(0) = 1$. $p=d=-0.5$

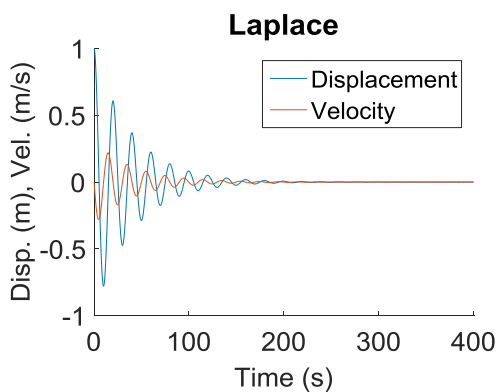


Figure 4.10 Laplace calculation of one DOF system with $m=1 \cdot 10^6$ kg, $F_{max}=1 \cdot 10^5$ N, $x'(0)=0$ and $x(0) = 1$. $p=-1.0$ $d=-0.5$

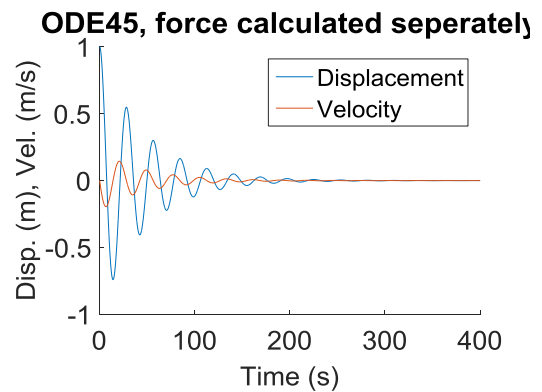


Figure 4.13 ODE45 calculation with 0.2 sec time delay of one DOF system with $m=1 \cdot 10^6$ kg, $F_{max}=1 \cdot 10^5$ N, $x'(0)=0$ and $x(0)=1$. $p=d=0.5$

4.5. VERIFICATION: TWO DOF

The next step is to extend the system to two degrees of freedom. A system with sway and yaw motions and two MoorMaster™ units is looked at. Eq. 4.38 and Eq. 4.39 show the equations of motion of the system with n MoorMaster™ units.

$$m \cdot \ddot{y} - F_{max} \cdot \sum_{i=1}^n p \cdot (y + y^{i*}) + d \cdot (\dot{y} + \dot{y}^{i*}) = 0 \quad \text{Eq. 4.38}$$

Where n is the number of MoorMaster™ units used, in this case two, and y^{i*} is the extra sway displacement caused by yaw, as given in Eq. 4.14.

$$I \cdot \ddot{\psi} - F_{max} \cdot \sum_{i=1}^n Pos_i \cdot [p \cdot (y + y^{i*}) + d \cdot (\dot{y} + \dot{y}^{i*})] = 0 \quad \text{Eq. 4.39}$$

Where Pos_i is the position of the MoorMaster™ units.

The expression for y^* as in Eq. 4.14 is complicated, therefore an approximation is used as in Eq. 4.40:

$$y^* = Pos \cdot \sin(\psi) \quad \text{Eq. 4.40}$$

To simplify this further, the approximation for small angles $\sin(\psi) \approx \psi$ is used. Figure 4.14 shows a comparison between the exact solution, the approximation and the further simplification. For this comparison a position of 50 meters forward of amidships is used, in order to get the maximum possible y^* for this ship. In reality the maximum forward position of a unit will be smaller, because the units attach to the parallel midship. For small angles up to approximately 0.2 radians, or 11.5 degrees, the approximation is close enough to the exact solution. The further simplification matches even better with the exact solution than the approximation. At an angle of 0.2 radians, the simplification has a 0.4% deviation from the exact solution.

This simplification is used, with the consequence that the model is only suitable for small angles up to about 11.5 degrees. However, since this would already mean an extra sway displacement of about 10 meters, it is safe to say this is not a problem for this situation. If the ship motions would get this big, the system would not be suitable for the situation anyway.

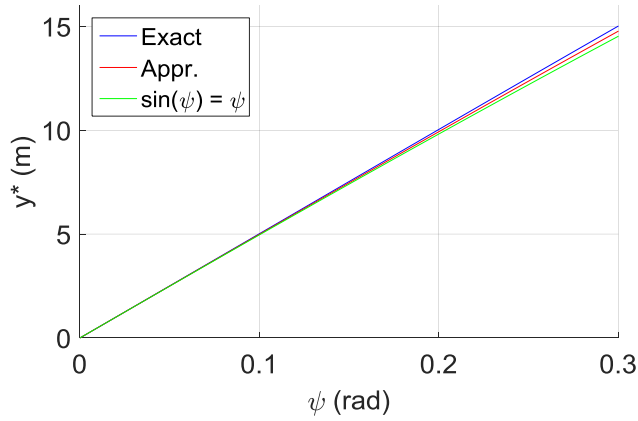


Figure 4.14 Comparison between exact calculation of y^* , approximation with Eq. 4.40 and further simplification with $\sin(\psi)=\psi$

First, Eq. 4.38 is solved. Using the simplification and a two unit system, Eq. 4.38 reduces to Eq. 4.41:

$$m \cdot \ddot{y} - 2 \cdot F_{max} \cdot (p \cdot y + d \cdot \dot{y}) - (F_{max} \cdot (Pos_1 + Pos_2)) \cdot (p \cdot \psi + d \cdot \dot{\psi}) = 0 \quad \text{Eq. 4.41}$$

The equation is solved using Laplace

$$\mathcal{L}\{y\} = Y \quad \text{Eq. 4.42}$$

$$\mathcal{L}\{\psi\} = \Psi \quad \text{Eq. 4.43}$$

Eq. 4.44 shows the Laplace transform of Eq. 4.41:

$$m \cdot (s^2 Y - s \cdot y(0) - \dot{y}(0)) - 2 \cdot F_{max} \cdot (d \cdot (sY - y(0)) + p \cdot Y) - (F_{max} \cdot (Pos_1 + Pos_2)) \cdot (p \cdot \Psi + d \cdot (s\Psi - \psi(0))) = 0 \quad \text{Eq. 4.44}$$

Which can be rewritten as Eq. 4.45.

$$Y = \frac{y(0) \cdot s + \dot{y}(0) - \frac{2 \cdot F_{max} \cdot d}{m} \cdot y(0) + \frac{F_{max}}{m} \cdot (Pos_1 + Pos_2) \cdot (p \cdot \Psi + d \cdot (s \cdot \Psi - \psi(0)))}{s^2 - \frac{2 \cdot F_{max} \cdot d}{m} \cdot s - \frac{2 \cdot F_{max} \cdot p}{m}} \quad \text{Eq. 4.45}$$

To improve readability, the constants κ , α_1 and β_1 are introduced, Eq. 4.46-Eq. 4.48:

$$\alpha_1 = \frac{d \cdot F_{max}}{m} \quad \text{Eq. 4.46}$$

$$\beta_1 = \sqrt{-\frac{2 \cdot p \cdot F_{max}}{m} - \frac{d^2 \cdot F_{max}^2}{m^2}} \quad \text{Eq. 4.47}$$

$$\kappa = \frac{F_{max}}{m} \cdot (Pos_1 + Pos_2) \quad \text{Eq. 4.48}$$

Again, the equation will be solve in two parts, Eq. 4.49 and Eq. 4.51.

$$Y_1 = y(0) \cdot \frac{s + \frac{\dot{y}(0)}{y(0)} - 2\alpha_1}{(s - \alpha)^2 + \beta_1^2} \quad \text{Eq. 4.49}$$

The solution of the first part is given in Eq. 4.50:

$$y_1 = y(0) \cdot e^{\alpha_1 t} \cdot \cos(\beta_1 t) + \left(\frac{\dot{y}(0) - \alpha_1 \cdot y(0)}{\beta_1} \right) \cdot e^{\alpha_1 t} \cdot \sin(\beta_1 t) \quad \text{Eq. 4.50}$$

With α and β as in Eq. 4.46 and Eq. 4.47 and κ as in Eq. 4.48

Next, the second part of the first equation of motion is solved:

$$Y_2 = \frac{\kappa \cdot (p \cdot \Psi + d \cdot (s \cdot \Psi - \psi(0)))}{(s - \alpha_1)^2 + \beta_1^2} \quad \text{Eq. 4.51}$$

The Laplace transform given in Eq. 4.52 is used to solve this

$$\mathcal{L} \left\{ \int_0^t f(t - \tau) \cdot g(\tau) d\tau \right\} = F(s) \cdot G(s) \quad \text{Eq. 4.52}$$

The solution of the second part is given in Eq. 4.53:

$$y_2 = \frac{\kappa \cdot p}{\beta_1} \int_0^t \psi(\tau) \cdot e^{\alpha_1(t-\tau)} \cdot \sin(\beta_1(t-\tau)) d\tau$$

$$+ \frac{\kappa \cdot d}{\beta_1} \cdot \int_0^t \dot{\psi}(\tau) \cdot e^{\alpha_1(t-\tau)} \cdot \sin(\beta_1(t-\tau)) d\tau$$

Eq. 4.53

With α , β and κ as in Eq. 4.46, Eq. 4.47 and Eq. 4.48.

The total solution to the equation of sway is given in Eq. 4.54:

$$y(t) = y(0) \cdot e^{\alpha_1 t} \cdot \cos(\beta_1 t) + \left(\frac{\dot{y}(0) - \alpha_1 \cdot y(0)}{\beta_1} \right) \cdot e^{\alpha_1 t} \cdot \sin(\beta_1 t)$$

$$+ \frac{\kappa \cdot p}{\beta_1} \int_0^t \psi(\tau) \cdot e^{\alpha_1(t-\tau)} \cdot \sin(\beta_1(t-\tau)) d\tau$$

$$+ \frac{\kappa \cdot d}{\beta_1} \cdot \int_0^t \dot{\psi}(\tau) \cdot e^{\alpha_1(t-\tau)} \cdot \sin(\beta_1(t-\tau)) d\tau$$

Eq. 4.54

With α , β and κ as in Eq. 4.46, Eq. 4.47 and Eq. 4.48.

Now the equation of yaw is solved, Eq. 4.55.

$$I \cdot \ddot{N} - F_{max} \cdot Pos_1 \cdot \left(p \cdot (y + Pos_1 \cdot \psi) + d \cdot (\dot{y} + Pos_1 \cdot \dot{\psi}) \right)$$

$$- F_{max} \cdot Pos_2 \cdot \left(p \cdot (y + Pos_2 \cdot \psi) + d \cdot (\dot{y} + Pos_2 \cdot \dot{\psi}) \right) = 0$$

Eq. 4.55

Which can be rewritten as Eq. 4.56:

$$I \cdot \ddot{\psi} - F_{max} \cdot (Pos_1 + Pos_2) \cdot (p \cdot y + d \cdot \dot{y}) - F_{max} \cdot (Pos_1^2 + Pos_2^2) \cdot (p \cdot \psi + d \cdot \dot{\psi}) = 0$$

Eq. 4.56

The Laplace transform of Eq. 4.56 is stated in Eq. 4.57:

$$I \cdot (s^2 \cdot \mu - s \cdot \psi(0) - \dot{\psi}(0)) - F_{max} \cdot (Pos_1 + Pos_2) \cdot (p \cdot Y + d \cdot (s \cdot Y - y(0))) - F_{max}$$

$$\cdot (Pos_1^2 + Pos_2^2) \cdot (p \cdot \Psi + (d \cdot s \cdot \Psi - \psi(0)))$$

Eq. 4.57

Similarly to the equation for sway, this is solved. The solution is shown in Eq. 4.58:

$$\begin{aligned} \psi(t) = & \psi(0) \cdot e^{\alpha_2 t} \cdot \cos(\beta_2 t) + \left(\frac{\dot{\psi}(0) - \alpha_2 \cdot \psi(0)}{\beta_2} \right) \cdot e^{\alpha_2 t} \cdot \sin(\beta_2 t) \\ & + \frac{R \cdot p}{\beta_2} \int_0^t y(\tau) \cdot e^{\alpha_2(t-\tau)} \cdot \sin(\beta_2(t-\tau)) d\tau \\ & + \frac{R \cdot d}{\beta_2} \cdot \int_0^t y(\tau) \cdot e^{\alpha_2(t-\tau)} \cdot \sin(\beta_2(t-\tau)) d\tau \end{aligned} \quad \text{Eq. 4.58}$$

With Q and R as in Eq. 4.59 and Eq. 4.60 and α and β as in Eq. 4.61 and Eq. 4.62.

$$Q = \frac{F_{max} \cdot (Pos_1^2 + Pos_2^2)}{I} \quad \text{Eq. 4.59}$$

$$R = \frac{F_{max} \cdot (Pos_1 + Pos_2)}{I} \quad \text{Eq. 4.60}$$

$$\alpha_2 = \frac{Q \cdot d}{2} \quad \text{Eq. 4.61}$$

$$\beta_2 = \sqrt{-Q \cdot p - \frac{Q^2 \cdot d^2}{4}} \quad \text{Eq. 4.62}$$

As with the one DOF case, a simple scenario is chosen to test the system: a mass of $1 \cdot 10^6 kg$, a moment of inertia of $3 \cdot 10^9 m^4$ and a maximum force of $1 \cdot 10^5 N$. The same steps are taken to extend the model: using ODE45 Matlab function instead of Laplace method, calculating differential equation per time step, using saturation to prevent forces larger than Fmax and finally calculating the force separately introducing a time delay of 0.2 sec. When using ODE45 and calculating the force separately, the exact y^* is used, instead of the approximation. Figure 4.15 - Figure 4.18 show the results for both the Laplace method as well as the ODE45 function with the force calculated separately with a 0.2 second time delay. The Matlab script of the two DOF sway and yaw model can be found in Appendix H.

The same can be done for surge and yaw. The Matlab script and results of the two DOF surge and yaw model can be found in Appendix I. In case of surge and yaw, it is clearly visible that the yaw angle settles at a non-zero value. If one zooms in on the surge plot, it can be seen that surge actually settles at a non-zero value as well. At this angle, the extra x displacement caused by the yaw angle, x^* equals the negative of the current surge displacement. Therefore, all units have a zero x-error. This effect is caused by the fact that the units can only push and pull on one side of the turning point, whereas with sway and yaw, there would be one unit on each side of the turning point.

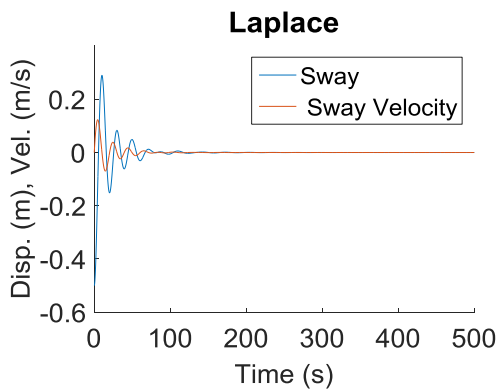


Figure 4.15 Sway Laplace calculation of two DOF sway and yaw system with $m=1*10^6$ kg, $I=3*10^9$ m⁴, $F_{max}=1*10^5$ N, $y'(0)=N(0)=0$ and $y(0)=-0.5$ and $N(0)=0.001$ rad. $p=d=-0.5$

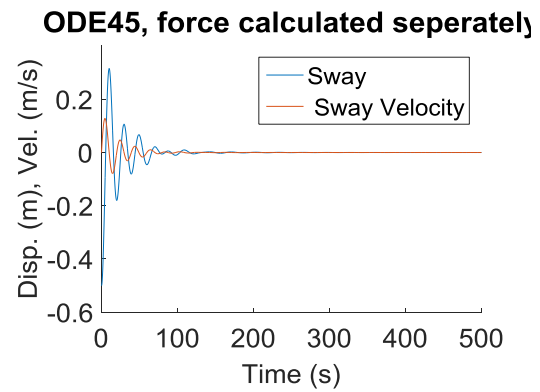


Figure 4.17 Sway ODE45 calculation with 0.2 sec time delay of two DOF sway and yaw system with $m=1*10^6$ kg, $I=3*10^9$ m⁴, $F_{max}=1*10^5$ N, $y'(0)=N(0)=0$ and $y(0)=-0.5$ and $N(0)=0.001$ rad. $p=d=-0.5$

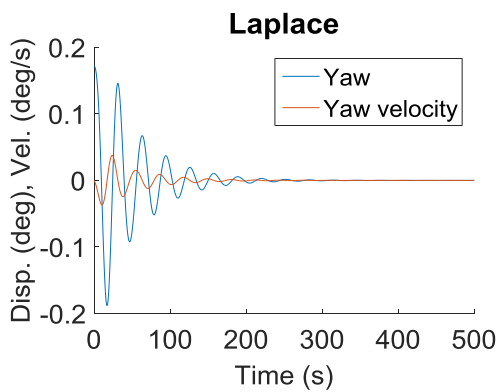


Figure 4.16 Yaw Laplace calculation of two DOF sway and yaw system with $m=1*10^6$ kg, $I=3*10^9$ m⁴, $F_{max}=1*10^5$ N, $y'(0)=N(0)=0$ and $y(0)=-0.5$ and $N(0)=0.001$ rad. $p=d=-0.5$

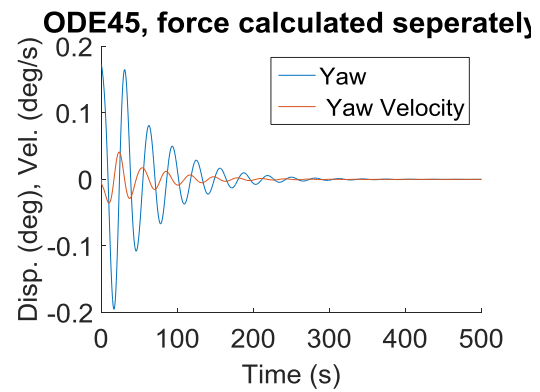


Figure 4.18 Yaw ODE45 calculation with 0.2 sec time delay of two DOF sway and yaw system with $m=1*10^6$ kg, $I=3*10^9$ m⁴, $F_{max}=1*10^5$ N, $y'(0)=N(0)=0$ and $y(0)=-0.5$ and $N(0)=0.001$ rad. $p=d=-0.5$

When looking at a two degrees of freedom system of surge and sway, the equations of motion get more complicated. The force of a MoorMaster™ unit is dependent on the total error in position, Eq. 4.63.

$$F_{unit} = F_{max} \cdot (p \cdot e + d \cdot \dot{e}) \quad \text{Eq. 4.63}$$

With the error e defined in Eq. 4.64

$$e = \sqrt{(x + x^*)^2 + (y + y^*)^2} \quad \text{Eq. 4.64}$$

With y^* and x^* as defined in paragraph 4.3, Eq. 4.13 and Eq. 4.14. The equations of motion are given in Eq. 4.65 and Eq. 4.66:

$$m \cdot \ddot{x} = \sum_{i=1}^n F_{unit,i} \cdot \cos(\alpha_i) \quad \text{Eq. 4.65}$$

$$m \cdot \ddot{y} = \sum_{i=1}^n F_{unit,i} \cdot \sin(\alpha_i) \quad \text{Eq. 4.66}$$

This is the point where the Laplace method is no longer an easy method to verify the Matlab functions. The Matlab script and results of the two DOF surge and sway model can be found in Appendix J. Given the comparison with the other two DOF systems and the one DOF system, it is safe to say the ODE45 function is also correct in this scenario.

4.6. VERIFICATION: THREE DOF

Cavotec advised that in a configuration of equispaced units, the central units are often in-effectively unutilised, while the fore and aft most units are easily overloaded. This can be solved by assigning the central units to purely control surge and the end units to purely control sway. This configuration is recommended by Cavotec when using a equispaced set-up.

This way, the three DOF model becomes a combination of the several, already verified, two DOF models. Units that are assigned to correct sway motion follow the sway and yaw two DOF model while units that are assigned to correct surge motion follow the surge and yaw two DOF model. The yaw equation of motion is a combination of the two, Eq. 4.67.

$$I \cdot \ddot{\psi} = \sum_{i=1}^n \left(\frac{1}{2} \cdot B - y^{i*} \right) \cdot F_{unit,i} \cdot \cos(\alpha_i) + \sum_{i=1}^n (Pos_i + x^{i*}) \cdot F_{unit,i} \cdot \sin(\alpha_i) \quad \text{Eq. 4.67}$$

Where α_i is 0 in case of a surge correcting unit and $\alpha_i = \frac{\pi}{2}$ in case of a sway correcting unit.

In order to model equispaced groups of units, the maximum force at a certain position is simply multiplied by the number of units in the group.

The Matlab script and results of a simple scenario can be found in Appendix K. As can be seen in the results, the issue with the remaining yaw angle in the surge and yaw two DOF model is solved by the sway correcting units.

So far, only simple scenarios are shown. The next step is applying the model to the case study, which requires the added mass matrix with coupling terms. The added mass matrix is incorporated in the differential equation function, see Appendix L. Also, the input parameters of the Large Rhine Vessel are implemented.

The final step before the PID settings can be set and results can be seen, is to apply the external force of the passing vessels. The data gathered with Ropes is imported and applied to the system. Appendix L shows the Matlab script and results for one case.

4.7. UNIT CONFIGURATION AND PD SETTING

There are many different configurations of MoorMaster™ units possible. One could for example work with equispaced single units or equispaced groups of units.

To determine a suitable configuration, the scenario with the highest external forces is looked at. This is the scenario with the 4 barge pushed convoy passing at a minimal distance. In this scenario there is a surge force amplitude of approximately 560 kN and a sway force amplitude of approximately 150 kN. To withstand these forces, six surge correcting units and one sway correcting unit are required, considering the maximum forces of a single unit. However, with only one sway correcting unit, the yaw angle would be difficult to correct, thus two sway correcting units is a minimum.

Considering the length of the parallel midship of the Large Rhine vessel, the chosen configuration is:

- two single sway correcting units at the outer ends of the midship
- three groups of two surge correcting units, equispaced between the sway correcting units.

Resulting in a total of eight MoorMaster™ units.

There are many algorithms to preliminary set a PD controller, however in practice, manual adjusting is almost always necessary (Cool, et al., 1979). The tuning algorithms are beyond the scope of this thesis, therefore the PD settings are tuned manually. If P and D are adjusted, using the maximum force scenario described above, until the ship motions are within the operational criteria limits, the result is a P of -5.0 and a D of -3.0.

4.8. VALIDATION OF SHIP MOTION MODEL

Though the programmed models of the reaction forces and ship motions are verified (the outcome is logical), they are not validated. It is recommended to validate the model, although this is outside the scope of this research. To validate the results of the calculations, two options are possible. The outcome of the model can be compared to full scale measurements or model tests can be performed. This paragraph shows suggestions how to validate the model.

4.8.1. FULL SCALE MEASUREMENTS

Cavotec is in possession of full scale measurement data. However, due to legal obligations they are unable to share this information at the moment. If in the future this data becomes available, it can be used to validate the model.

4.8.2. MODEL TESTS

To validate the physical model as well as the combination of Ropes with the physical model, a series of possible model tests are proposed.

First the tests to validate the physical model itself are described, then the tests to validate the combination with Ropes is explained.

4.8.2.1. TEST SET-UP

The profile of the ARK and the quay is built to scale in the tank. The moored vessel is secured with attached movable arms, containing force measuring devices and actuators. A second vessel is pulled past the moored vessel.

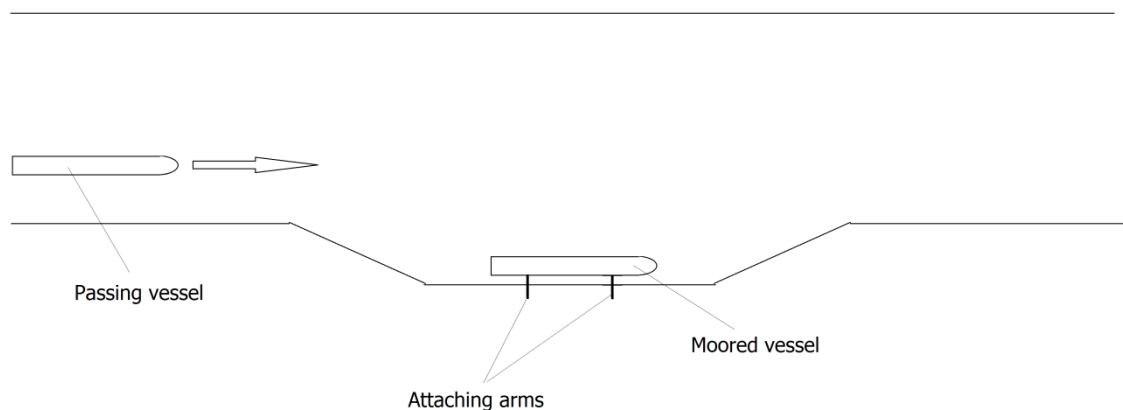


Figure 4.19 Test set-up

The testing consists of two parts, generating the input and output of the physical model.

VALIDATING PHYSICAL MODEL

First the forces acting on the vessel caused by a passing vessel are measured, to create input for the physical model. The moored vessel is restrained and the exciting forces are measured using force measuring devices.

Second the ship is no longer restrained, but the arms will work similar to the full scale mooring system. This will be explained later in this paragraph. The same vessel as used in the first test is pulled past at the same conditions. The motions of the arms are registered and compared to the output of the physical model.

The arms are attached in the same configuration as the full scale mooring system. The forces acting on them will be measured and then run through a PID regulator with the same settings as in the physical model. The forces dictated by the PID regulator will be fed to the actuators in the moving arms. The difference with the full scale mooring system is that this system does not work with vacuum pads. An error should be produced if the forces exceed the scaled maximum forces of the MoorMasterTM units. To restrain the vessel, the PID values should simply be set to zero.

VALIDATING COMBINATION WITH ROPES

The combination with ropes can be tested by simulating the run done in the model tests with Ropes and using the output of Ropes as the input of the physical model. The output of the physical model is again compared to the motions of the model test vessel.

A simpler version of the tests would be to use a straight channel with no incline at the bottom instead of the ARK profile. This simplifies the test set-up greatly, however it cannot be validated whether the influence of the harbour geometry is modelled correctly.

4.9. SUMMARY MODELING MOORED VESSEL

In this chapter, a model is written to determine the reaction forces of the MoorMaster™ units and the resulting ship motions. The model is also verified.

4.9.1. PHYSICAL MODEL SHIP MOTIONS

The equation of motion of a vessel theoretically consists of four parts:

- The mass and added mass times the acceleration
- The retardation function, representing damping, times the velocity
- The hydrostatic spring coefficient times the displacement
- The external forces

The retardation and added mass are dependent on the frequency of the motions. The studied situation in this thesis consists of very low frequency motions. Therefore the damping of the ship will be neglected. The added mass can be considered constant at these low frequencies. To determine the added mass, the vessel is run through Delfrac, a 3-D diffraction program developed at the Delft University of Technology. Of course the MoorMaster™ units do introduce damping to the system. Since the MoorMaster™ units only produce forces in the horizontal plane and the horizontal motions are expected to be the most critical, only the motions in the horizontal plane will be considered: surge, sway and yaw. The hydrostatic spring coefficient is only relevant for vertical motions and zero for non-vertical motions. The equation of motion is based on the manoeuvring model, see Eq. 4.2.

F_{ext} is the external force acting on the ship, consisting of the hydrodynamic force caused by the passing vessel and the applied force by the MoorMaster™ units, see Eq. 4.4. The external hydrodynamic force is modelled with the output from the Ropes simulations.

4.9.2. PHYSICAL MODEL MOORMASTER™ UNITS

The forces acting on the ship result in a certain offset from the neutral position of a MoorMaster™ unit. This offset is translated into an error in x direction and an error in y direction. The MoorMaster™ unit responds to the error in displacement with a reaction force, with the aim of getting the unit, and thus ship, back in the neutral position. The extra displacement of a unit caused by the yaw angle of the vessel is described in Eq. 4.13 and Eq. 4.14. The magnitude and angle of the force of a single unit are determined by Eq. 4.5-Eq. 4.7.

Paragraphs 4.4-4.6 show the verification of the model, in steps from 1 DOF to the full 3 DOF model.

To determine a suitable configuration, the scenario with the highest external forces is looked at. To withstand these forces and considering the length of the parallel midship of the Large Rhine vessel, the chosen configuration is:

- two single sway correcting units at the outer ends of the midship
- three groups of two surge correcting units, equispaced between the sway correcting units.

Resulting in a total of eight MoorMaster™ units.

The PD settings are tuned manually. If P and D are adjusted, using the maximum force scenario described above, until the ship motions are within the operational criteria limits, the result is a P of -5.0 and a D of -3.0.

Paragraph 4.8 shows recommendations to validate the model.

5. CONSTRUCTION CALCULATION

To assess the suitability of the mooring system, it is essential to determine whether the construction of an inland vessel can cope with the loads of the mooring system. In previous chapters the forces and configuration of the MoorMaster™ units are determined. In this chapter, it is explained how these forces are used to calculate the stress on the hull of a case study vessel, a "Damen Riverliner 1145E". The results of the construction calculation are displayed in chapter 6, along with the other results.

The maximum force one unit will exert on the hull is 100 kN in surge direction or 200 kN in sway direction. The surface of one suction pad is assumed to be 2 m², based on drawings of the units and the statement of Cavotec that the pressure exerted on the hull is never more than 1 atmosphere. Based on the drawings, the dimensions are assumed to be approximately 1.60x1.25 m.

The yield strength of the most common steel used in the construction of ships is 235 MPa. However, the load of the MoorMaster™ units is not the only source of stress in the ships side hull. Lloyd's rules state that the permissible stress due to longitudinal bending is 137 MPa. The permissible combined stress, being the sum of stresses due to longitudinal bending and local loading, is 177 MPa (Lloyd's Register Group Limited, 2016). This would mean a 25% safety margin on the 235 MPa yielding stress.

It is beyond the scope of this research to calculate the longitudinal bending moment stress and identify the other local loadings. This is different for most vessels, not a single value can be calculated to suit every Large Rhine vessel. What is done, is a basic level calculation for an example ship, determining the stresses caused by the MoorMaster™ units. If the stress caused by the MoorMaster™ units combined with the global bending stress and other local loadings is below 177 MPa, there should be no structural problems.

5.1. BASIC CASE STUDY CALCULATION LOAD IN SWAY DIRECTION

Lloyd's rules for inland shipping dictate that the frame spacing for a 109.95 m dry cargo inland vessel should be 500-640 mm. The corresponding side shell plate thickness is 8 mm for a 500 mm frame spacing, or 9.5 mm for a 640 mm frame spacing. (Lloyd's Register Group Limited, 2016).

First, a calculation for a load in sway direction is performed. Some assumptions have to be made considering the construction of the vessel. The construction of a dry cargo vessel, a "Damen Riverliner 1145E", is used as a case study. Figure 5.1 shows the cross section of the cargo hold.

The thickness of the side shell plating of the case study ship is 9mm. The ship has a transverse frame spacing of 500mm. The transverse stiffeners used are 140x8 bulb flats. Apart from these stiffeners, two t-shape profiles are used as longitudinal stiffeners. The estimated dimensions of the cross section of the longitudinal stiffeners is shown in Figure 5.2. The longitudinal stiffeners are estimated from Figure 5.1 to be at a height of 2000 and 2800 mm from the bottom of the ship. The longest unsupported length, in height direction, is 1250mm, between the bilge bracket and the lowest longitudinal stiffener.

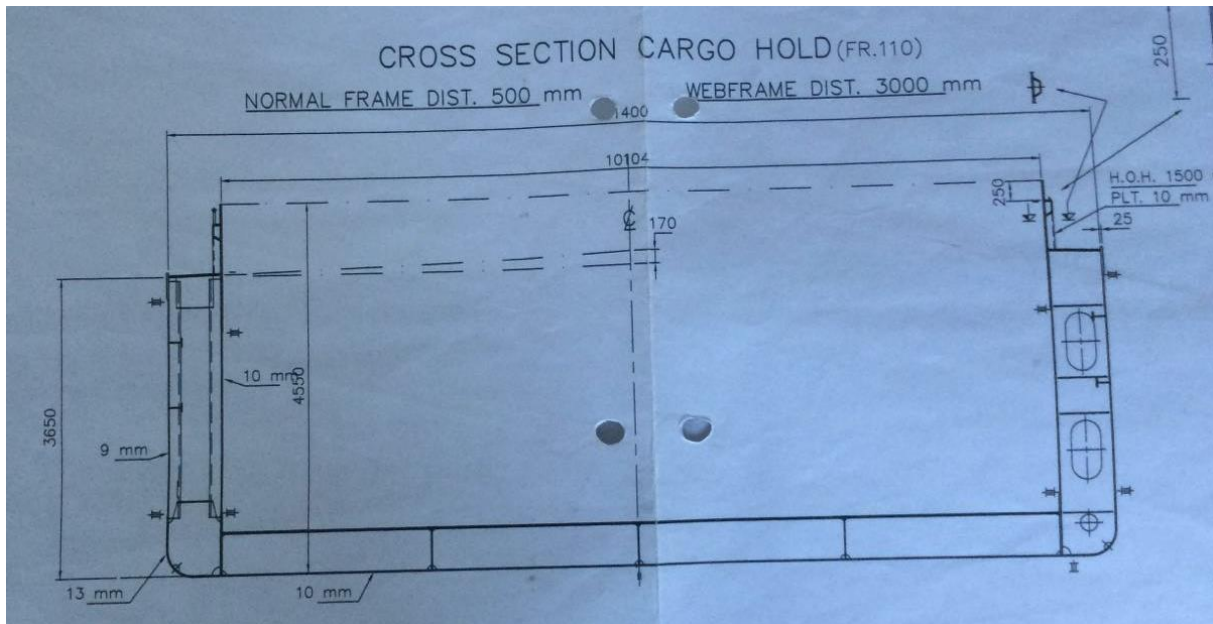


Figure 5.1 Cross section of cargo hold of "Damen Riverliner 1145E"

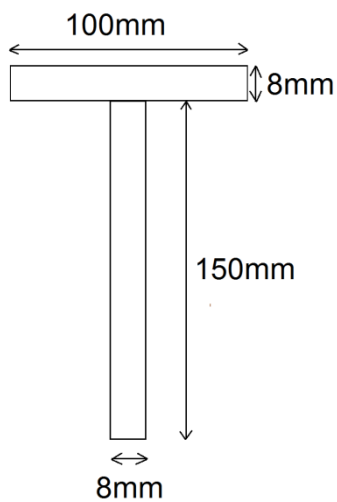


Figure 5.2 Estimated cross section of longitudinal stiffeners of "Damen Riverliner 1145E"

The construction calculations are performed using an FEM software package, 'ANSYS'. The Ansys script file can be found in Appendix N. The side shell plating and the t-shape stiffener are modelled as plates using shell elements. The bulb flats are modelled as a beam element with the characteristics of the 140x8 bulb flats, with an offset from the mid plane of the plate. Some estimations are made considering characteristics of the bulb flats, such as the warping constant. After having run some variations of these constants, it was confirmed that they have little to no effect on the results.

The top and bottom of the plate are simply supported and on the sides symmetry restrictions are applied. A load of 100 kN/m^2 is applied to the surface of the plate.

5.1.1. VERIFICATION OF ANSYS MODEL

Basic hand calculations are performed to verify the Ansys model, using only the plate and bulb flat profile.

To calculate the stress in the steel plate, Eq. 5.1 is used.

$$\sigma = \frac{M \cdot y}{I} \quad \text{Eq. 5.1}$$

With σ the stress at a certain point in the plate, M the occurring bending moment at that point, y the distance from the neutral axis and I the moment of inertia around the neutral axis. To determine the maximum stress, the maximum occurring moment, the maximum distance from the neutral axis and the moment of inertia around the neutral axis need to be calculated.

First, the neutral axis of the plate plus stiffener is calculated, using the effective plate width. The effective plate width of a plate attached to secondary stiffeners is determined by Lloyd's to be the greater of $40 \cdot t_p$, t_p being the plate thickness, or 600 mm, but never larger than the actual frame spacing.

This also results in the maximum distance to the neutral axis. Next, the moment of inertia around the neutral axis is determined, also using the effective plate width. The maximum occurring moment is calculated using Eq. 5.2, the maximum bending moment in a beam, simply supported at both ends:

$$M_{max} = \frac{Q \cdot l}{8} \quad \text{Eq. 5.2}$$

Where l is the length of the plate and Q is defined as in Eq. 5.3:

$$Q = q \cdot l \quad \text{Eq. 5.3}$$

With q defined as in Eq. 5.4:

$$q = p \cdot s \quad \text{Eq. 5.4}$$

With p the load in the structure in N/m^2 and s the stiffener spacing.

The hand calculation results in a maximum stress of 121.870 MPa, while the Ansys model, minus the t-shape stiffener, calculates a maximum stress of 119.746 MPa. The difference between the two methods is less than 2%.

5.2. BASIC CASE STUDY CALCULATION LOAD IN SURGE DIRECTION

For the loads in surge direction, Eq. 5.5 is used.

$$\sigma = \frac{F}{A} \quad \text{Eq. 5.5}$$

Where F is the total force exerted on the hull, 100 kN, and A is the surface of the intersection of the plate, $t \cdot h$, h being the height of the MoorMaster™ unit.

6. RESULTS

In chapter 3, the simulation of passing vessels is explained. This results in the forces acting on the moored vessel due to passing vessels. These forces are used to model the ship motions, in chapter 4. Chapter 5 describes the method used to calculate the stress on the hull caused by the MoorMaster™ units. In this chapter, the results of all three chapters are shown. First the forces on the moored vessel, the results from the Ropes simulations, are shown. Next, the resulting ship motions, the outcome of the ship motion model, are displayed. Last, the results from the construction calculations are shown.

6.1. ROPES SIMULATIONS

This paragraph shows and explains the results from Ropes. Surge and sway forces are focused on, because these are critical in mooring criteria.

In general, the Ropes computations result in smooth curves. However, when the passing distance is very small, some peaks arise in the surge force. This can be seen in Figure 6.1.

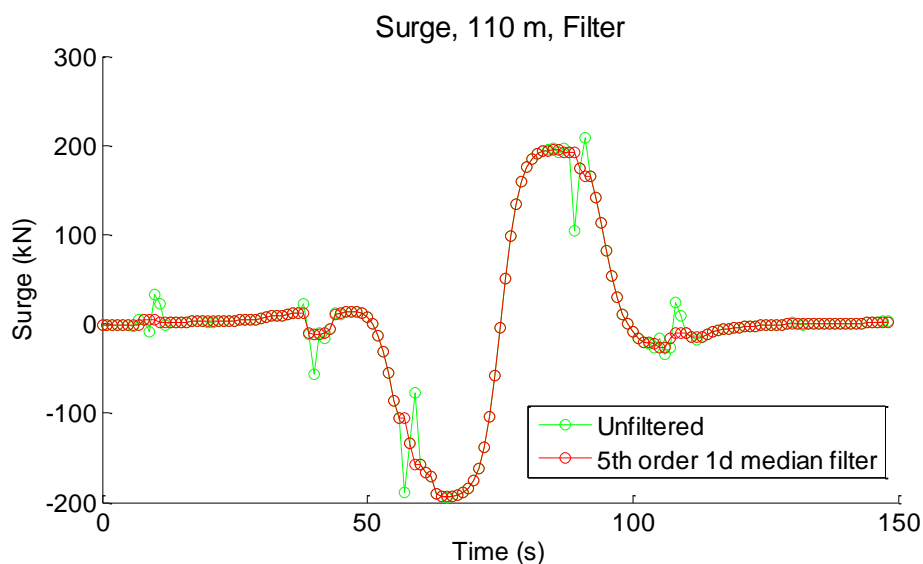


Figure 6.1 1-d 5th order median filter to filter out peaks

The peaks are a consequence of the numerical method, not a natural phenomenon. The cause is the fact that the passing vessel sails over the slope at the side of the canal. The peaks appear at the points where the front or aft of the passing vessel passes the end and beginning of the slope. This is demonstrated in Figure 6.2 and Figure 6.3. Figure 6.2 shows the simulation at 90 seconds, where one of the peaks in Figure 6.1 is found. Here, the front of the passing vessel is at the beginning of the slope. Figure 6.3 shows the simulation at 109 seconds, where another peak is found. The aft of the vessel is at the beginning of the slope. The peaks are explained by the sudden change in panel distribution. In the panel method, the influence of each panel on each other is taken into account. A sudden change in the distance between the panels in combination with the passing vessel moving at a speed of one panel per time step, or a Courant number of 1, can cause some instability in the simulation.

Because the peaks are only a modelling error, a 1-d 5th order median filter is used to filter the peaks, see Figure 6.1. A fairly smooth curve is obtained. The signals of the 135 and 200 m passing vessels at the smallest passing distance are processed in the same way.

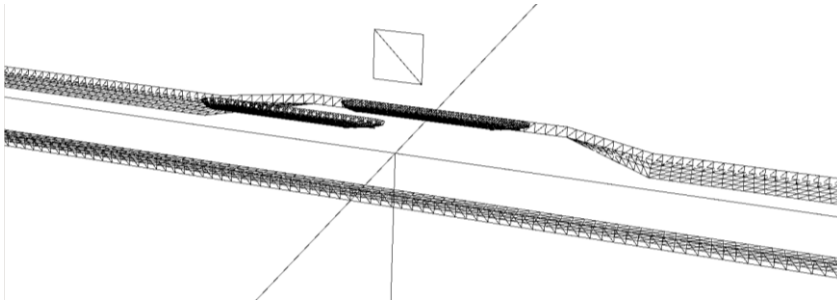


Figure 6.2 Simulation at 90 sec.

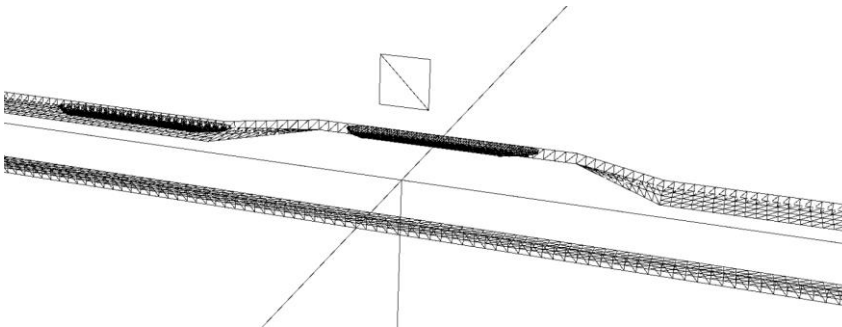


Figure 6.3 Simulation at 109 sec.

The surge forces at different passing distances are compared, see Figure 6.4. It is clear that a smaller passing distance generates a greater force. The passing distance of 88.2 m is reversed from the others, because the passing vessel is sailing in the opposite direction. Figure 6.5 shows the same figure for sway forces. The same increase in force with decrease in passing distance is observed.

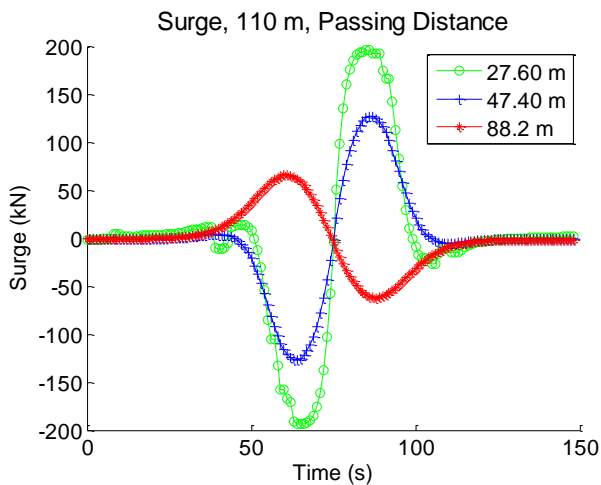


Figure 6.4 Surge force for different passing distances. (110 m vessel passing). Filtered

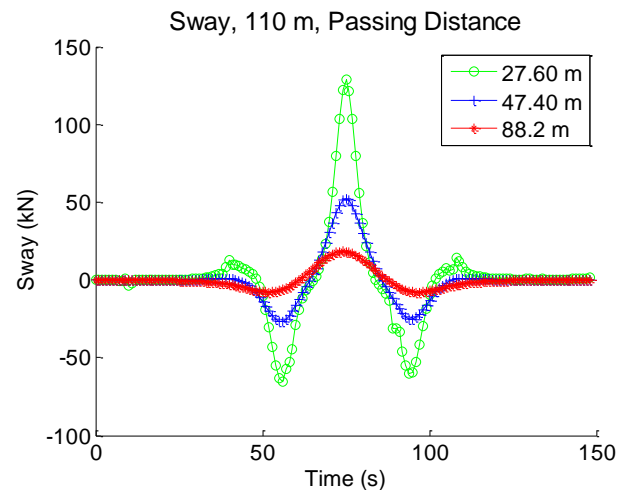


Figure 6.5 Sway force for different passing distances. (110 m vessel passing)

An increase in drift angle only shows a slight increase in force, see Figure O.1 in Appendix O. This is because only the extra water suppression of the drift angle is calculated, the free surface wave effects are not accounted for in these simulations.

When the ship is empty, a much smaller part of the vessel is below water, which reduces the pressure area and thus the forces. This does not necessarily mean that the resulting motions will be smaller. Figure O.2 in Appendix O shows the difference between the full and empty loading conditions.

Figure 6.6 and Figure 6.7 show the surge and sway forces for different passing vessels. As is to be expected, the larger the passing vessel, the larger the hydrodynamic forces on the moored vessel.

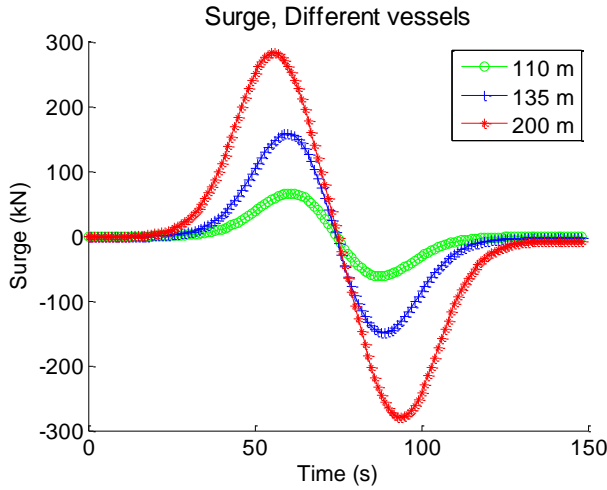


Figure 6.6 Surge force for different passing vessels (88.2 m passing distance)

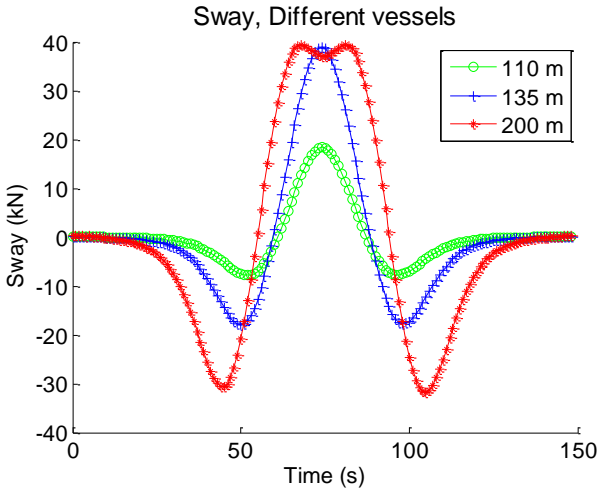


Figure 6.7 Sway force for different passing vessels (88.2 m passing distance)

6.2. PHYSICAL MODEL SHIP MOTIONS

Using the models described in chapter 3.3, the resulting ship motions for each scenario simulated with Ropes can be calculated. Because the smaller the forces are, the smaller the motions will be, the results of the scenario with the biggest forces are shown in these results.

Figure 6.8 shows the hydromechanical force caused by the passing vessel in this most critical scenario. The 200 m 4 barge pushed convoy passing at the smallest passing distance of 33.35 m, fully loaded and at a speed of 18 km/h.

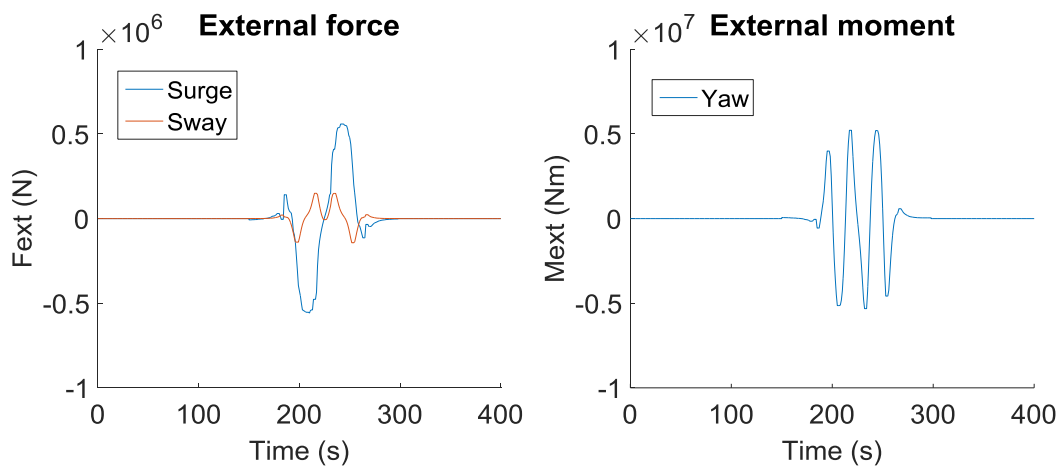


Figure 6.8 External forces and moment caused by 200m 4 barge convoy at 18 km/h, at a passing distance of 33.35m, P=-5, D=-3

The resulting ship motions are calculated with the MoorMaster™ unit configuration as determined in chapter 4.7. This is a configuration with 6 surge correcting units and 2 sway correcting units, with a PD setting of P=-5 and D=-3. Figure P.1 in Appendix P shows the forces the units exert on the ship.

Figure 6.9, Figure 6.10 and Figure 6.11 show the resulting ship motions, including the criteria for 90-100% loading efficiency. As can be seen in the figures, with this MoorMaster™ unit configuration, the ship motions stay within the criteria. Even when looking at the combined sway and yaw motions, at the fore and aft end of the ship, the motions are within the criteria, see Figure 6.12. Relative to the criteria, the yaw motions are largest, almost exceeding the criteria at one point.

When choosing a lower PD setting, larger motions are expected. Whether the forces exerted by the units also get smaller, is more difficult to predict. The forces are the product of P and the error, plus the product of D and the derivative of the error. The forces will get smaller, if P decreases more than the error increases. If the error increases more than P decreases, the forces will get larger.

It turns out the second case applies here. Figure Q.1, Figure Q.2 and Figure Q.3 in Appendix Q show the ship motions with a PD setting of P=2.5 and D=1.5, half of the previously used setting. As expected, the motions are larger than before. Figure P.2 in Appendix P shows the forces the units exert on the ship.

These are slightly larger than they were for the higher PD setting, meaning the increase in error is larger than the decrease in P.

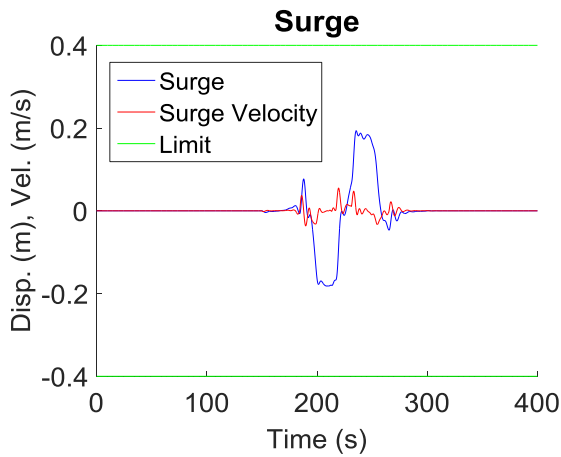


Figure 6.9 Resulting surge motions caused by 200m 4 barge convoy at 18 km/h, at a passing distance of 33.35m, P=-5, D=-3

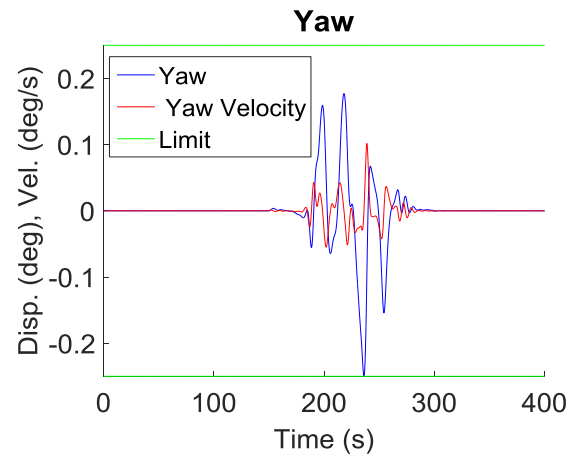


Figure 6.11 Resulting yaw motions caused by 200m 4 barge convoy at 18 km/h, at a passing distance of 33.35m, P=-5, D=-3

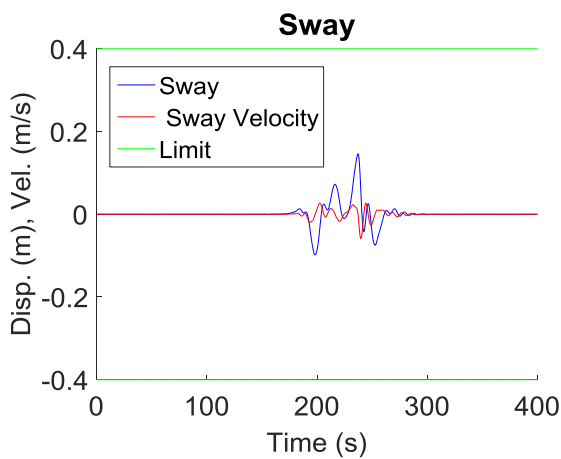


Figure 6.10 Resulting sway motions caused by 200m 4 barge convoy at 18 km/h, at a passing distance of 33.35m, P=-5, D=-3

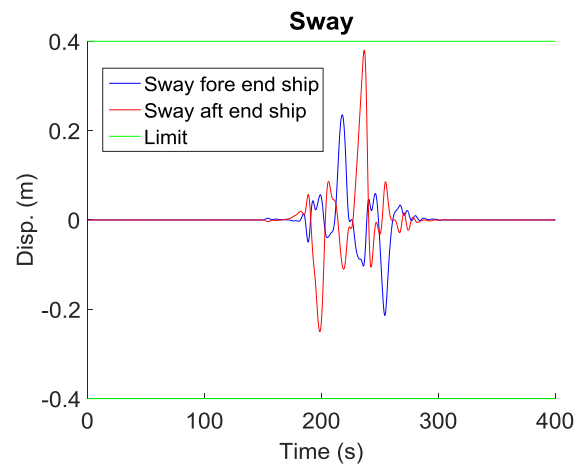


Figure 6.12 Resulting sway motions at fore and aft end caused by 200m 4 barge convoy at 18 km/h, at a passing distance of 33.35m, P=-5, D=-3

Another scenario that is looked into, is two Large Rhine vessels passing after each other. First, Figure Q.4 - Figure Q.7 in Appendix Q show the results of a 110m Large Rhine vessel passing at 47.40 m, likely to be the most common case. The curves are much smoother than the curves of the scenario described before, the pushed convoy sailing as close to the moored vessel as possible. The scattered peaks are likely to be another effect of the numerical method.

The motions caused by the first passing are cancelled out before the motions caused by the second passing begin, thus not affecting each other. The graphs are displayed in Figure Q.9 - Figure Q.11 in Appendix Q. Figure Q.8 in Appendix Q shows the external forces and moments of two vessels passing after each other. Figure P.4 in Appendix P shows the force the units exert on the moored vessel.

Of course, when two vessels would be passing very shortly after each other, where the second vessels passes before the forces of the first vessels are diminished, it is a different story. The forces of two passing events cannot simply be added up, because the pressure wave of the first vessel influences the pressure wave of the second vessel.

6.3. CONSTRUCTION CALCULATION

The maximum stress in the side shell plating and stiffeners due to the load of the MoorMaster™ units in sway direction is very much dependent on the (web) frame configuration of the vessel. The solutions of the FEM calculation for the load in sway direction on the "Damen Riverliner 1145E" are displayed in Figure 6.13- Figure 6.14. Figure 6.13 shows the stress in x direction, while Figure 6.14 shows the stress in y direction. The maximum observed stress is 119.773 MPa, in y direction. In this case, y direction is in the length of the vessel.

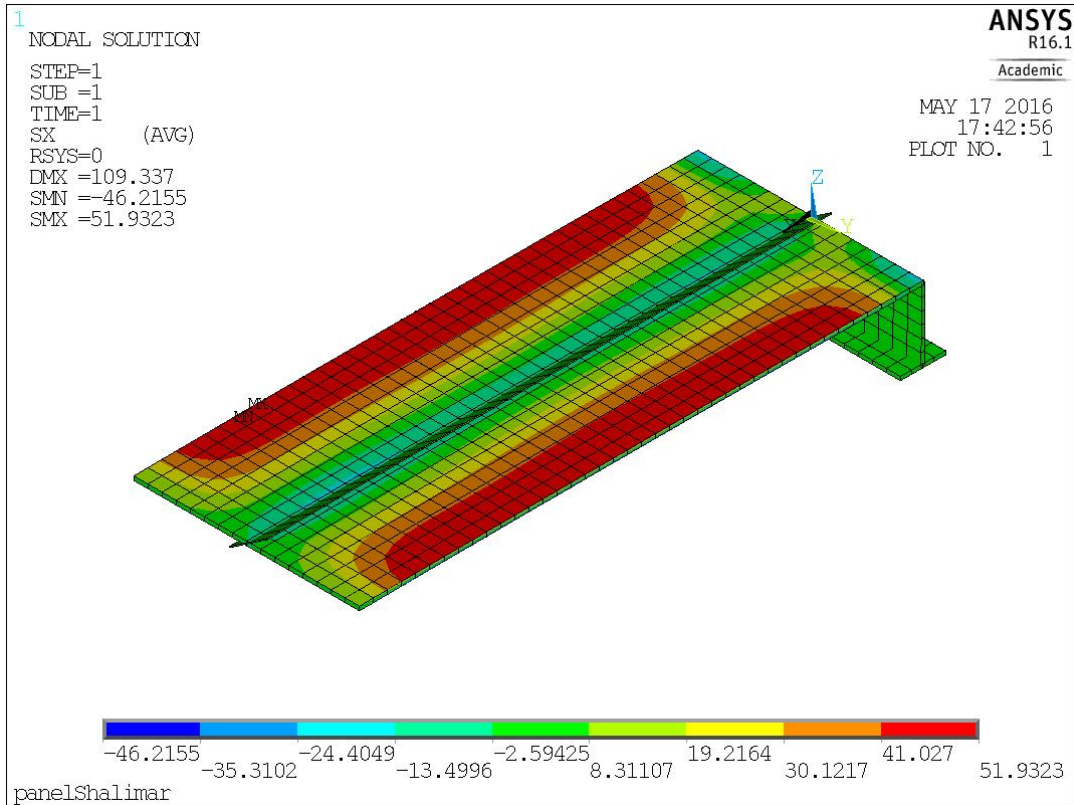


Figure 6.13 Stress in x direction in side plating due to load of 100 kN/m² in sway direction

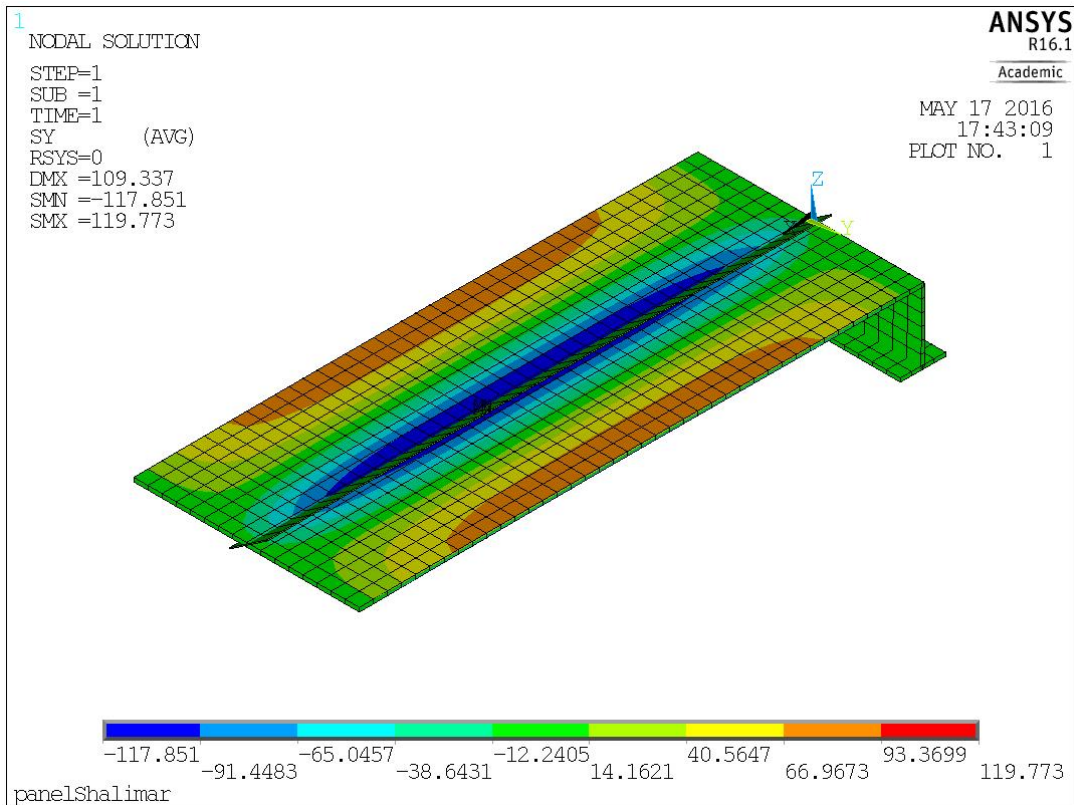


Figure 6.14 Stress in y direction in side plating due to load of 100 kN/m² in sway direction

For the loads in surge direction, it is only dependent on the plate thickness. Table 6.1 shows the stresses for different side shell plate thicknesses.

Table 6.1 Maximum stress in side shell plating and stiffeners due to force in surge direction

Plate thickness	Stress
8 mm	12.50 MPa
9.5 mm	10.53 MPa

These stresses are based on the maximum possible forces which are exerted by the MoorMaster™ units. When these stresses, together with the stress due to longitudinal bending and other local loads does not exceed 177 MPa, it is safe.

7. CONCLUSIONS

The main question of this research is:

- Is the MoorMaster™ 200 system a suitable mooring solution for (un)loading vessels at landing quays in inland waterways in the sense that there is no need for passing vessels to reduce speed?

A case study is performed on a 110 m Large Rhine vessel, moored at a quay side in the Amsterdam Rijnkanaal.

To determine the suitability of the MoorMaster™ system for an inland waterway, the following questions are answered:

- What are the forces produced by passing ships at cruising speed on the moored vessel?

Passing ships produce forces up to 560 kN in surge direction and 150 kN in sway direction, sailing at 18 km/h, the maximum allowed speed. For more detailed figures, see 6.1.

- What are the reaction forces of the MoorMaster™ units?
 - a) What configuration of MoorMaster™ units is needed to keep the moored vessel in place?

In this case study, two single sway correcting units at the outer ends of the midship and three groups of two surge correcting units, equispaced between the sway correcting units are needed to keep the moored vessel in place, resulting in a total of eight MoorMaster™ units.

- b) What are the forces produced by the MoorMaster™ units on the moored vessel in order to keep it in place?

The MoorMaster™ units each exert a maximum of 200 kN in sway direction, or 100 kN in surge direction.

- c) How should 'to keep it in place' be defined; what are the tolerances or boundaries for motions from an operational point of view?

For an (un)loading efficiency of 90-100%, the ship motions should not exceed the following:

- $A_{Surge} \leq 400 \text{ mm}$
- $A_{Sway} \leq 400 \text{ mm}$
- $A_{Yaw} \leq 0.25 \text{ deg}$

- What are the resulting motions of the moored vessel?

The resulting motions of the moored vessel are within the operational criteria. For more detailed figures, see 6.2.

- Can the construction of a typical inland vessel withstand these forces?

This is dependent on the stiffener configuration of the vessel and the other loads, besides the MoorMaster™ units, the vessel is coping with. Decreasing the PD settings is not a way to reduce the forces acting on the hull of the vessel.

Based on the results, the answer to the main question is:

For the studied case study and for the studied suitability criteria, given that the global bending stress combined with local loading does not exceed 57 MPa, the MoorMaster™ 200 system is a suitable mooring solution.

8. DISCUSSION & RECOMMENDATIONS

The results give a clear indication that the MoorMaster™ 200 system is suitable for the case studied. However, there are some items to keep into consideration.

8.1. RESEARCH SCOPE

Please be reminded that all passing events in this research are simulated at 18 km/h. To be able to say, legally and scientifically, that there is no need for passing vessels to reduce speed, a ship of maximum allowed dimensions has to be able to sail past at maximum allowed speed. However, in practice a 200 m 4 barge pushed convoy sailing at 18 km/h may never actually happen. When sailing at a more realistic speed of 10 km/h, the forces get reduced over 40%. It could be helpful to look more detailed into the operational profile. How often does a 4 barge pushed convoy actually pass and at what speed? Is eight units financially attractive or would it be more profitable to install less units and not be able to (un)load when a 200 m convoy passes at 18 km/h?

In this research, the focus is on the Amsterdam Rijnkanaal and only single passing vessels are looked at. For future research, it is recommended to investigate the effect of the shape and size of the waterway. It is mentioned that Ropes is a suitable tool for this research, because it gives good results for straight channels. When investigating other shapes of waterways, a different numerical method needs to be used, which incorporates second order wave free surface effects. The same goes for investigating the effect of larger drift angles.

Apart from that, the passing of several ships at once (crossings), should be looked into, as well as two vessels passing very shortly after each other. The forces of two vessels passing cannot simply be added up, as they have a large effect on each other. When looking into two vessels passing at once, the validity of Ropes should certainly be re-evaluated as well.

In this research, the main criteria for suitability is the ability to (un)load the vessel efficiently. There are of course other fields of interest that should be looked into before taking the system in operation. Not only the (un)loading of the vessel is determined by the ship motions, but the comfort of the people on board as well. Especially in inland shipping, where many captains are ship owners and families live on board, this should not be ignored as a factor. If being moored at a MoorMaster™ is uncomfortable, ship owners will likely choose other options.

8.2. LITERATURE

Very little literature is written to date about the MoorMaster™ system, which is likely due to it being relatively new. This thesis only looks into the MoorMaster™ 200 units. There are also other units available, such as the MoorMaster™ 400, which has a higher maximum force per unit. It can be interesting to look into other types and thus other configurations. It is recommended to consult Cavotec about the optimal solution for each case. Having said that, advice and literature from Cavotec is not independent research, which could mean a more optimistic view than an independent party would have.

No literature could be found on the subject of inland shipping motion criteria. The criteria of ship motions for (un)loading that are used are originally meant for container vessels of 100-200 m, which is exactly what is researched. However, they are not specifically designed for inland shipping. It may be possible that for inland shipping, some other criteria could apply.

Lastly, when looking at inland shipping, shallow and restricted waters are key. Research on the hydromechanics in these circumstances still has a long way to go as far as understanding all phenomenon and being able to predict them.

8.3. MODELLING IMPROVEMENTS

The model that is presented in this research is a first step towards predicting the ship motions of a vessel moored with MoorMaster™ units. A lot of extensions and improvements could be made.

In Ropes, the passing events are simulated using both a fully loaded as well as an empty moored vessel. Due to time limitation, only the added mass and thus ship motions of the fully loaded moored vessel are calculated. The forces on the empty moored vessel are much smaller than on the fully loaded vessel, considering the much smaller wet surface. However, the mass and moment of inertia of the empty vessel is also much smaller, meaning the ship motions do not necessarily have to be smaller than those of the fully loaded vessel. The model could be improved by adding different loading conditions.

Extending the model to six DOF instead of three gives great insight in the complete motions of the vessel. Even though the horizontal motions are most critical for (un)loading the vessel, vertical motions are of some effect as well. Apart from (un)loading the vessel, the vertical motion behaviour also determines the comfort of the people on board.

Optimisation of the PD settings by an expert is also recommended in the process of finding the optimal solution.

8.4. RESULTS

When simulating vessels close to the shore and sailing over the talus, accuracy declines. This is clearly visible in the results. Peaks occur and the motions are much more irregular than at greater passing distances. Despite these peaks and irregularities, the amplitude of the motion does not seem to be affected by this. This means the results are still useful for the goal of this research.

It should also be noted, that decreasing the PD settings does not decrease the forces exerted by the MoorMaster™ units. This is not a solution to decrease the load on the hull of the vessel. The cause is that when the settings are decreased, the motions of the vessel get larger. Even though constants are decreased, the increase in error results in the same forces, or even larger.

8.5. VALIDATION

Because of the high passing velocity and the depth of the canal, the depth-based Froude number is relatively high at 0.65. Even though a correction factor is taken into account, it may be worth looking into the validity of the model used by Ropes at this high depth-based Froude number.

Even though the ship motion model is extensively verified, it is not validated. There was no time or resources for model tests and full scale data unfortunately was not available due to legal issues. In the future, Cavotec might be able to release the full scale data to validate the model. It is recommended to validate the results with either model tests or full scale measurements.

8.6. STRUCTURAL STRENGTH

To ensure the structural integrity of an inland vessel when mooring with the MoorMaster™ system, a structural analysis needs to be performed. There is no standard calculation that can be done to ensure

structural integrity for all inland vessels. Most vessels are unique and therefore require their own calculations. Apart from that, repairs done over the years can have an influence as well. However, most of these calculations and values are usually already known, since many of these are needed for the classification of the vessel. Therefore, it does not have to be a lot of work to determine suitability per ship.

8.7. MOORMASTER™ SYSTEM

Though the MoorMaster™ system is effective in this case study, its efficiency is questionable. The simulations with Ropes show that the forces on the moored vessel in surge direction are almost four times larger than in sway direction. The MoorMaster™ system is however more suited to correct in sway direction. The maximum force of one unit is twice as high in sway direction as it is in surge direction. This indicates that a different mooring solution, more focussed on correcting surge motions, is more efficient in this case.

The PID configurator in the MoorMaster™ units responds to the error in displacement. The system may work faster if the units would respond to forces instead of motions, or a combination of both.

9. REFERENCES

Binnenvaartpolitiereglement, 2004. *Bijlage 13. Toegestane afmetingen van een schip of een samenstel op de vaarwegen, bedoeld in artikel 9.02, eerste lid.* sl:Scheepvaartverkeerswet.

Binnenvaartpolitiereglement, 2004. *Artikel 6.20 Hinderlijke waterbeweging.* sl:Scheepvaartverkeerswet.

Cavotec MoorMaster Limited, 2012. *Description of MoorMaster 200 C/B as Required for Numeric Modeling*, Christchurch, New Zealand: Cavotec MoorMaster Limited.

Coférence Européenne des Ministres des Transports, 1992. *Resolution No. 92/2 New Classification of Inland Waterways*, Athens, Greece: CEMT.

Cool, J., Schijff, F. & Viersma, T., 1979. Instellen van een regelaar. In: *Regeltechniek*. Amsterdam/Brussel: B.V. Uitgeversmaatschappij Elsevier Argus, pp. 256-279.

de Bont, J., 2010. *Validation of numerical models for motions of ships moored with MoorMasterTM units, in a harbour under influence of ocean waves*, Master Thesis: Delft University of Technology, Royal Haskoning.

de Bont, J. et al., 2010. *Calculations of the Motions of a Ship Moored with MoorMaster Units*. Liverpool, UK, PIANC MMX Congress.

de Koning Gans, H., Huijsmans, R. & Pinkster, J., 2007. *A Method to Predict Forces on Passing Ships under Drift*. Ann Arbor, Michigan, International Conference on Numerical Ship Hydrodynamics.

Deyzen, A. v., Lem, J. V. D., Beimers, P. & Bont, J. D., 2014. *The Effect of Active Motion Dampening Systems on the Behaviour of Moored Ships*. San Fransisco, USA, PIANC World Congress.

Dienst Verkeer en Scheepvaart, 2008. *Vaarwegen in Nederland*, sl: Rijkswaterstaat.

Elzinga, T., Iribarren, J. & Jensen, O., 1992. Movements of Moored Ships in Harbours. *Coastal Engineering Proceedings*, Issue No. 23, pp. 3216-3229.

Goedhart, G., 2002. *Criteria for (un)-loading Container Ships*, Delft, The Netherlands: Delft University of Technology, Master Thesis.

Jensen, O. et al., 1990. Criteria for Ship Movement in Harbours. *Coastal Engineering Proceedings*, Issue No 22, pp. 3074-3087.

Journée, J., 2000. *Hydromechanic Coefficients for Calculating Time Domain Motions of Cutter Suction Dredges by Cummins Equations*, Delft: Delft University of Technology, Ship Hydromechanics Laboratory.

Journée, J. & Adegeest, L., 2003. *Theoretical Manual of "SEAWAY for windows"*, Delft University of Technology: AMARCON (Advanced Maritime Consulting).

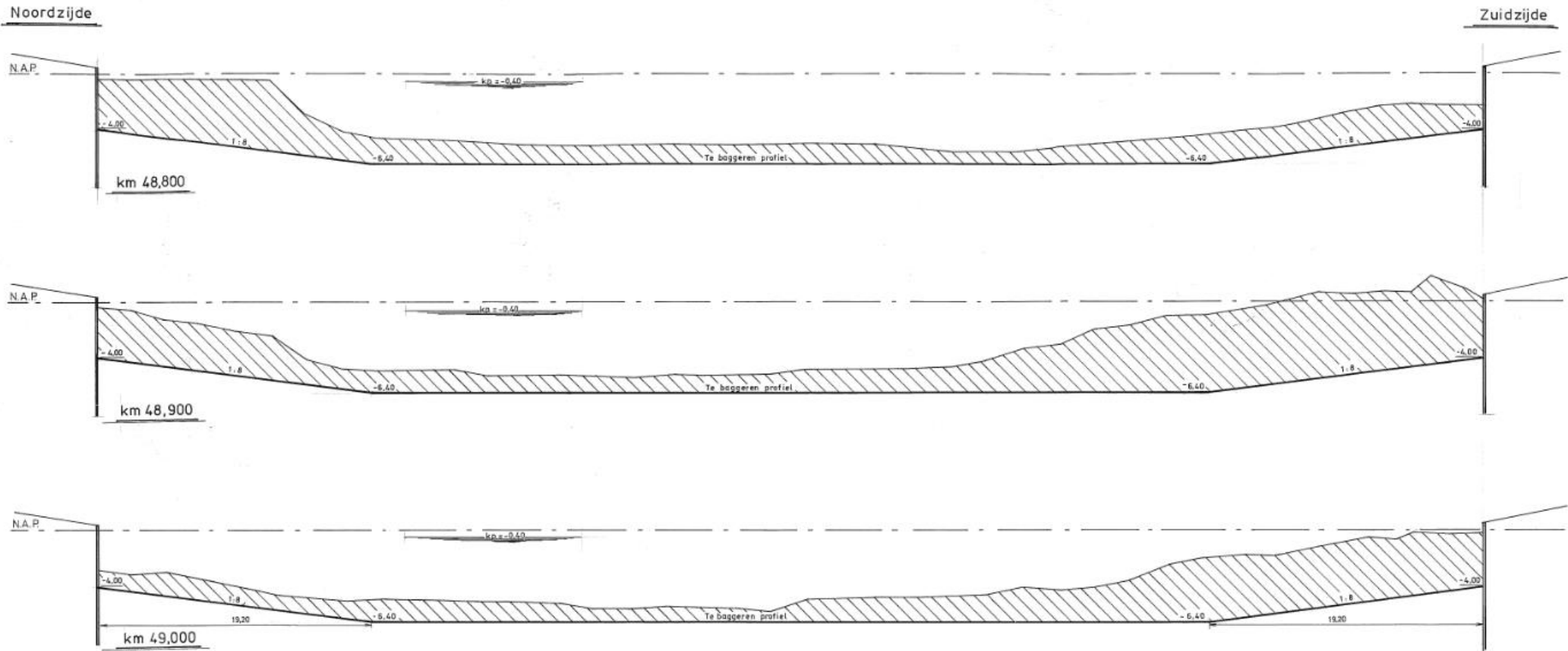
Journée, J. & Massie, W., 2001. Rigid Body Dynamics. In: *Offshore Hydromechanics*. Delft: Delft University of Technology, pp. 6-1 - 6-44.

Katz, J. & Plotkin, A., 1991. Fundamentals of Inviscid, Incompressible Flow. In: *Low-Speed Aerodynamics; From Wing Theory to Panel Methods*. Singapore: McGraw-Hill, Inc., pp. 25-51.

Katz, J. & Plotkin, A., 1991. General Solution of the Incompressible, Potential. In: *Low-Speed Aerodynamics; From Wing Theory to Panel Methods*. Singapore: McGraw-Hill, Inc., pp. 52-87.

- Lievens, L., 2010. *Nieuw dwarsprofiel voor het Amsterdam-Rijnkanaal*, Delft: TU Delft, Deltares, Rijkswaterstaat.
- Lloyd's Register Group Limited, 2016. Part 3, Chapter 3, Section 2; Part 4, Chapter 1, Section 5. In: *Rules and Regulations for the Classification of Inland Waterway Ships*. Londen: sn, pp. 52-54; 204-206.
- Lloyd's Register Group Limited, 2016. Part 3, Chapter 4, Section 6 Maximum permissible stresses. In: *Rules and Regulations for the Classification of Inland Waterways*. Londen: sn, p. 78.
- Moes, H. & Terblanche, L., 2010. *Motion Criteria for the Efficient (Un)Loading of Container Vessels*. Delft, The Netherlands, Port Infrastructure Seminar TU Delft.
- Pinkster Marine Hydrodynamics BV, 2013. *Ropes - User manual*, sl: Pinkster Marine Hydrodynamics BV.
- Pinkster, J., 1995. *Hydrodynamic Interaction Effects in Waves*. The Hague, The Netherlands, The International Society of Offshore and Polar Engineers.
- Pinkster, J., 2006. De bewegingsvergelijking van het schip in een horizontaal vlak. In: *Bewegen en Sturen II Manoeuvreren; Deel II: Sturen en Manoeuvreren*. Delft: Delft University of Technology, pp. 5.1-5.8.
- Pinkster, J. & Pinkster, H., 2014. *A Fast, User-Friendly, 3-D Potential Flow Program for the Prediction of Passing Vessel Forces*. San Francisco, USA, PIANC World Congress.
- Remery, G., 1974. *Mooring Forces Induced by Passing Ships*. Dallas, Texas, Offshore Technology Conference.
- Rijkswaterstaat, 2009. *Scheepvaartinformatie Hoofdvaarwegen*, Den Haag: Ministerie van Verkeer en Waterstaat.
- Rijkswaterstaat, 2011. *Richtlijnen Vaarwegen 2011*. sl:Directoraat-Generaal Rijkswaterstaat.
- Schär, C., 2015. *The Courant-Friedrichs-Levy (CFL) Stability Criterion*, ETH Zürich : Institut für Atmosphäre und Klima.
- Talstra, H. & Bliet, A., 2014. *Loads on Moored Ships due to Passing Ships in a Straight Harbour Channel*. San Francisco, USA, PIANC World Congress.
- Terblanche, L. & van der Molen, W., 2013. *Numerical Modeling of Long Waves and Moored Ship Motions*. Sydney, N.S.W, Australasian Port and Harbour Conference.
- Thorensen, C. A., 2014. Berthing requirements. In: *Port Designer's Handbook*. Westminster, London: ICE Publishing, pp. 99-142.
- van den Boom, H., Pluijm, M. & Pauw, W., 2014. *Ropes; Joint Industry Project on Effect of Passing Ships on Moored Vessels*. San Francisco, USA, PIANC World Congress.
- van der Hout, A. & de Jong, M., 2014. *Passing Ship Effect in Complex Geometries and Currents*. San Francisco, USA, PIANC World Congress.
- Verheij, H., Meerten, H. v. & Giri, S., 2012. *Onderzoek Bodemerisatie Amsterdam-Rijnkanaal*, Utrecht: Deltares.
- Wictor, E. & van den Boom, H., 2014. *Full Scale Measurements of Passing Ship Effects*. San Francisco, USA, PIANC World Congress.

APPENDIX A. CROSS SECTION OF AMSTERDAM-RIJNKANAAL

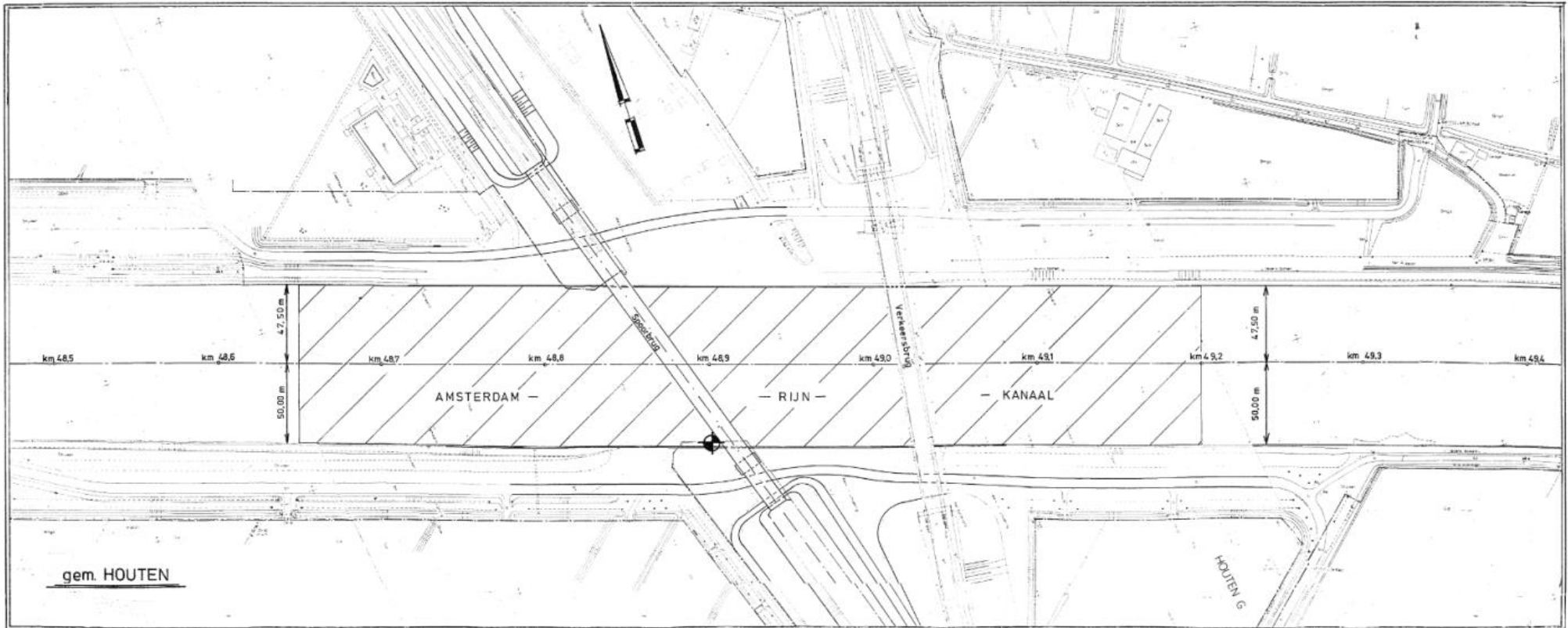


Dwarsprofielen

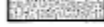
Schaal 1:200

Situatie

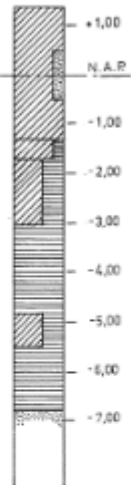
Schaal 1:2000



Verklaring

-  te baggeren specie
- maten in meters
- hoogtematen in meters t.o.v. N.A.P.
-  op situatie : baggervak
- bestand profiel
- te baggeren profiel
-  plaats grondboring
-  klei
-  veen
-  zand

Grondboring



79 307 032 v56

	opgen.	getek.	gecalq.	gekant.	gezien	akkoord	
d.d.	april 79	april 79	april 79				
par.	len	len	len				
gew.							
<p>Amsterdam-Rijnkanaal VERRUIMING VAN km 48,650 – km 49,200 in de gemeente HOUTEN.</p>				<p>O.O. nr. U 2057 DIENST 1979</p>			
<p>Situatie's en dwarsprofielen.</p>				<p>met 1 tekening</p>			
RIJKSWATERSTAAT DIREKTIE UTRECHT HOOFDAFDELING AN					SCHAAL : diverse A1 N ^o 79.218 N.W.N		

APPENDIX B. CLASSIFICATION OF EUROPEAN INLAND WATERWAYS

(Coférence Européenne des Ministres des Transports, 1992)

CLASSIFICATION OF EUROPEAN INLAND WATERWAYS

Type of inland waterways	Classes of navigable waterways	Motor vessels and barges					Pushed convoys					Minimum height under bridges ^{2/}	Graphical symbols on maps	
		Type of vessel: General characteristics					Type of convoy: General characteristics							
		Designation	Maximum length	Maximum beam	Draught ^{7/}	Tonnage		Length	Beam	Draught ^{7/}	Tonnage			
			L(m)	B(m)	d(m)	T(t)		L(m)	B(m)	d(m)	T(t)	H(m)		
1	2	3	4	5	6	7	8	9	10	11	12	13	14	
OF REGIONAL IMPORTANCE	To West of Elbe	I	Barge	38.5	5.05	1.80-2.20	250-400						4.0	=====
		II	Kampine-Barge	50-55	6.6	2.50	400-650						4.0-5.0	=====
		III	Gustav Koenigs	67-80	8.2	2.50	650-1,000						4.0-5.0	=====
	To East of Elbe	I	Gross Finow	41	4.7	1.40	180						3.0	=====
		II	BM-500	57	7.5-9.0	1.60	500-630						3.0	=====
		III	6/	67-70	8.2-9.0	1.60-2.00	470-700		118-132	8.2-9.0	1.60-2.00	1,000-1,200	4.0	=====
OF INTERNATIONAL IMPORTANCE	IV	Johann Welker	80-85	9.5	2.50	1,000-1,500		85	9.5 ^{5/}	2.50-2.80	1,250-1,450	5.25 or 7.00 ^{4/}	=====	
	Va	Large Rhine vessels	95-110	11.4	2.50-2.80	1,500-3,000		95-110 ^{1/}	11.4	2.50-4.50	1,600-3,000	5.25 or 7.00 or 9.10 ^{4/}	=====	
	Vb							172-185 ^{1/}	11.4	2.50-4.50	3,200-6,000	4/	=====	
	VIa							95-110 ^{1/}	22.8	2.50-4.50	3,200-6,000	7.00 or 9.10 ^{4/}	=====	
	VIb	3/	140	15.0	3.90			185-195 ^{1/}	22.8	2.50-4.50	6,400-12,000	7.00 or 9.10 ^{4/}	=====	
	VIc						 	270-280 ^{1/} 195-200 ^{1/}	22.8 33.0-34.2 ^{1/}	2.50-4.50 2.50-4.50	9,600-18,000 9,600-18,000	9.10 ^{4/}	=====	
	VII						 8/	285	33.0-34.2 ^{1/}	2.50-4.50	14,500-27,000	9.10 ^{4/}	=====	

APPENDIX C. CLASSIFICATION OF RIJKSWATERSTAAT

Table 8: Classification of inland navigation fleet, *Rijkswaterstaat* 2010

CEMT Class	Motor vessels							Pushed convoys (Barge)				
	RWS Class	Characteristics of reference vessel**			Classification		RWS Class	Characteristics of reference pushed convoy**				
		Designation	Beam	Length	Draught (laden)	Cargo capacity		Beam and length	Combination	Beam	Length	Draught (laden)
		m	m	m	t	m		m	m	m		
0	M0	Other				1-250	B ≤ 5.00 of L ≤ 38.00					
I	M1	Péniche	5.05	38.5	2.5	251-400	B = 5.01-5.10 and L ≥ 38.01	BO1		5.2	55	1.9
II	M2	Kempenaar	6.6	50-55	2.6	401-650	B = 5.11-6.70 and L ≥ 38.01	BO2		6.6	60-70	2.6
III	M3	Hagenaar	7.2	55-70	2.6	651-800	B = 6.71-7.30 and L ≥ 38.01	BO3		7.5	80	2.6
	M4	Dortmund Eems (L ≤ 74 m)	8.2	67-73	2.7	801-1050	B = 7.31-8.30 and L = 38.01-74.00	BO4		8.2	85	2.7
	M5	Ext. Dortmund Eems (L > 74 m)	8.2	80-85	2.7	1051-1250	B = 7.31-8.30 and L ≥ 74.01					
IVa	M6	Rhine-Herne Vessel (L ≤ 86 m)	9.5	80-85	2.9	1251-1750	B = 8.31-9.60 and L = 38.01-86.00	BI	Europa I pushed 	9.5	85-105	3.0
	M7	Ext. Rhine-Herne (L > 86 m)	9.5	105	3.0	1751-2050	B = 8.31-9.60 and L ≥ 86.01		convoy			
IVb												
Va	M8	Large Rhine Vessel (L ≤ 111 m)	11.4	110	3.5	2051-3300	B = 9.61-11.50 and L = 38.01 - 111.00	BI-1	Europa II pushed 	11.4	95-110	3.5
	M9	Extended Large Rhine Vessel (L > 111 m)	11.4	135	3.5	3301-4000	B = 9.61-11.50 and L ≥ 111.01	BIa-1	Europa IIa pushed 	11.4	92-110	4.0
								BIIL-1	Europa II long 	11.4	125-135	4.0
Vb							BI-2i	2-barge pushed 	11.4	170-190	3.5-4.0	
VIa	M10	Ref. vessel 13.5 * 110 m	13.50	110	4.0	4001-4300	B = 11.51-14.30 and L = 38.01 - 111.00	BI-2b	2-barge pushed 	22.8	95-145	3.5-4.0
	M11	Ref. vessel 14.2 * 135 m	14.20	135	4.0	4301-5600	B = 11.51-14.30 and L ≥ 111.01		convoy wide 			
	M12	Rhinemax Vessel	17.0	135	4.0	≥ 5601	B ≥ 14.31 and L ≥ 38.01					
Vib							BI-4	4-barge pushed convoy 	22.8	185-195	3.5-4.0	
Vic							BI-6i	6-barge pushed 	22.8	270	3.5-4.0	
VIIa							BI-6b	6-barge pushed 	34.2	195	3.5-4.0	

* In classes I, IV, V and higher the headroom has been adjusted for 2, 3 and 4 layers of containers respectively (headroom on canals relative to reference high water level = 1% exceedance/year)

** The characteristics of the reference vessels have a margin of error of ± 1 metre in the length, and ± 10 cm in the beam.

Classification		RWS Class	Characteristics of reference coupled unit**				Classification		Headroom * incl. 30 cm spare headroom
Cargo capacity	Beam and length		Combination	Beam	Length	Draught (laden)	Cargo capacity	Beam and length	
t	m			m	m	m	t	m	m
0-400	B<=5.20 and L= all	C1I	2 péniches long 	5.05	77-80	2.5	<= 900	B<= 5.1 and L=all	5.25*
		C1b	2 péniches wide 	10.1	38.5	2.5	<= 900	B=9.61-12.60 and L<= 80.00	5.25*
401-600	B=5.21-6.70 and L=all								6.1
601-800	B=6.71-7.60 and L=all								6.4
801-1250	B=7.61-8.40 and L=all								6.6
									6.4
1251-1800	B=8.41-9.60 and L=all								7.0*
									7.0*
		C2I	Class IV + Europa I long 	9.5	170-185	3.0	901-3350	B=5.11-9.60 and L=all	7.0*
1801-2450	B=9.61-15.10 and L<=111.00								9.1*
2451-3200	B=9.61-15.10 and L<=111.00								9.1*
3201-3950	B=9.61-15.10 and L=111.01-146.00								9.1*
3951-7050	B=9.61-15.10 and L>=146.01	C3I	Class Va + Europa II long 	11.4	170-190	3.5-4.0	3351-7250	B=9.61-12.60 and L>=80.01	9.1*
3951-7050	B=15.11-24.00 and L<=146.00	C2b	Class IV + Europa I wide 	19.0	85-105	3.0	901-3350	B=12.61-19.10 and L<=136.00	7.0* only for class IV coupled unit
		C3b	Class Va +Europa II wide 	22.8	95-110	3.5-4.0	3351-7250	B>19.10 and L<=136	9.1*
7051-12000 (7051-9000)	B=15.11-24.00 and L=146.01-200	C4	Class Va + 3 Europa II 	22.8	185	3.5-4.0	>=7251	B>12.60 and L>=136.01	9.1*
12001-18000 (12001-15000)	B=15.11-24.00 and L>=200.01								9.1*
12001-18000 (12001-15000)	B>=24.01 and L=all								9.1*

- NB: 1: A reference vessel is a vessel whose dimensions determine the dimensions of the waterway and the engineering structures on or in it.
2: New waterways and enlarged waterways are based on the largest reference vessel within a CEMT class.
3: Classes M3, M4, M6, M8, M10 and M11 may be used only for the renovation of existing waterways, locks and bridges.
4: The smallest dimensions of a reference vessel represent the lower threshold for categorising a waterway in a particular standardised class.

APPENDIX D. PASSING LOCKS ARK

Table D.1 Passings in locks in ARK in 2011

Passages Klasse VI t.o.v. totaal over heel 2011			
			Percentage t.o.v. totaal
Bernhardsluis	Vla	667	2,9%
	Vlb	311	1,4%
	Vlc	0	0,0%
	VI totaal	978	4,3%
	Binnenvaart totaal	22.879	
<hr/>			
Irenesluis	Vla	1.020	2,7%
	Vlb	535	1,4%
	Vlc	0	0,0%
	VI totaal	1.555	4,1%
	Binnenvaart totaal	38.083	

APPENDIX E. POTENTIAL FLOW; BOUNDARY CONDITIONS AND SINGULARITIES

In this appendix some elements of using potential flow in the panel method are further elaborated on. The boundary conditions that can be applied to the Laplace equation are displayed and some singularities that are elementary solutions to the Laplace equation are shown.

BOUNDARY CONDITIONS

When using potential flow, several boundary conditions can be applied in order to solve the Laplace equation. These are elaborated on below. (Journée & Adegeest, 2003)

SEABED BOUNDARY CONDITION

Fluid particles cannot penetrate the bottom of the waterway. Therefore:

$$\frac{\partial \Phi}{\partial z} = 0 \text{ for } z = -h \quad \text{Eq. E.1}$$

Where h is the water depth.

DYNAMIC BOUNDARY CONDITION AT THE FREE SURFACE

The dynamic boundary condition at the free surface entails that the pressure, p , at the free surface of the fluid is equal to the atmospheric pressure. The pressure in the fluid is given by the Bernoulli equation, Eq. E.2.

$$\frac{\partial \Phi}{\partial t} + \frac{1}{2} \cdot (u^2 + v^2 + w^2) + \frac{p}{\rho} + g \cdot z = 0 \quad \text{Eq. E.2}$$

Linearizing the Bernoulli equation and applying it to the fluid surface gives Eq. E.3:

$$\frac{\partial^2 \Phi}{\partial t^2} + g \cdot \frac{\partial \Phi}{\partial z} = 0 \text{ for } z = 0 \quad \text{Eq. E.3}$$

KINEMATIC BOUNDARY CONDITION ON THE OSCILLATING BODY SURFACE

The velocity of a water particle at the surface of the body (vessel), is equal to the velocity of the body in that point itself. The outward normal velocity at a point on the surface of the body is given by

$$\frac{\partial \Phi}{\partial n} = v_n(x, y, z) = \sum_{j=1}^6 v_j \cdot f_j \quad \text{Eq. E.4}$$

Where v_n is the outward normal velocity, x, y, z the location of the point on the body, v_j oscillatory velocities and f_j generalised direction-cosines.

RADIATION CONDITION

The radiation condition states that infinitely far from the body, the effects of the oscillation body are not present anymore. Thus, at a distance R of the body, the potential of the fluid tends to zero as R goes to infinity, Eq. E.4.

$$\lim_{R \rightarrow \infty} \Phi = 0 \quad \text{Eq. E.5}$$

SYMMETRIC OR ANTI-SYMMETRIC CONDITION

Because of the symmetric shape of ships, some simplifications are possible to the potential equations.

SINGULARITIES

The singularities explained below are elementary solution to the Laplace equation. They are used in numerical method such as the panel method to solve the potential flow field.

SOURCES/SINKS

One of the basic solutions to the Laplace equation is a source or sink (a source with a negative strength is often called a sink). The potential of a source element, placed at the origin of a spherical coordinate system is given in Eq. E.6. (Katz & Plotkin, 1991).

$$\Phi = -\frac{\sigma}{4\pi r} \quad \text{Eq. E.6}$$

Where σ is the source strength and r the radial distance from the point source. Figure E.1 gives a visual representation of a source and sink.

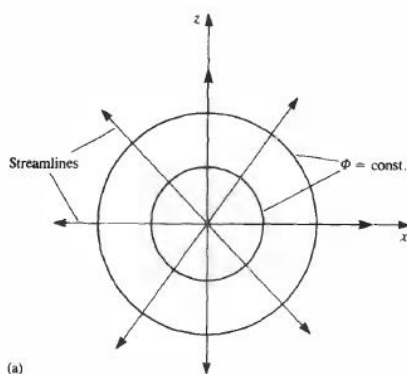


Figure E.1 Visual representation of source (Katz & Plotkin, 1991)

DOUBLET

Another basic solution is the doublet. It is a combination of a source and a sink. The potential is given in Eq. E.7.

$$\Phi = \frac{\mu}{4\pi} \bar{n} \cdot \nabla \left(\frac{1}{r} \right) \quad \text{Eq. E.7}$$

Where μ is the doublet strength and n the normal vector pointing into the objects surface. Figure E.2 gives a visual representation of a doublet. (Katz & Plotkin, 1991)

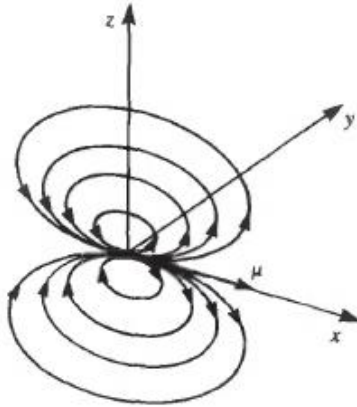


Figure E.2 Visual representation of a doublet (Katz & Plotkin, 1991)

VORTICES

The last basic solution that will be discussed here is the vortex. This singularity only has a tangential velocity component. The potential of a vortex is given in Eq. E.8.

$$\Phi = -\frac{\Gamma}{2\pi} \theta + C \quad \text{Eq. E.8}$$

Where Γ is the circulation, and C is an arbitrary constant. Figure E.3 shows a visual representation of a vortex. (Katz & Plotkin, 1991)

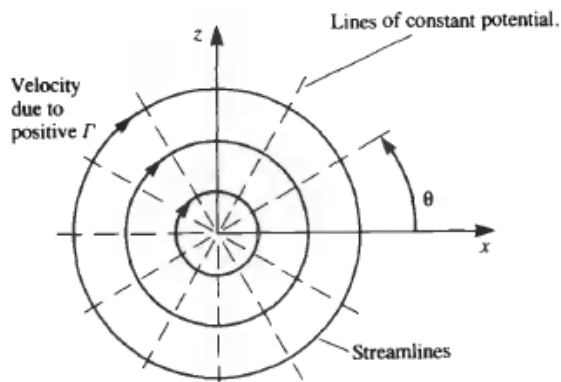


Figure E.3 Visual representation of a vortex (Katz & Plotkin, 1991)

APPENDIX F. ROPES DESCRIPTION AND SENSITIVITY STUDY

In this appendix, the input interface of Ropes and a sensitivity study are presented.

INPUT INTERFACE

The input of Ropes mainly consists of two parts: the vessels and the harbour geometry. There are several parent vessels which can be scaled to match the desired vessel. The loading condition can also be changed as well as initial position, heading, drift angle and velocity. Figure F.1 shows the main input screen for a simulation in Ropes. In the upper window, the vessels are described. In the lower window, the harbour geometry is described. Below, the time step and number of steps, the water depth and the density of water are asked.

Edit simulation

Description: Run110_E_47400_0

Vessel(s)

Index	Description	LPP [m]	B [m]	T [m]	Speed	X [m]	Y [m]	Heading [deg]
1	Run110_E_47400_0	109.95	11.424	0.825	-	0	-67.8	0
2	Inland barge Klasse V Passing	109.95	11.424	3.45	5 m/s	-375	-20.4	0

Buttons: Add... Remove Edit...

Harbour parts

Index	Description	X [m]	Y [m]	Heading [deg]
1	ARK2	0	0	0

Buttons: Add... Remove Edit...

Quay

Quay present

Simulation

Number of output time steps: 150

Output time step: 1 s

Waterdepth: 6 m

Density of water: 1000 kg / m³

Buttons: Preview... OK Cancel

Figure F.1 Simulation input Ropes

Figure F.2 shows the input panel for vessels. A parent vessel is selected which most resembles the wanted vessel. In 'Main dimensions (fully loaded)', the parent vessel can be scaled to match the simulated vessel. A loading condition can be selected by altering the draft, heel and trim in 'Loading condition'. The initial position, heading and direction of track can be set as well as the speed.

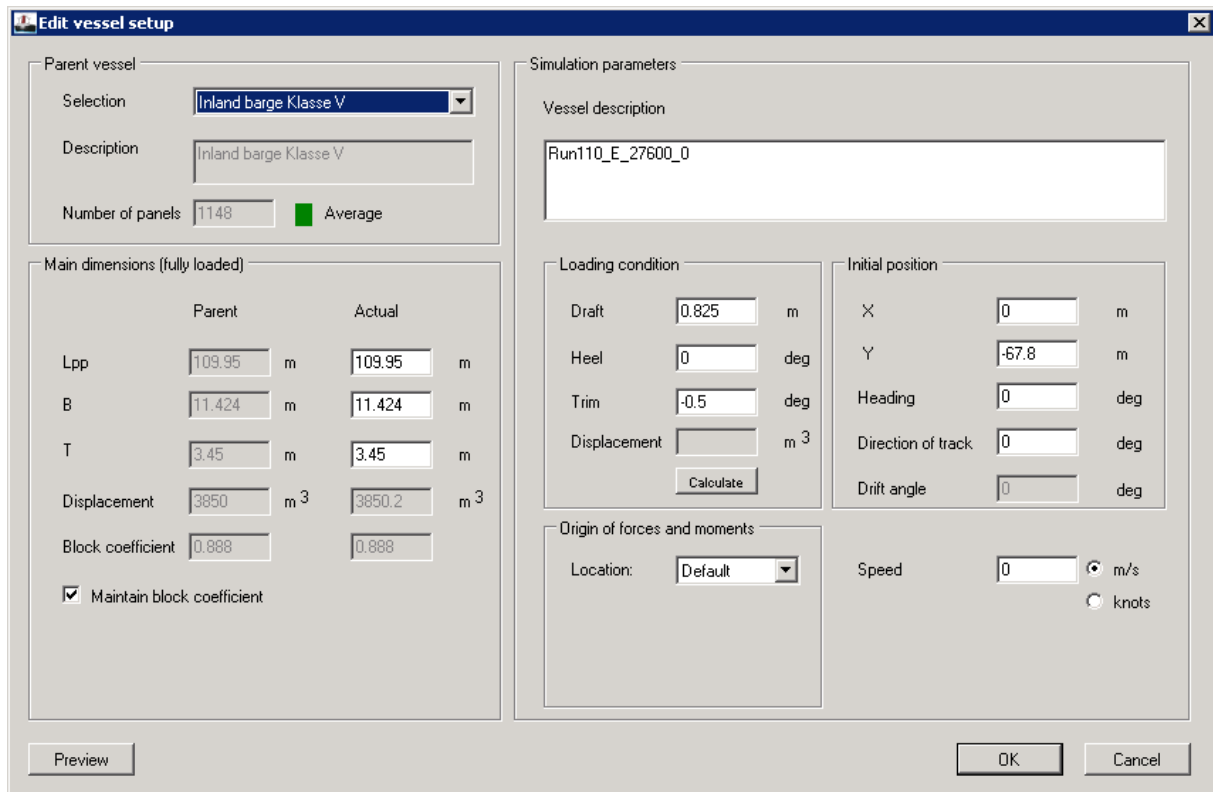


Figure F.2 Vessel input Ropes

SENSITIVITY STUDY

To get a feeling of the influence of certain simulation parameters, first a simple straight canal is simulated. The parent hull for an inland class V barge is used for both the moored ship and the passing ship (110 m). The moored ship is moored at the side of the canal half way through, the passing vessel is sailing by in the middle of the canal. The time step, sailing distance and canal length are varied to obtain a relation.

TIME STEP

Using a ship speed of 5 m/s, the time step is varied from 0.50 seconds to 2.00 seconds. With the standard panel size of 5 m used in Ropes, this means the Courant number is varied from 0.5 to 2.00. The total simulation time is kept constant, by varying the number of steps. Figure F.3 and Figure F.5 show the surge force for varying time steps. Figure F.4 and Figure F.6 show the sway force for varying time steps. When looking at Figure F.3 and Figure F.4, the difference between the time steps seems non-existent. Figure F.5 and Figure F.6 zoom in on the peaks of the graphs. The calculated points are on the exact same graph, however with increasing time step, some detail is lost. The time step does not seem to be a sensitive input parameter, however in order to prevent a Courant number higher than 1, a 1.00 second time step will be used.

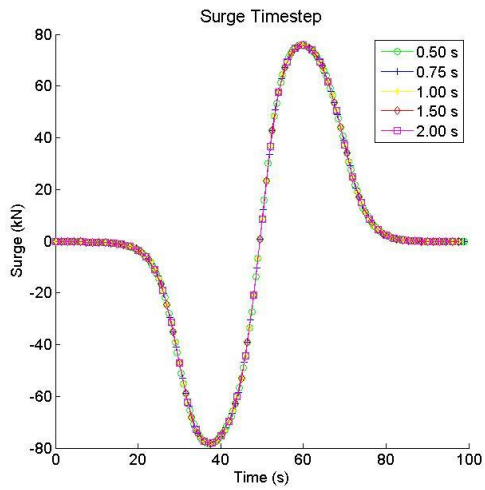


Figure F.3 Surge force for varying time step

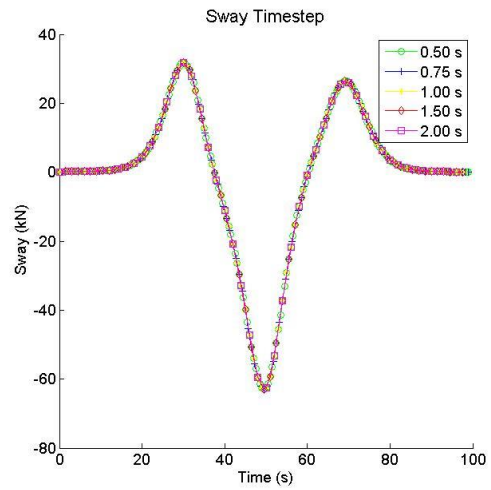


Figure F.4 Sway force for varying time step

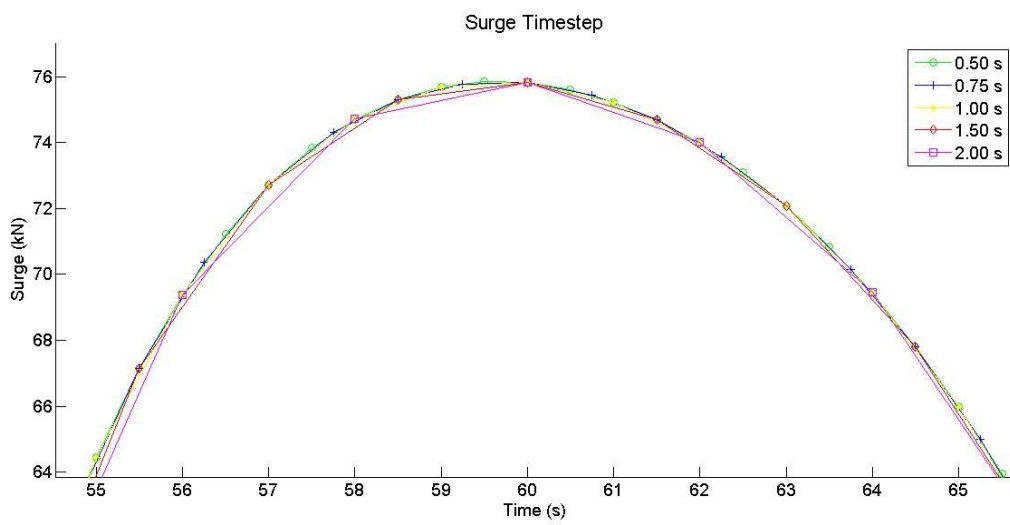


Figure F.5 Surge force for varying time step, zoom

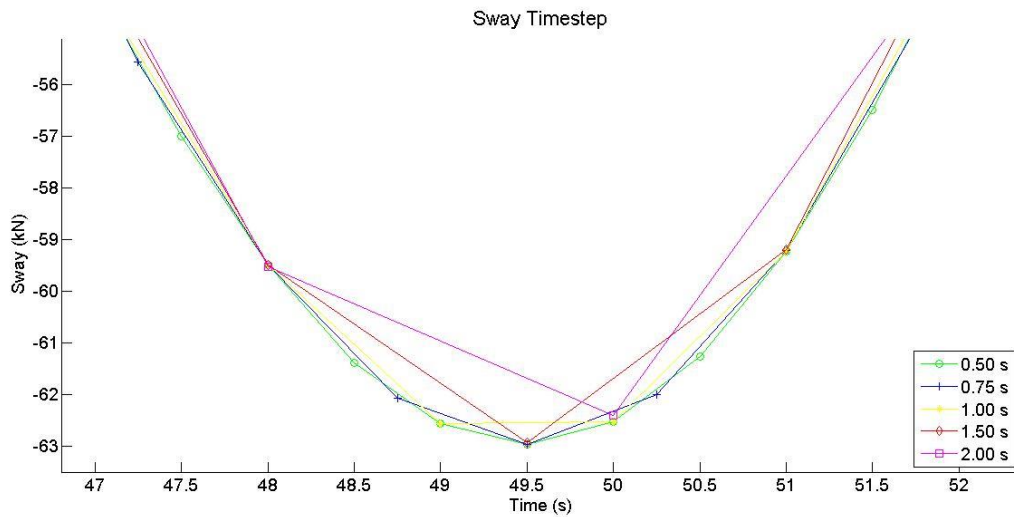


Figure F.6 Sway force for varying time step, zoom

SAILING DISTANCE

The distance sailed by the passing vessel, where half of the distance is sailed before the moored vessel, and half after, is varied from 300 to 600 m. Figure F.7 and Figure F.8 show the surge and sway force respectively. It is obvious that the sailing distance does not affect the shape of the curves. However to have a complete view of the effects of the passing ship, at least 500 m should be sailed in this case. In selecting the sailing distance, one should take care to incorporate the entire event. This is of course dependent on the size of the moored vessel and the harbour geometry.

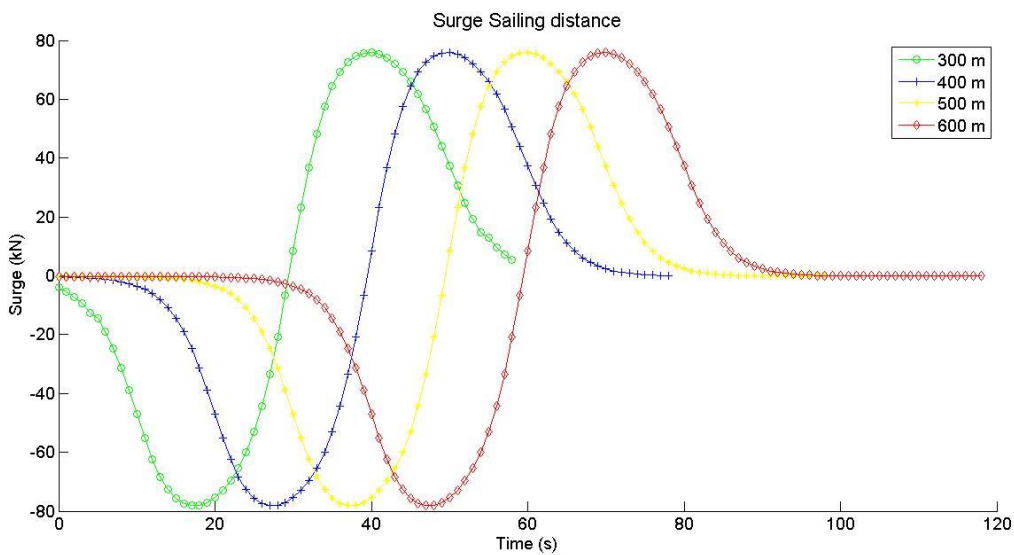


Figure F.7 Surge force for varying sailing distance

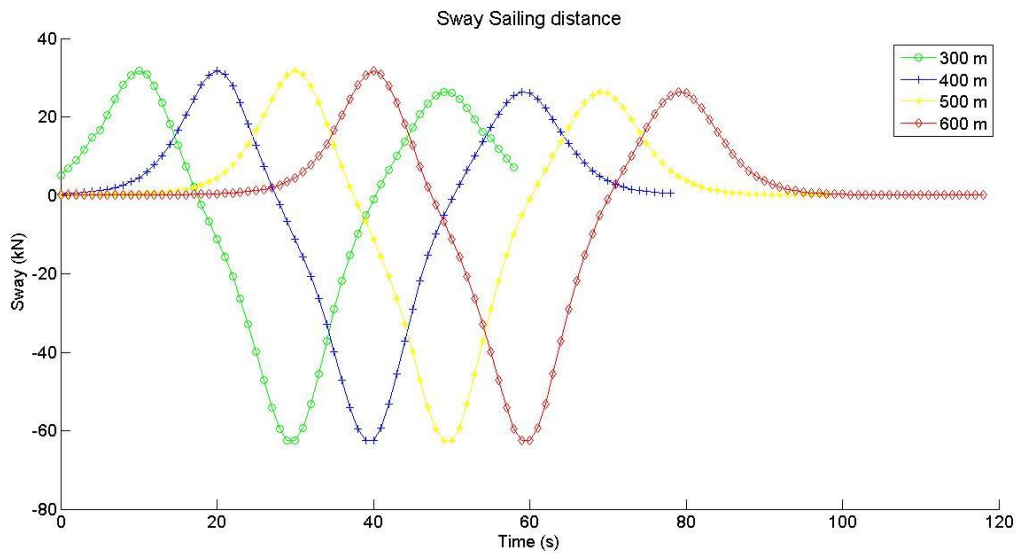


Figure F.8 Sway force for varying sailing distance

CANAL LENGTH

If the canal is not made long enough, effects will be visible caused by the end of the canal. The sailing distance is kept at 500 m, while the canal length is varied from 500 to 1000 m. Figure F.9 shows the surge force and , Figure F.11 a zoom at the first seconds. Figure F.10 shows the sway force and Figure F.12 the heave force. While for the sway force, the canal length does not seem to have much effect and the surge force is only influenced in the beginning of the simulation, which is not at the peak, the heave is strongly affected by the canal length. Two times the sailing distance seems to be an appropriate waterway length.

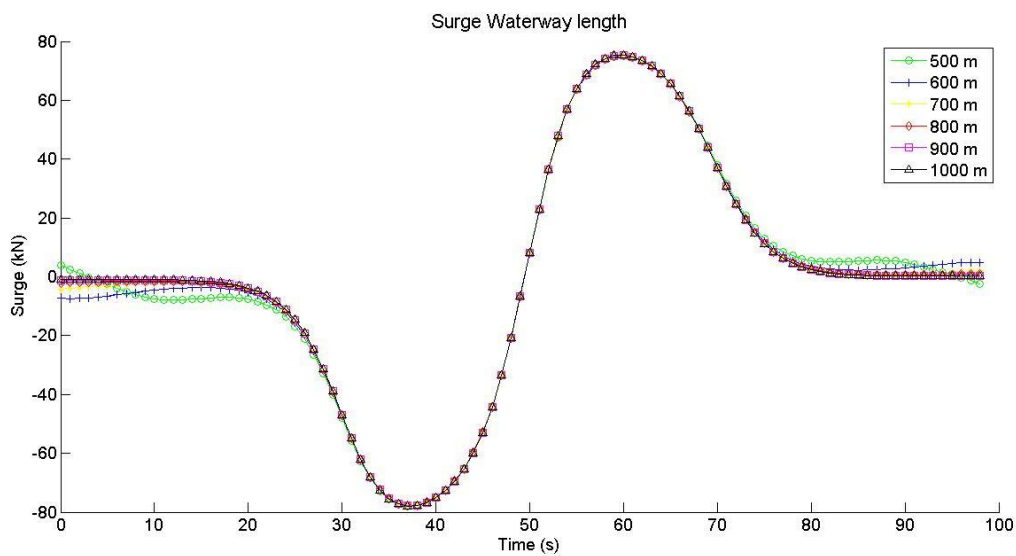


Figure F.9 Surge force for varying waterway length

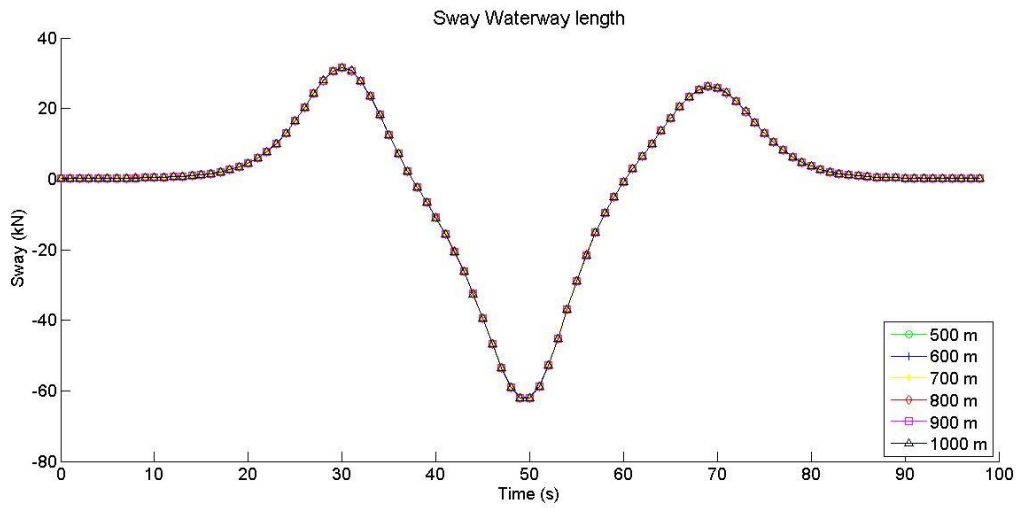


Figure F.10 Sway force for varying waterway length

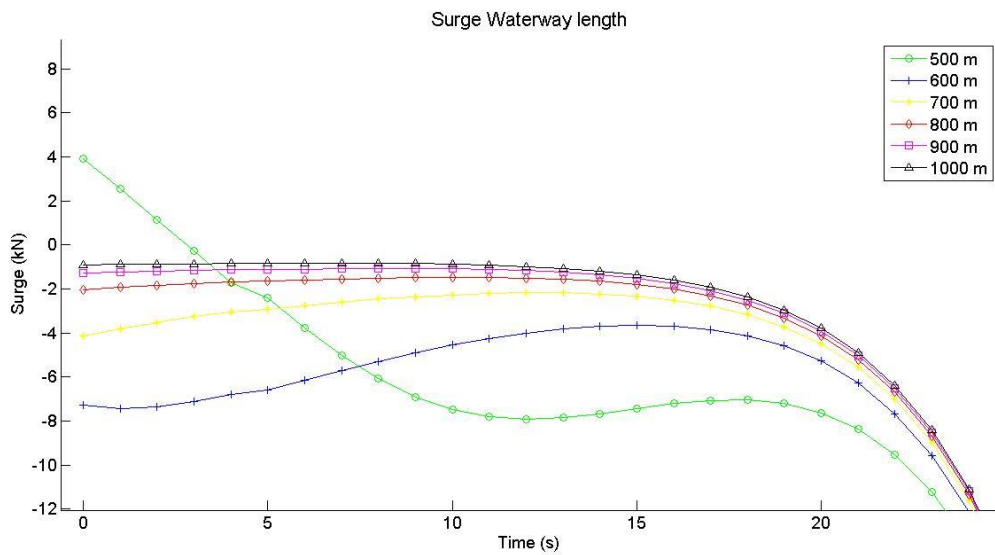


Figure F.11 Surge force for varying waterway length, zoom

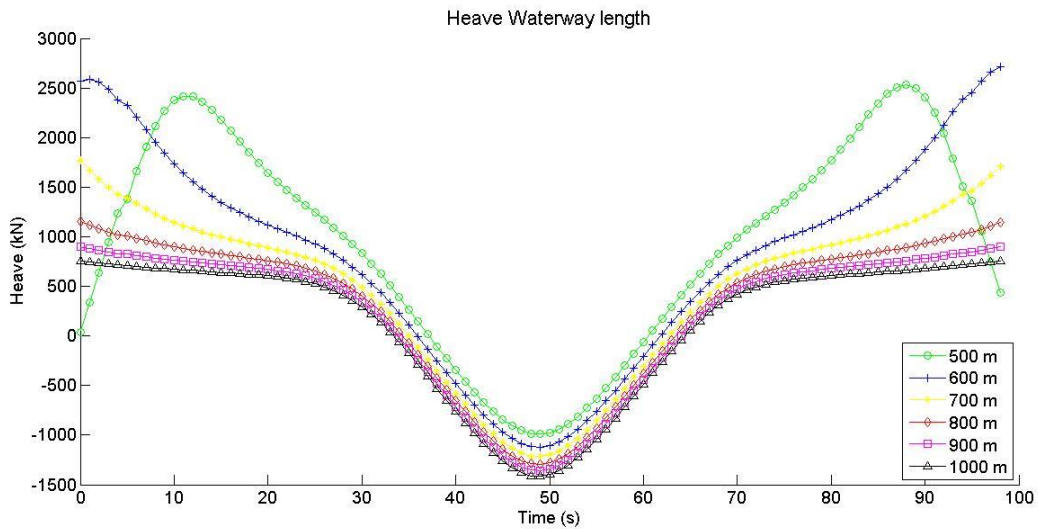


Figure F.12 Heave force for varying waterway length

HARBOUR GEOMETRY

Next, the harbour geometry of the ARK is modelled. In Figure 2.4 the cross section of the ARK is displayed. The width of the flat bottom will be taken as 61.6 m. This makes the total width of the ARK 100 m.

In the new harbour geometry, a new sailing distance is necessary. Figure F.13 and Figure F.14 show the surge and sway force for a sailing distance of 500 m, 750 m and 1000 m. For this harbour geometry, a sailing distance of 750 m is chosen.

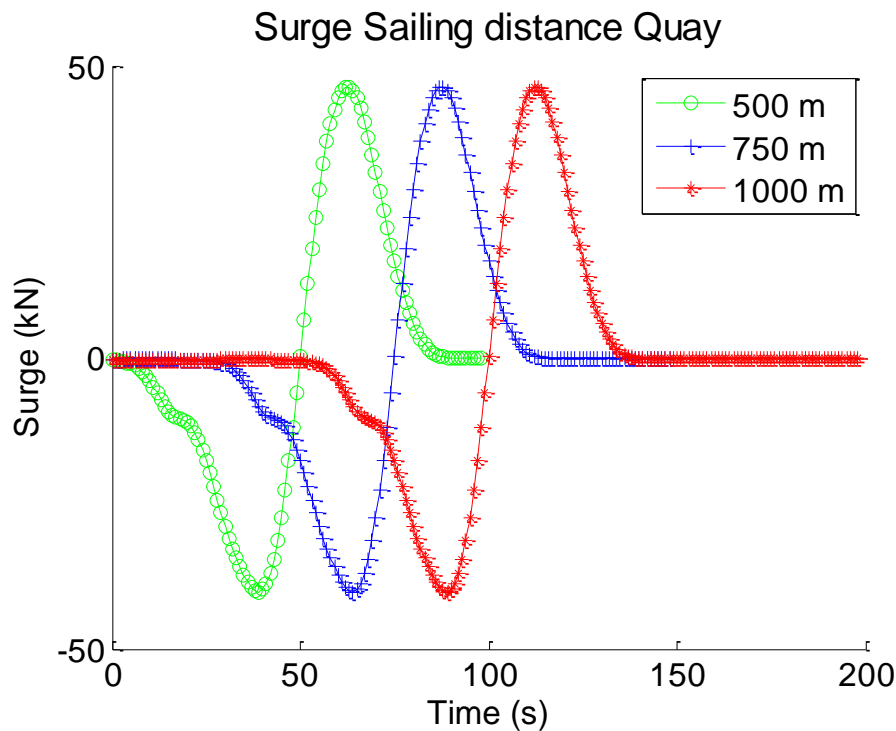


Figure F.13 Surge force for varying sailing distances with quay

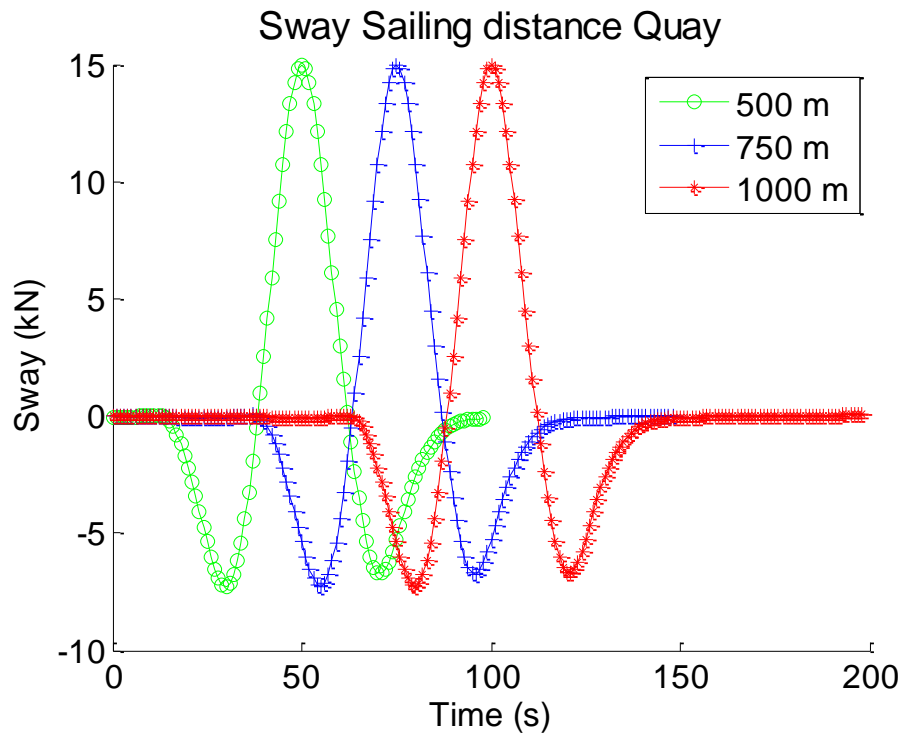


Figure F.14 Sway force for varying sailing distances with quay

Earlier it was concluded that the canal should be twice as long as the sailing distance. In this case that would imply a 1500 m waterway. To check, a waterway of 1500 m and 1250 m are simulated. The results of the are shown in Figure F.15 and Figure F.16. As with the straight channel, surge and sway do not show a great deviation, but heave is already significantly changed when changing the length to 1250. The length of the waterway will thus be kept at 1500 m.

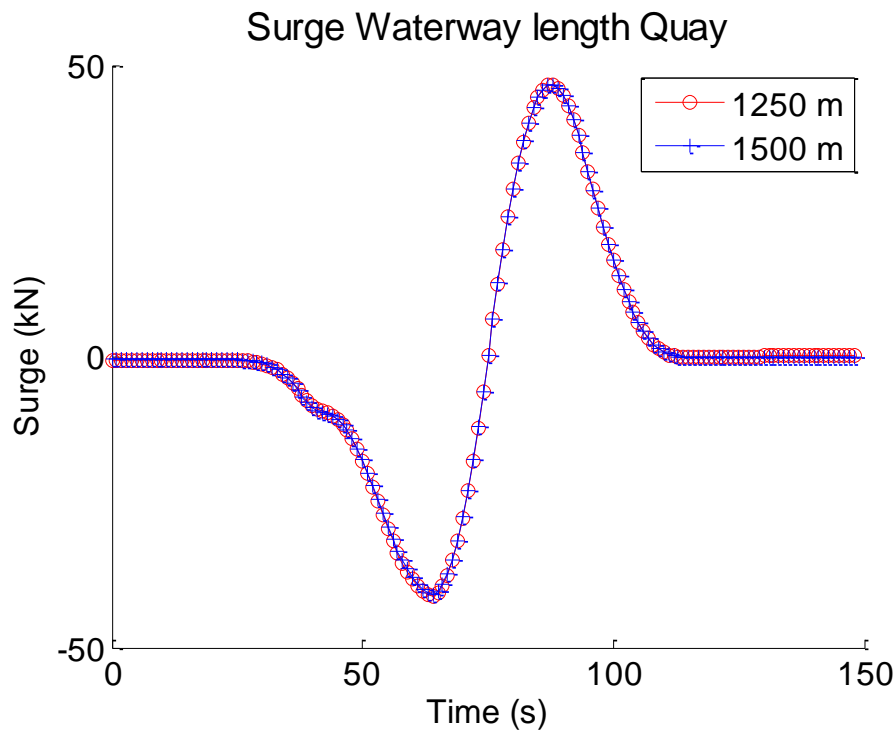


Figure F.15 Surge force for varying waterway length with quay

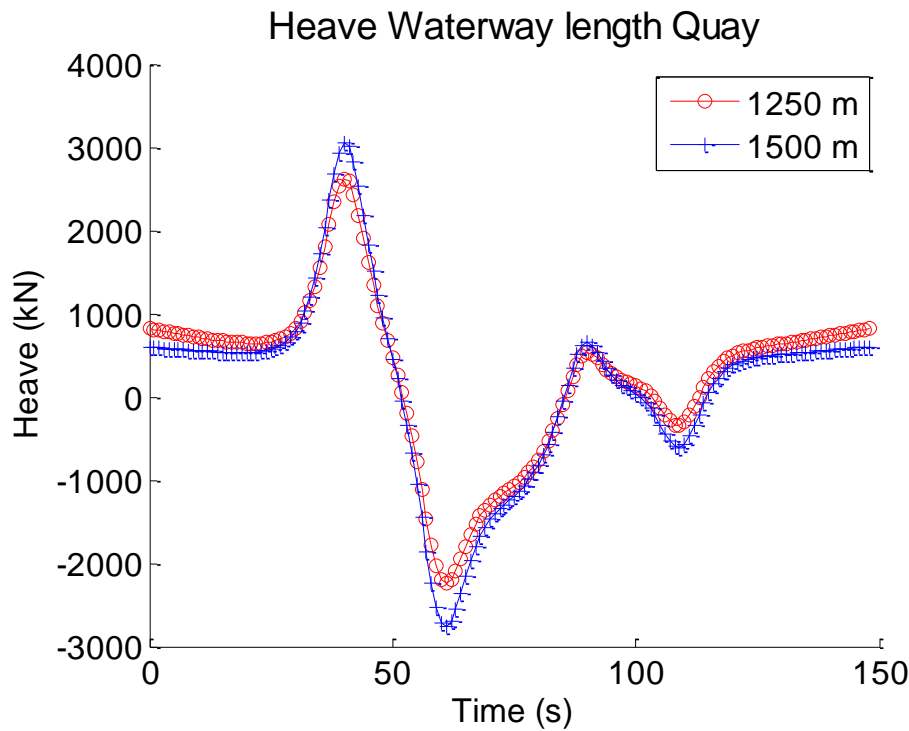


Figure F.16 Heave force for varying waterway length with quay

PANEL SIZE

To improve the computing time, it is investigated if the default size of 5 m per panel can be increased without much loss of accuracy. The panel size is systematically varied in three regions, to be known as the walls directly surrounding the moored vessel, the walls up to the starting point of the sailing vessel plus a margin and the outer part of the walls. Figure F.17 shows the three regions in red, region 1, blue region 2, and yellow, region 3.

In order to keep all motions within 1% deviation from the default panel size, the panel size in region 1 can be increased to 6 m per panel. The other regions will have to remain 5 m per panel. Since this alteration will not reduce the computation time significantly, the standard 5 m/panel will be used.

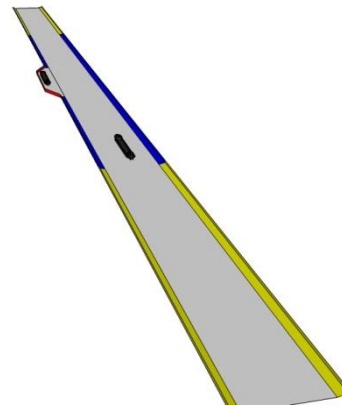


Figure F.17 Regions panelsizes

APPENDIX G. MATLAB SCRIPT ONE DOF MODEL

```
clear
```

TIME

```
T_step = 0.1;           % Timestep in s
T_sim = 400;           % Simulation time in s
T = linspace(0,T_sim,(T_sim/T_step)+1).'; % Generate time vector
```

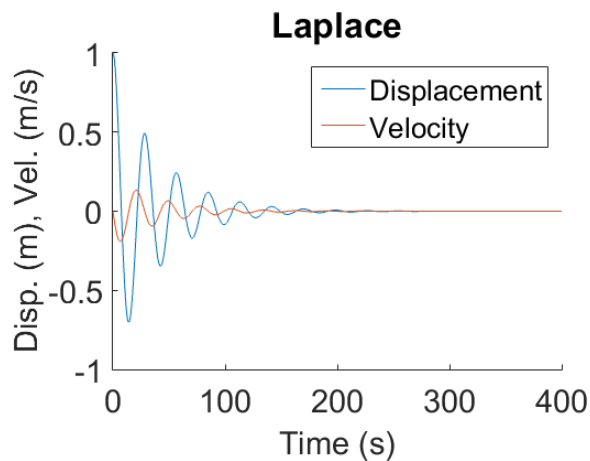
VARIABLES

```
p=-0.5;           % proportional gain
d=-0.5;           % differential gain
u_0=1;            % initial value displacement in m
du_0=0;           % initial value velocity in m/s
Fmax=100000;      % maximum force unit in N
m=1000000;        % mass of system in kg
```

LAPLACE

```
u=zeros(length(T),1);
du=zeros(length(T),1);
a=(d*Fmax)/(2*m);
b=sqrt(-(p*Fmax/m)-(d^2*Fmax^2)/(4*m^2));

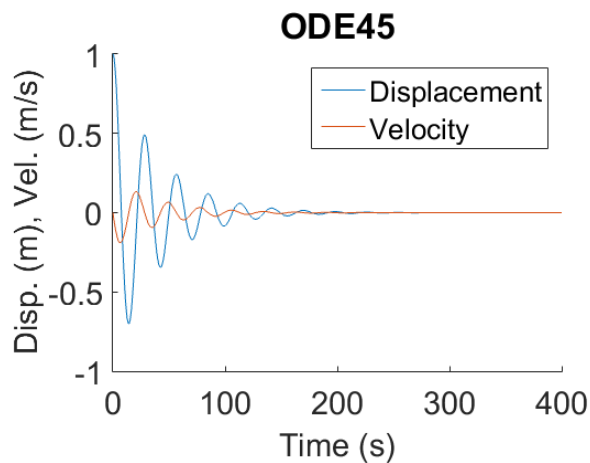
for i=1:length(T)
    u(i)= u_0*exp(a*T(i))*cos(b*T(i))+(du_0/b-u_0*(a/b))*exp(a*T(i))*sin(b*T(i));
    if i==1
        du(i)=du_0;
    else
        du(i)=(u(i)-u(i-1))/T_step;
    end
end
figure
hold on
plot(T,u);
plot(T,du);
title('Laplace', 'FontSize', 24);
xlabel('Time (s)', 'FontSize', 22);
ylabel('Disp. (m), vel. (m/s)', 'FontSize', 22);
legend('Displacement', 'Velocity');
set(gca, 'fontsize', 22)
```



ODE45

```
[t,y] = ode45(@(t,y) MydiffOneDOF(t,y,m,Fmax,d,p), [T(1),T(length(T))], [u_0 du_0]);
```

```
figure
hold on
plot(t,y);
title('ODE45', 'FontSize', 24);
xlabel('Time (s)', 'FontSize', 22);
ylabel('Disp. (m), vel. (m/s)', 'FontSize', 22);
legend('Displacement', 'velocity');
set(gca, 'fontsize', 22)
```



ODE45 PER TIME STEP

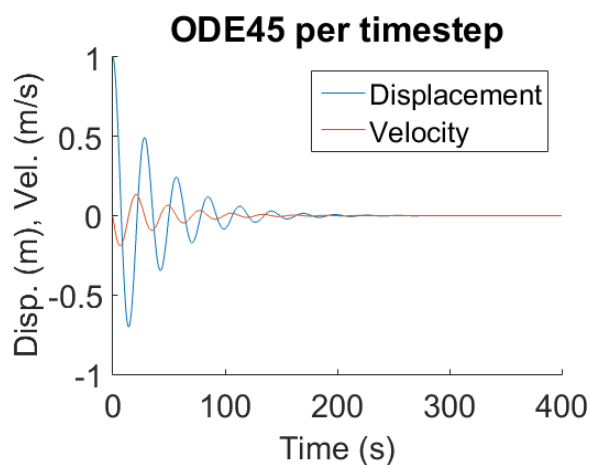
```
for i=1:length(T)
    if i==1 % First time step, use initial values for displacement and velocity
        [t,y] = ode45(@(t,y) MydiffOneDOF(t,y,m,Fmax,d,p), [T(i),T(i+1)], [u_0 du_0]);
    elseif i==length(T) % Last time step, use time length of one more time step
        [t,y] = ode45(@(t,y) MydiffOneDOF(t,y,m,Fmax,d,p), [T(i),T(i)+T_step], [U(i-1) du(i-1)]);
    else % Every other timestep, use time length form this time step until the next, use previous outcomes for displacement and velocity
        [t,y] = ode45(@(t,y) MydiffOneDOF(t,y,m,Fmax,d,p), [T(i),T(i+1)], [U(i-1) du(i-1)]);
    end
end
```

```

end
    U(i,:) = y(41,1); % displacement
    du(i,:) = y(41,2); % velocity
end

figure
hold on
plot(T,U);
plot(T,du);
title('ODE45 per timestep', 'FontSize', 24);
xlabel('Time (s)', 'FontSize', 22);
ylabel('Disp. (m), Vel. (m/s)', 'FontSize', 22);
legend('Displacement', 'velocity');
set(gca, 'fontsize',22)

```



ODE45 PER TIME STEP WITH SATURATION

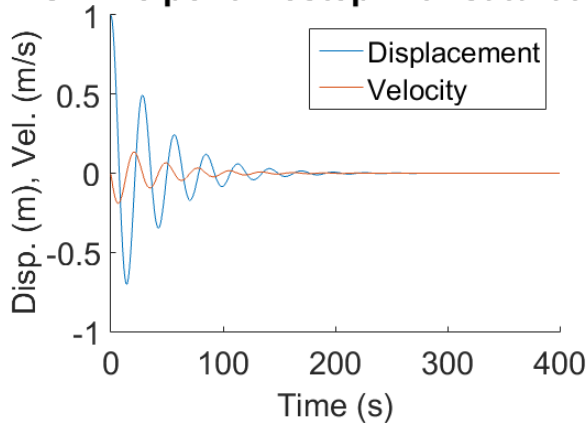
```

for i=1:length(T)
    if i==1 % First time step, use initial values for displacement and velocity
        [t,y] = ode45(@(t,y) MydiffOneDOFSat(t,y,m,Fmax,d,p), [T(i),T(i+1)], [u_0 du_0]);
    elseif i==length(T) % Last time step, use time length of one more time step
        [t,y] = ode45(@(t,y) MydiffOneDOFSat(t,y,m,Fmax,d,p), [T(i),T(i)+T_step], [U(i-1)
du(i-1)]);
    else % Every other timestep, use time length form this time step until the next, use
previous outcomes for displacement and velocity
        [t,y] = ode45(@(t,y) MydiffOneDOFSat(t,y,m,Fmax,d,p), [T(i),T(i+1)], [U(i-1) du(i-
1)]);
    end
    U(i,:) = y(41,1); % displacement
    du(i,:) = y(41,2); % velocity
end

figure
hold on
plot(T,U);
plot(T,du);
title('ODE45 per timestep with saturation', 'FontSize', 24);
xlabel('Time (s)', 'FontSize', 22);
ylabel('Disp. (m), Vel. (m/s)', 'FontSize', 22);
legend('Displacement', 'velocity');
set(gca, 'fontsize',22)

```

ODE45 per timestep with saturation



ODE45 PER TIME STEP WITH SATURATION, FORCE CALCULATED SEPERATELY WITH TIME DELAY

```

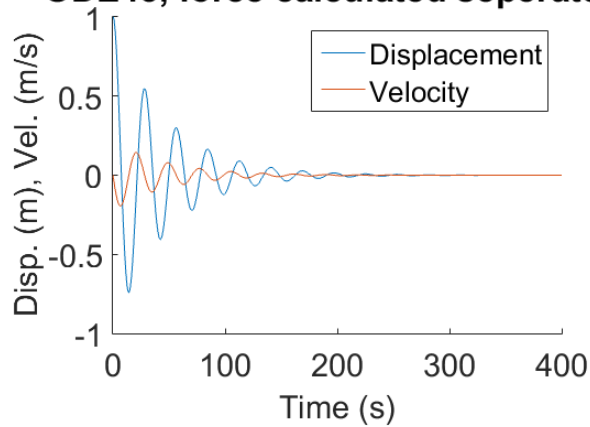
for i=1:length(T)
    if i==1 || i==2           %Due to time delay, first two time steps no force
        Fex=0;
    elseif (d*Fmax*dU(i-2)+p*Fmax*U(i-2)) >= Fmax % if force larger than max, use max force
        Fex=Fmax;
    elseif (d*Fmax*dU(i-2)+p*Fmax*U(i-2)) <= -Fmax
        Fex=-Fmax;
    else
        Fex=d*Fmax*dU(i-2)+p*Fmax*U(i-2); % calculate force using displacement and
        velocities of two time steps ago
    end

    if i==1 % First time step, use initial values for displacement and velocity
        [t,y] = ode45(@(t,y) MydiffOneDOFsep(t,y,m,Fex), [T(i),T(i+1)], [u_0 du_0]);
    elseif i==length(T) % Last time step, use time length of one more time step
        [t,y] = ode45(@(t,y) MydiffOneDOFsep(t,y,m,Fex), [T(i),T(i)+T_step], [U(i-1) dU(i-
1)]);
    else % Every other timestep, use time length form this time step until the next, use
    previous outcomes for displacement and velocity
        [t,y] = ode45(@(t,y) MydiffOneDOFsep(t,y,m,Fex), [T(i),T(i+1)], [U(i-1) dU(i-1)]);
    end
    U(i,:) = y(41,1); % displacement
    dU(i,:) = y(41,2); % velocity
end

figure
hold on
plot(T,U);
plot(T,dU);
title('ODE45, force calculated seperately', 'FontSize', 24);
xlabel('Time (s)', 'FontSize', 22);
ylabel('Disp. (m), Vel. (m/s)', 'FontSize', 22);
legend('Displacement', 'velocity');
set(gca, 'fontsize',22)

```

ODE45, force calculated separately



DIFFERENTIAL FUNCTIONS

```
function dy = MydiffOneDOF(t,y, m, Fmax, d, p)
```

```
dy(1,1)= y(2);
```

```
dy(2,1)=((d*Fmax*y(2))+(p*Fmax*y(1)))/m;
```

```
function dy = MydiffOneDOFsat(t,y, m, Fmax, d, p)
```

```
if (d*Fmax*y(2))+(p*Fmax*y(1)) >= Fmax
```

```
dy(1,1)= y(2);
```

```
dy(2,1)=Fmax/m;
```

```
elseif (d*Fmax*y(2))+(p*Fmax*y(1)) <= -Fmax
```

```
dy(1,1)= y(2);
```

```
dy(2,1)=-Fmax/m;
```

```
else
```

```
dy(1,1)= y(2);
```

```
dy(2,1)=((d*Fmax*y(2))+(p*Fmax*y(1)))/m;
```

```
end
```

```
function dy = MydiffOneDOFsep(t,y, m, Fext)
```

```
dy(1,1)= y(2);
```

```
dy(2,1)=Fext/m;
```

```
end
```

[Published with MATLAB® R2015a](#)

APPENDIX H. MATLAB SCRIPT TWO DOF MODEL: SWAY AND YAW

TIME

```
T_step = 0.1; % Timestep in s
T_sim = 500; % Simulation time in s
T = linspace(0,T_sim,(T_sim/T_step)+1).'; % Generate time vector
```

VARIABLES

```
B=11;
p=-0.5;
d=-0.5;
u_0=[-0.5 0.003];
du_0=[0 0];
Fmax=100000;
m=1000000;
I=3*10^9;
Pos = [-30 40];

% Constants:
a_1 = (d*Fmax)/(m);
b_1 = sqrt(-(2*p*Fmax/m)-(d^2*Fmax^2)/(m^2));
k = (Fmax/m)*sum(Pos);
Q = Fmax*sum(Pos.^2)/I;
R = Fmax*sum(Pos)/I;
a_2 = Q*d/2;
b_2 = sqrt(-Q*p-a_2^2);
```

LAPLACE

```
u=zeros(length(T),2);
du=zeros(length(T),2);

% Convolution integrals
int_11=zeros(length(T),1);
int_12=zeros(length(T),1);
int_21=zeros(length(T),1);
int_22=zeros(length(T),1);

int_1total = zeros(length(T),1);
int_2total = zeros(length(T),1);

for i=1:length(T)

    if i==1
    elseif i==2
    else
        int_11(i) = (k*p/b_1)*integral(@(tau) interp1(T,u(:,2),tau).*exp(a_1*(T(i)-tau)).*sin(b_1*(T(i)-tau)),T(2),T(i));
        int_12(i) = (k*d/b_1)*integral(@(tau) interp1(T,du(:,2),tau).*exp(a_1*(T(i)-tau)).*sin(b_1*(T(i)-tau)),T(2),T(i));
```

```

    int_21(i) = (R*p/b_2)*integral(@(tau) interp1(T,u(:,1),tau).*exp(a_2*(T(i)-
tau)).*sin(b_2*(T(i)-tau)),T(2),T(i));
    int_22(i) = (R*d/b_2)*integral(@(tau) interp1(T,du(:,1),tau).*exp(a_2*(T(i)-
tau)).*sin(b_2*(T(i)-tau)),T(2),T(i));

    int_1total(i) = int_11(i)+int_12(i);
    int_2total(i) = int_21(i)+int_22(i);
end
% Calculation Laplace

    u(i,1)= u_0(1)*exp(a_1*T(i))*cos(b_1*T(i)) + ((du_0(1)-
a_1*u_0(1))/b_1)*exp(a_1*T(i))*sin(b_1*T(i)) + int_1total(i);
    u(i,2)= u_0(2)*exp(a_2*T(i))*cos(b_2*T(i)) + ((du_0(2)-
a_2*u_0(2))/b_2)*exp(a_2*T(i))*sin(b_2*T(i)) + int_2total(i);

% Differential
if i==1
    du(i,:)=du_0(1,:);
else
    du(i,)=(u(i,:)-u(i-1,:))/T_step;
end

end

```

ODE45

```

[l,w] = ode45(@(l,w) MydifftwoDOF(l,w,m,I,Fmax,d,p,Pos), [T(1),T(length(T))], [u_0(1) du_0(1)
u_0(2) du_0(2)]);

```

ODE45 PER TIME STEP

```

u_1=zeros(length(T),2);
du_1=zeros(length(T),2);

for i=1:length(T)
    if i==1 % First time step, use initial values for displacement and velocity
        [t_1,y_1] = ode45(@(t_1,y_1) MydifftwoDOF(t_1,y_1,m,I,Fmax,d,p,Pos), [T(i),T(i+1)],
[u_0(1) du_0(1) u_0(2) du_0(2)]);
    elseif i==length(T)% Last time step, use time length of one more time step
        [t_1,y_1] = ode45(@(t_1,y_1) MydifftwoDOF(t_1,y_1,m,I,Fmax,d,p,Pos),
[T(i),T(i)+T_step], [u_1(i-1,1) du_1(i-1,1) u_1(i-1,2) du_1(i-1,2)]);
    else % Every other timestep, use time length form this time step until the next, use
previous outcomes for displacement and velocity
        [t_1,y_1] = ode45(@(t_1,y_1) MydifftwoDOF(t_1,y_1,m,I,Fmax,d,p,Pos), [T(i),T(i+1)],
[u_1(i-1,1) du_1(i-1,1) u_1(i-1,2) du_1(i-1,2)]);
    end

    u_1(i,1) = y_1(end,1); % displacement
    u_1(i,2) = y_1(end,3);
    du_1(i,1) = y_1(end,2); % velocity
    du_1(i,2) = y_1(end,4);

end

```

ODE45 PER TIME STEP WITH SATURATION

```

u_2=zeros(length(T),2);
du_2=zeros(length(T),2);

for i=1:length(T)
    if i==1 % First time step, use initial values for displacement and velocity
        [t_2,y_2] = ode45(@(t_2,y_2) MydifftwoDOFsat(t_2,y_2,m,I,Fmax,d,p,Pos), [T(i),T(i+1)],
[u_0(1) du_0(1) u_0(2) du_0(2)]);
    elseif i==length(T) % Last time step, use time length of one more time step
        [t_2,y_2] = ode45(@(t_2,y_2) MydifftwoDOFsat(t_2,y_2,m,I,Fmax,d,p,Pos),
[T(i),T(i)+T_step], [u_2(i-1,1) du_2(i-1,1) u_2(i-1,2) du_2(i-1,2)]);
    else % Every other timestep, use time length form this time step until the next, use
previous outcomes for displacement and velocity
        [t_2,y_2] = ode45(@(t_2,y_2) MydifftwoDOFsat(t_2,y_2,m,I,Fmax,d,p,Pos), [T(i),T(i+1)],
[u_2(i-1,1) du_2(i-1,1) u_2(i-1,2) du_2(i-1,2)]);
    end

    u_2(i,1) = y_2(end,1); % displacement
    u_2(i,2) = y_2(end,3);
    du_2(i,1) = y_2(end,2); % velocity
    du_2(i,2) = y_2(end,4);

end

```

ODE45 per time step with saturation, force calculated seperately with time delay

```

U=zeros(length(T),2);
dU=zeros(length(T),2);
y_extra=zeros(length(T),length(Pos));
dy_extra=zeros(length(T),length(Pos));

for i=1:length(T)

    if i==1 || i==2
        Fextotal(i)=0;
        Mextotal(i)=0;
    else
        for j=1:length(Pos)
            y_extra(i,j) = Pos(j)*sin(U(i-2,2))+(B/2)-(B/2)*cos(U(i-2,2));
            dy_extra(i,j) = (y_extra(i,j)-y_extra(i-1,j))/T_step;

            Fex(i,j)=Fmax*(p*(U(i-2,1)+y_extra(i,j))+d*(dU(i-2,1)+dy_extra(i,j)));
            if Fex(i,j) >= Fmax
                Fex(i,j)=Fmax;
            elseif Fex(i,j) <= -Fmax
                Fex(i,j) = -Fmax;
            end
            Mex(i,j)=Pos(j)*Fex(i,j);
        end
        Fextotal(i) = sum(Fex(i,:));
        Mextotal(i) = sum(Mex(i,:));
    end
end

```

```

if i==1 % First time step, use initial values for displacement and velocity
    [t,y] = ode45(@(t,y) MydiftwoDOFsep(t,y,m, I, Fextotal(i), Mexttotal(i)),
[T(i),T(i+1)], [u_0(1,1) du_0(1,1) u_0(1,2) du_0(1,2)]);
    elseif i==length(T) % Last time step, use time length of one more time step
        [t,y] = ode45(@(t,y) MydiftwoDOFsep(t,y,m,I,Fextotal(i),Mexttotal(i)),
[T(i),T(i)+T_step], [U(i-1,1) dU(i-1,1) U(i-1,2) dU(i-1,2)]);
    else % Every other timestep, use time length form this time step until the next, use
previous outcomes for displacement and velocity
        [t,y] = ode45(@(t,y) MydiftwoDOFsep(t,y,m,I,Fextotal(i),Mexttotal(i)), [T(i),T(i+1)],
[U(i-1,1) dU(i-1,1) U(i-1,2) dU(i-1,2)]);
    end
    U(i,1) = y(41,1); % displacement
    U(i,2) = y(41,3);
    du(i,1) = y(41,2); % velocity
    du(i,2) = y(41,4);
end

U(:,2)=rattodeg(U(:,2));
du(:,2)=rattodeg(du(:,2));

u(:,2)=rattodeg(u(:,2));
du(:,2)=rattodeg(du(:,2));

```

DIFFERENTIAL FUNCTIONS

```

function dy = MydiftwoDOF(t,y, m, I, Fmax, d, p, Pos)

dy(1,1)= y(2);
dy(2,1)= (2*Fmax*(p*y(1)+d*y(2))+Fmax*sum(Pos)*(p*y(3)+d*y(4)))/m;
dy(3,1)= y(4);
dy(4,1)= (Fmax*sum(Pos)*(p*y(1)+d*y(2))+Fmax*sum(Pos.^2)*(p*y(3)+d*y(4)))/I;

```

```

function dy = MydiftwoDOFsat(t,y, m, I, Fmax, d, p, Pos)
Fex = zeros(length(Pos),1);
Mex = zeros(length(Pos),1);

for j=1:length(Pos)
    Fex(j)=Fmax*(p*y(1)+d*y(2))+Fmax*Pos(j)*(p*y(3)+d*y(4));
    if Fex(j) >= Fmax
        Fex(j)=Fmax;
    elseif Fex(j) <= -Fmax
        Fex(j) = -Fmax;
    end
    Mex(j)=Pos(j)*Fex(j);
end
Fextotal = sum(Fex);
Mexttotal = sum(Mex);

```

```
dy(1,1)= y(2);  
dy(2,1)= Fexttotal/m;  
dy(3,1)= y(4);  
dy(4,1)= Mexttotal/I;
```

```
function dy = MydifftwoDOFsep(t,y, m, I, Fext, Mext)  
  
    dy(1,1)= y(2);  
    dy(2,1)=Fext/m;  
    dy(3,1)= y(4);  
    dy(4,1)=Mext/I;  
end
```

[Published with MATLAB® R2015a](#)

TIME

```
T_step = 0.1;           % Timestep in s
T_sim = 400;           % Simulation time in s
T = linspace(0,T_sim,(T_sim/T_step)+1).'; % Generate time vector
```

VARIABLES

```
p=-0.5;
d=-0.5;
B = 11;
u_0=[1 0.001];
du_0=[0 0];
Fmax=100000;
m=1000000;
I=3*10^9;
Pos = [-30 40];

% Constants:
a_1 = (d*Fmax)/(m);
b_1 = sqrt(-(2*p*Fmax/m)-(d^2*Fmax^2)/(m^2));
k = (Fmax/m)*sum(Pos);
Q = Fmax*sum(Pos.^2)/I;
R = Fmax*sum(Pos)/I;
a_2 = Q*d/2;
b_2 = sqrt(-Q*p-a_2^2);
```

ODE45

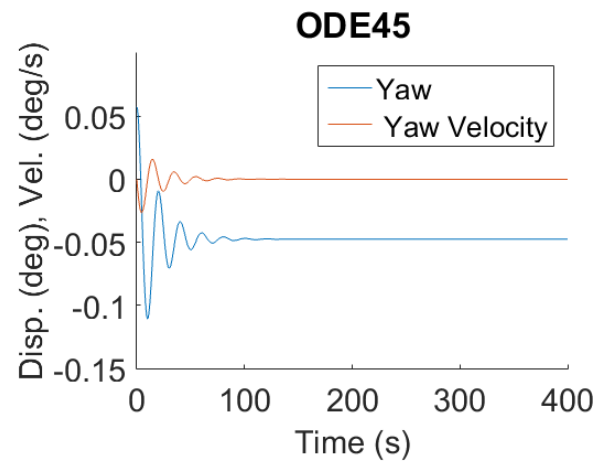
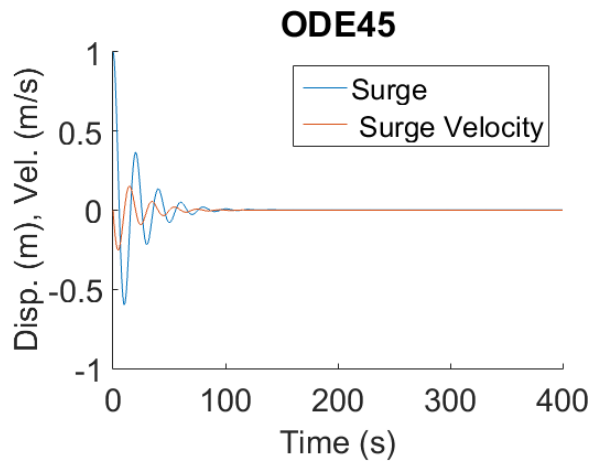
```
[t,w] = ode45(@(t,w) MydiffTwoDOFSurge(t,w,m,I,Fmax,d,p,Pos,B), [T(1),T(length(T))], [u_0(1)
du_0(1) u_0(2) du_0(2)]);

w(:,3) = radtodeg(w(:,3));
w(:,4) = radtodeg(w(:,4));

figure
hold on
plot(t,w(:,1:2));
title('ODE45', 'FontSize', 24);
xlabel('Time (s)', 'FontSize', 22);
ylabel('Disp. (m), Vel. (m/s)', 'FontSize', 22);
legend('Surge', ' Surge Velocity');
set(gca, 'fontsize',22)

figure
hold on
plot(t,w(:,3:4));
title('ODE45', 'FontSize', 24);
xlabel('Time (s)', 'FontSize', 22);
ylabel('Disp. (deg), Vel. (deg/s)', 'FontSize', 22);
```

```
Legend('Yaw', 'Yaw Velocity');
set(gca, 'fontSize', 22)
```



ODE45 PER TIME STEP

```
U_1=zeros(length(T),2);
du_1=zeros(length(T),2);

for i=1:length(T)
    if i==1
        [t_1,x_1] = ode45(@(t_1,x_1) MydifftwoDOFSurge(t_1,x_1,m,I,Fmax,d,p,Pos,B),
[T(i),T(i+1)], [u_0(1) du_0(1) u_0(2) du_0(2)]);
    elseif i==length(T)
        [t_1,x_1] = ode45(@(t_1,x_1) MydifftwoDOFSurge(t_1,x_1,m,I,Fmax,d,p,Pos,B),
[T(i),T(i)+T_step], [U_1(i-1,1) du_1(i-1,1) U_1(i-1,2) du_1(i-1,2)]);
    else
        [t_1,x_1] = ode45(@(t_1,x_1) MydifftwoDOFSurge(t_1,x_1,m,I,Fmax,d,p,Pos,B),
[T(i),T(i+1)], [U_1(i-1,1) du_1(i-1,1) U_1(i-1,2) du_1(i-1,2)]);
    end

    U_1(i,1) = x_1(end,1);
    U_1(i,2) = x_1(end,3);
    du_1(i,1) = x_1(end,2);
    du_1(i,2) = x_1(end,4);

end

U_1(:,2) = radtodeg(U_1(:,2));
du_1(:,2) = radtodeg(du_1(:,2));

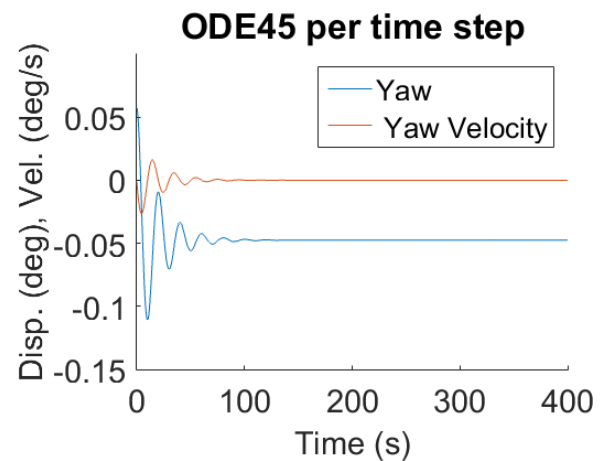
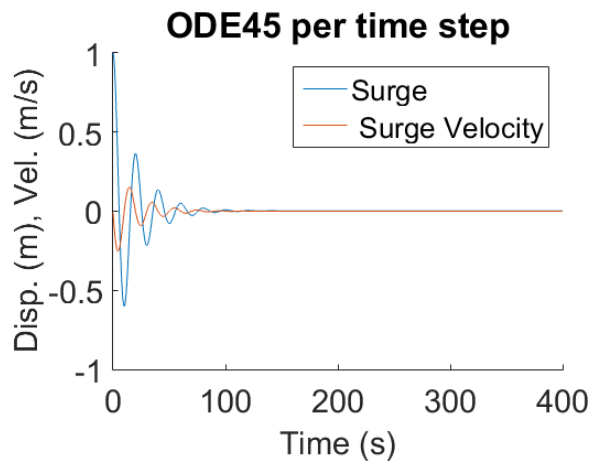
figure
hold on
plot(T,U_1(:,1));
plot(T,du_1(:,1));
title('ODE45 per time step', 'FontSize', 24);
xlabel('Time (s)', 'FontSize', 22);
ylabel('Disp. (m), Vel. (m/s)', 'FontSize', 22);
legend('Surge', 'Surge velocity');
set(gca, 'fontSize', 22)
```

figure

```

hold on
plot(T,U_1(:,2));
plot(T,dU_1(:,2));
title('ODE45 per time step', 'FontSize', 24);
xlabel('Time (s)', 'FontSize', 22);
ylabel('Disp. (deg), Vel. (deg/s)', 'FontSize', 22);
legend('Yaw',' Yaw Velocity');
set(gca, 'fontsize',22)

```



ODE45 PER TIME STEP WITH SATURATION, FORCE CALCULATED SEPERATELY WITH TIME DELAY

```

U=zeros(length(T),2);
dU=zeros(length(T),2);

for i=1:length(T)

    if i==1 || i==2
        Fextotal(i)=0;
        Mexttotal(i)=0;
    else
        for j=1:length(Pos)
            x_extra(i,j) = Pos(j)*cos(U(i-2,2))-Pos(j)+(B/2)*sin(U(i-2,2));
            dx_extra(i,j) = (x_extra(i,j)-x_extra(i-1,j))/T_step;

            Fex(i,j)=Fmax*(p*(U(i-2,1)+x_extra(i,j))+d*(dU(i-2,1)+dx_extra(i,j)));
            if Fex(i,j) >= Fmax
                Fex(i,j)=Fmax;
            elseif Fex(i,j) <= -Fmax
                Fex(i,j) = -Fmax;
            end

            Mex(i,j)=(B/2)*Fex(i,j);

        end
        Fextotal(i) = sum(Fex(i,:));
        Mexttotal(i) = sum(Mex(i,:));
    end
end

```

```

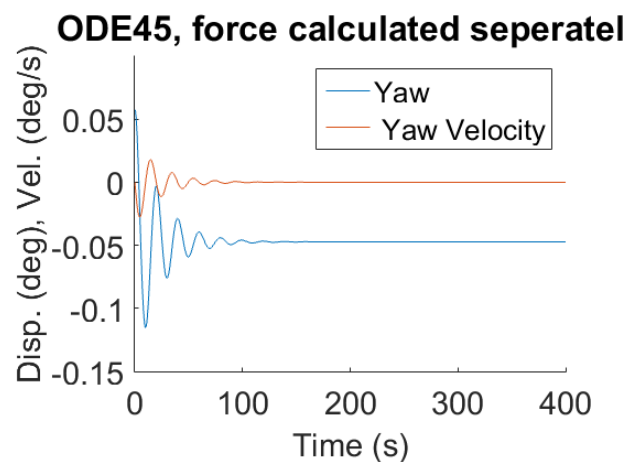
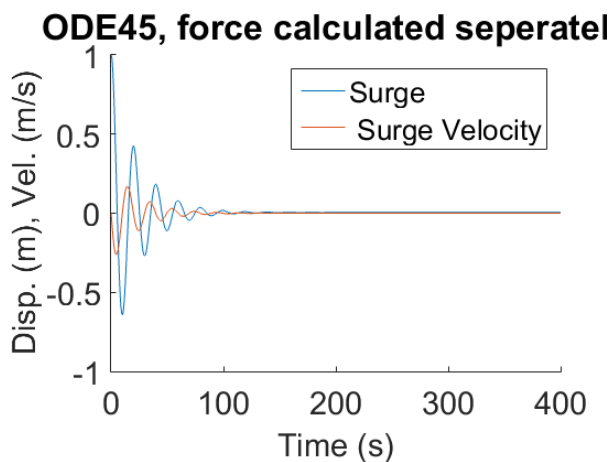
if i==1 % First time step, use initial values for displacement and velocity
    [t,x] = ode45(@(t,x) MydifftwoDOFsep(t,x,m, I, Fexttotal(i), Mexttotal(i)),
    [T(i),T(i+1)], [u_0(1,1) du_0(1,1) u_0(1,2) du_0(1,2)]);
    elseif i==length(T) % Last time step, use time length of one more time step
    [t,x] = ode45(@(t,x) MydifftwoDOFsep(t,x,m,I,Fexttotal(i),Mexttotal(i)),
    [T(i),T(i)+T_step], [U(i-1,1) dU(i-1,1) U(i-1,2) dU(i-1,2)]);
    else % Every other timestep, use time length form this time step until the next, use
    previous outcomes for displacement and velocity
    [t,x] = ode45(@(t,x) MydifftwoDOFsep(t,x,m,I,Fexttotal(i),Mexttotal(i)), [T(i),T(i+1)],
    [U(i-1,1) dU(i-1,1) U(i-1,2) dU(i-1,2)]);
    end
    U(i,1) = x(41,1); % displacement
    U(i,2) = x(41,3);
    dU(i,1) = x(41,2); % velocity
    dU(i,2) = x(41,4);
end

U(:,2) = radtodeg(U(:,2));
dU(:,2) = radtodeg(dU(:,2));

figure
hold on
plot(T,U(:,1));
plot(T,dU(:,1));
title('ODE45, force calculated seperately', 'FontSize', 24);
xlabel('Time (s)', 'FontSize', 22);
ylabel('Disp. (m), Vel. (m/s)', 'FontSize', 22);
legend('Surge', ' Surge Velocity');
set(gca, 'fontsize',22)

figure
hold on
plot(T,U(:,2));
plot(T,dU(:,2));
title('ODE45, force calculated seperately', 'FontSize', 24);
xlabel('Time (s)', 'FontSize', 22);
ylabel('Disp. (deg), Vel. (deg/s)', 'FontSize', 22);
legend('Yaw', ' Yaw Velocity');
set(gca, 'fontsize',22)

```



DIFFERENTIAL FUNCTIONS

```
function dx = MydifftwoDOFsurge(t,x, m, I, Fmax, d, p, Pos, B)

n = length(Pos);

dx(1,1)= x(2);
dx(2,1)= (n*Fmax*(p*x(1)+d*x(2))+Fmax*(p*(sum(Pos)*(cos(x(3))-
1)+(B/2)*sin(x(3)))+d*((B/2)*cos(x(3))*x(4)-sum(Pos)*sin(x(3))*x(4)))/m;
dx(3,1)= x(4);
dx(4,1)= (1/2)*B*(n*Fmax*(p*x(1)+d*x(2))+Fmax*(p*(sum(Pos)*(cos(x(3))-
1)+(B/2)*sin(x(3)))+d*((B/2)*cos(x(3))*x(4)-sum(Pos)*sin(x(3))*x(4)))/I;
```

```
function dx = MydifftwoDOFsep(t,x, m, I, Fext, Mext)

dx(1,1)= x(2);
dx(2,1)=Fext/m;
dx(3,1)= x(4);
dx(4,1)=Mext/I;

end
```

[Published with MATLAB® R2015a](#)

APPENDIX J. MATLAB SCRIPT TWO DOF MODEL: SURGE AND SWAY

```
clear
```

TIME

```
T_step = 0.1; % Timestep in s
T_sim = 400; % Simulation time in s
T = linspace(0,T_sim,(T_sim/T_step)+1).'; % Generate time vector
```

VARIABLES

```
p=-0.5;
d=-0.5;
B = 11;
u_0=[1 -1];
du_0=[0 0];
Fmax=100000;
m=1000000;
I=3*10^9;
Pos = [-30 40];
```

ODE45 PER TIME STEP

```
U_1=zeros(length(T),2);
dU_1=zeros(length(T),2);

for i=1:length(T)
    if i==1
        [t_1,y_1] = ode45(@(t_1,y_1) MydifftwoDOFxy(t_1,y_1,m,Fmax,d,p), [T(i),T(i+1)],
[u_0(1) du_0(1) u_0(2) du_0(2)]);
    elseif i==length(T)
        [t_1,y_1] = ode45(@(t_1,y_1) MydifftwoDOFxy(t_1,y_1,m,Fmax,d,p), [T(i),T(i)+T_step],
[U_1(i-1,1) dU_1(i-1,1) U_1(i-1,2) dU_1(i-1,2)]);
    else
        [t_1,y_1] = ode45(@(t_1,y_1) MydifftwoDOFxy(t_1,y_1,m,Fmax,d,p), [T(i),T(i+1)],
[U_1(i-1,1) dU_1(i-1,1) U_1(i-1,2) dU_1(i-1,2)]);
    end

    U_1(i,1) = y_1(end,1);
    U_1(i,2) = y_1(end,3);
    dU_1(i,1) = y_1(end,2);
    dU_1(i,2) = y_1(end,4);

end

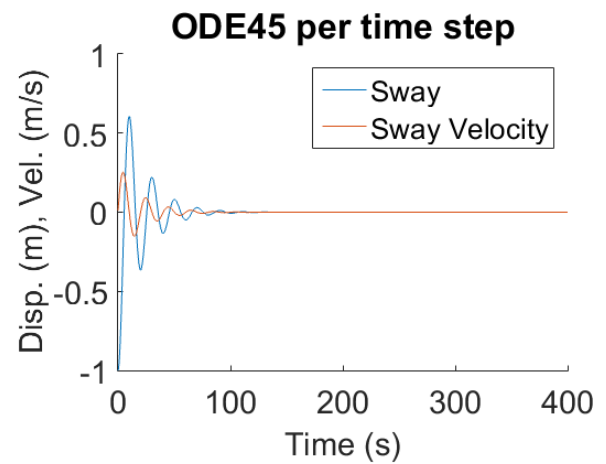
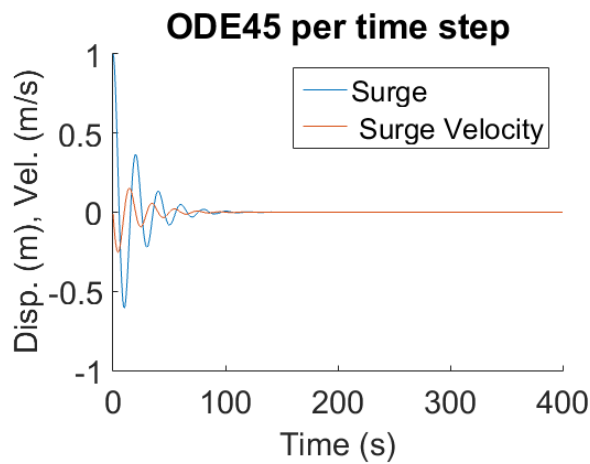
figure
hold on
plot(T,U_1(:,1));
plot(T,dU_1(:,1));
title('ODE45 per time step', 'FontSize', 24);
xlabel('Time (s)', 'FontSize', 22);
```

```

ylabel('Disp. (m), Vel. (m/s)', 'FontSize', 22);
legend('Surge', 'Surge Velocity');
set(gca, 'fontsize', 22)

figure
hold on
plot(T,U_1(:,2));
plot(T,du_1(:,2));
title('ODE45 per time step', 'FontSize', 24);
xlabel('Time (s)', 'FontSize', 22);
ylabel('Disp. (m), Vel. (m/s)', 'FontSize', 22);
legend('Sway', 'Sway Velocity');
set(gca, 'fontsize', 22)

```



ODE45 PER TIME STEP WITH SATURATION, FORCE CALCULATED SEPERATELY WITH TIME DELAY

```

u=zeros(length(T),2);
du=zeros(length(T),2);

for i=1:length(T)

    if i==1 || i==2
        Fextotal_x(i)=0;
        Fextotal_y(i)=0;
    else
        for j=1:length(Pos)
            Fex(i,j)=(Fmax*(p*sqrt(U(i-2,1)^2+U(i-2,2)^2)+d*((U(i-2,1)*du(i-2,1)+U(i-2,2)*du(i-2,2))/(sqrt(U(i-2,1)^2+U(i-2,2)^2)))));
            if Fex(i,j) >= Fmax
                Fex(i,j)=Fmax;
            elseif Fex(i,j) <= -Fmax
                Fex(i,j) = -Fmax;
            end
            Fex_x(i,j) = Fex(i,j)*cos(atan2(U(i-1,2),U(i-1,1)));
            Fex_y(i,j) = Fex(i,j)*sin(atan2(U(i-1,2),U(i-1,1)));
        end
    end
end

```

```

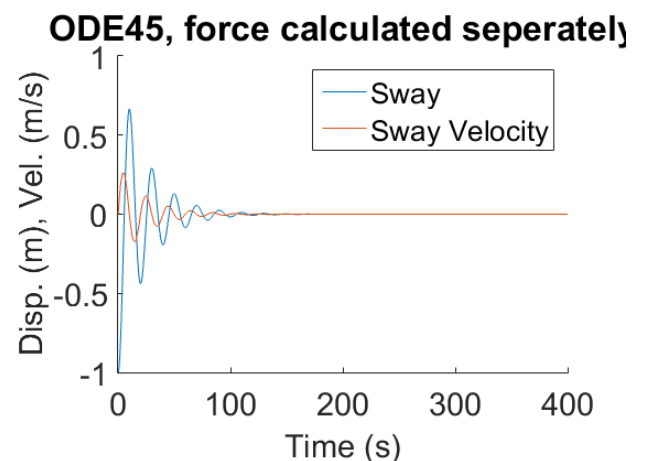
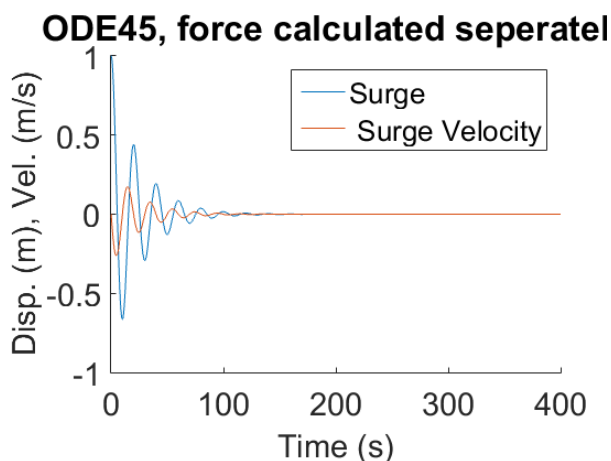
Fextotal_x(i) = sum(Fex_x(i,:));
Fextotal_y(i) = sum(Fex_y(i,:));
end

if i==1 % First time step, use initial values for displacement and velocity
    [t,y] = ode45(@(t,y) MydiftwoDOFsepxy(t,y,m, Fextotal_x(i), Fextotal_y(i)),
[T(i),T(i+1)], [u_0(1,1) du_0(1,1) u_0(1,2) du_0(1,2)]);
elseif i==length(T) % Last time step, use time length of one more time step
    [t,y] = ode45(@(t,y) MydiftwoDOFsepxy(t,y,m,Fextotal_x(i), Fextotal_y(i)),
[T(i),T(i)+T_step], [U(i-1,1) dU(i-1,1) U(i-1,2) dU(i-1,2)]);
else % Every other timestep, use time length form this time step until the next, use
previous outcomes for displacement and velocity
    [t,y] = ode45(@(t,y) MydiftwoDOFsepxy(t,y,m,Fextotal_x(i), Fextotal_y(i)),
[T(i),T(i+1)], [U(i-1,1) dU(i-1,1) U(i-1,2) dU(i-1,2)]);
end
U(i,1) = y(41,1); % displacement
U(i,2) = y(41,3);
dU(i,1) = y(41,2); % velocity
dU(i,2) = y(41,4);
end

figure
hold on
plot(T,U(:,1));
plot(T,dU(:,1));
title('ODE45, force calculated seperately', 'FontSize', 24);
xlabel('Time (s)', 'FontSize', 22);
ylabel('Disp. (m), vel. (m/s)', 'FontSize', 22);
legend('Surge', ' Surge Velocity');
set(gca, 'fontsize',22)

figure
hold on
plot(T,U(:,2));
plot(T,dU(:,2));
title('ODE45, force calculated seperately', 'FontSize', 24);
xlabel('Time (s)', 'FontSize', 22);
ylabel('Disp. (m), vel. (m/s)', 'FontSize', 22);
legend('Sway', 'Sway Velocity');
set(gca, 'fontsize',22)

```



DIFFERENTIAL FUNCTIONS

```
function dy = MydifftwoDOFxy(t,y, m, Fmax, d, p)
```

```
dy(1,1)= y(2);  
dy(2,1)=  
2*(Fmax*(p*sqrt(y(1)^2+y(3)^2)+d*((y(1)*y(2)+y(3)*y(4))/(sqrt(y(1)^2+y(3)^2))))*cos(atan2(y(3),y(1)))/m;  
dy(3,1)= y(4);  
dy(4,1)=  
2*(Fmax*(p*sqrt(y(1)^2+y(3)^2)+d*((y(1)*y(2)+y(3)*y(4))/(sqrt(y(1)^2+y(3)^2))))*sin(atan2(y(3),y(1)))/m;
```

```
function dy = MydifftwoDOFsepxy(t,y, m, Fextx, Fexty)
```

```
dy(1,1)= y(2);  
dy(2,1)=Fextx/m;  
dy(3,1)= y(4);  
dy(4,1)=Fexty/m;  
end
```

[Published with MATLAB® R2015a](#)

APPENDIX K. MATLAB SCRIPT THREE DOF MODEL

TIME

```
T_step = 0.1; % Timestep in s
T_sim = 400; % Simulation time in s
T = linspace(0,T_sim,(T_sim/T_step)+1).'; % Generate time vector
```

VARIABLES

```
B = 11;
p=-0.5;
d=-0.5;
u_0=[0.5 -0.5 0];
du_0=[0 0 0];
m=1000000;
I=3*10^9;
Pos = [-30 -16 5 26 40];
Setting = [0 1 1 1 0]; % 0 is sway correcting, 1 is surge correcting
n= length(Pos);
```

PREPARE VECTORS

```
U = zeros(length(T),3);
dU = zeros(length(T),3);
error_x = zeros(length(T),n);
error_y = zeros(length(T),n);
x_extra = zeros(length(T),n);
y_extra = zeros(length(T),n);
error = zeros(length(T),n);
d_error = zeros(length(T),n);
F_unit = zeros(length(T),n);
angle_unit = zeros(length(T),n);
F_x = zeros(length(T),n);
F_y = zeros(length(T),n);
M = zeros(length(T),n);
F_xtotal = zeros(length(T),1);
F_ytotal = zeros(length(T),1);
M_total = zeros(length(T),1);
```

CALCULATION

```
% for each time step
for i=1:length(T)

    if i==1 || i==2
    else
        % for each unit:
        for j=1:n
            % error by yaw
            x_extra(i,j) = Pos(j)*cos(U(i-2,3))-Pos(j)+(B/2)*sin(U(i-2,3));
            y_extra(i,j) = Pos(j)*sin(U(i-2,3))+((B/2)-(B/2)*cos(U(i-2,3)));
```

```

%error x
error_x(i,j) = U(i-2,1)+x_extra(i,j);
% error y
error_y(i,j) = U(i-2,2)+y_extra(i,j);

if Setting(j) == 1 % in case of surge correcting unit
% error unit
    error(i,j) = error_x(i,j);
    Fmax = 100000;
else % in case of sway correcting unit
    error(i,j) = error_y(i,j);
    Fmax = 200000;
end
% derivative of total error
d_error(i,j) = (error(i,j) - error(i-1,j))/T_step;

% total force
F_unit(i,j) = Fmax*(p*error(i,j)+d*d_error(i,j));
if F_unit(i,j) <= -Fmax
    F_unit(i,j) = -Fmax;
elseif F_unit(i,j) >= Fmax
    F_unit(i,j) = Fmax;
end

% x force and y force
if Setting(j)
    F_x(i,j) = F_unit(i,j);
    F_y(i,j) = 0;
else
    F_y(i,j) = F_unit(i,j);
    F_x(i,j) = 0;
end
% moment
M(i,j) = F_y(i,j)*(Pos(j)+x_extra(i,j))+F_x(i,j)*(0.5*B-y_extra(i,j));
end

%F_xtotal
F_xtotal(i) = sum(F_x(i,:));
%F_ytotal
F_ytotal(i) = sum(F_y(i,:));
%M_total
M_total(i) = sum(M(i,:));
end

if i==1 % First time step, use initial values for displacement and velocity
    [t,y] = ode45(@(t,y) MydiffthreeDOFsep(t,y,m,I, F_xtotal(i), F_ytotal(i), M_total(i)),
    [T(i),T(i+1)], [u_0(1) du_0(1) u_0(2) du_0(2) u_0(3) du_0(3)]);
elseif i==length(T) % Last time step, use time length of one more time step
    [t,y] = ode45(@(t,y) MydiffthreeDOFsep(t,y,m,I, F_xtotal(i), F_ytotal(i), M_total(i)),
    [T(i),T(i)+T_step], [U(i-1,1) dU(i-1,1) U(i-1,2) dU(i-1,2) U(i-1,3) dU(i-1,3)]);
else % Every other timestep, use time length from this time step until the next, use
previous outcomes for displacement and velocity
    [t,y] = ode45(@(t,y) MydiffthreeDOFsep(t,y,m,I, F_xtotal(i), F_ytotal(i), M_total(i)),
    [T(i),T(i+1)], [U(i-1,1) dU(i-1,1) U(i-1,2) dU(i-1,2) U(i-1,3) dU(i-1,3)]);
end
U(i,1) = y(end,1); % displacement

```

```

U(i,2) = y(end,3);
U(i,3) = y(end,5);

dU(i,1) = y(end,2); % velocity
dU(i,2) = y(end,4);
dU(i,3) = y(end,6);

end

```

FIGURES

```

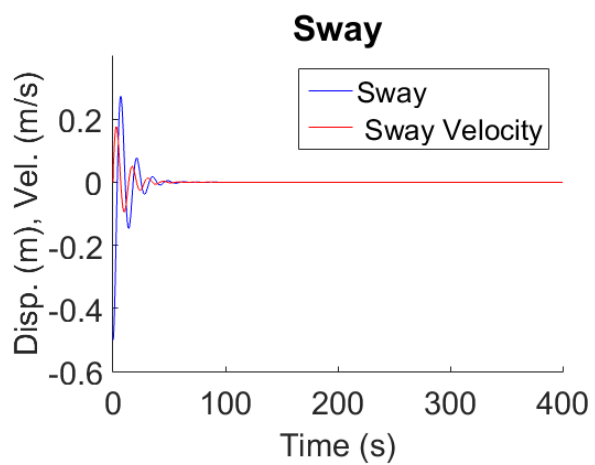
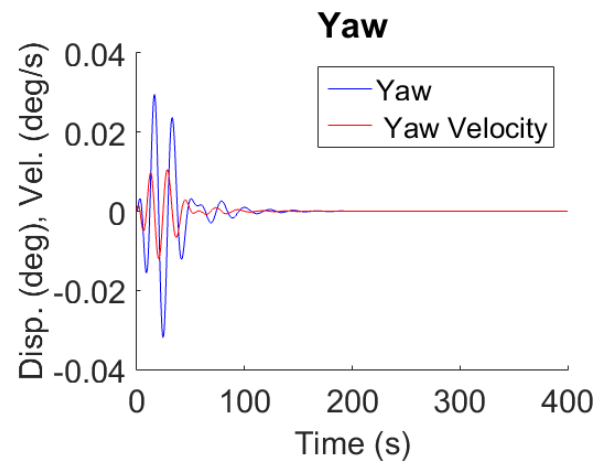
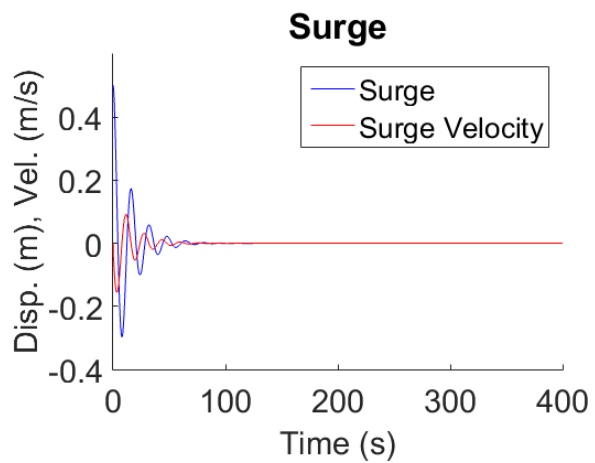
% rad --> degree
U(:,3) = radtodeg(U(:,3));
dU(:,3) = radtodeg(dU(:,3));

figure
hold on
plot(T,U(:,1), 'b');
plot(T,dU(:,1), 'r');
title('Surge', 'FontSize', 24);
xlabel('Time (s)', 'FontSize', 22);
ylabel('Disp. (m), Vel. (m/s)', 'FontSize', 22);
legend('Surge','Surge Velocity');
set(gca, 'fontsize',22)

figure
hold on
plot(T,U(:,2), 'b');
plot(T,dU(:,2), 'r');
title('Sway', 'FontSize', 24);
xlabel('Time (s)', 'FontSize', 22);
ylabel('Disp. (m), Vel. (m/s)', 'FontSize', 22);
legend('Sway',' Sway Velocity');
set(gca, 'fontsize',22)

figure
hold on
plot(T,U(:,3), 'b');
plot(T,dU(:,3), 'r');
title('Yaw', 'FontSize', 24);
xlabel('Time (s)', 'FontSize', 22);
ylabel('Disp. (deg), Vel. (deg/s)', 'FontSize', 22);
legend('Yaw',' Yaw Velocity');
set(gca, 'fontsize',22)

```



DIFFERENTIAL FUNCTION

```
function dy = MydiffthreeDOFsep(t,y, m, I, F_x, F_y, M)

    dy(1,1)= y(2);
    dy(2,1)= F_x/m;
    dy(3,1)= y(4);
    dy(4,1)= F_y/m;
    dy(5,1)= y(6);
    dy(6,1)= M/I;
end
```

[Published with MATLAB® R2015a](#)

APPENDIX L. MATLAB SCRIPT THREE DOF MODEL WITH COUPLING TERMS, CASE STUDY INPUT VARIABLES AND EXTERNAL FORCE

TIME

```
T_step = 0.1; % Timestep in s
T_sim = 1000; % Simulation time in s
T = linspace(0,T_sim,(T_sim/T_step)+1).'; % Generate time vector
```

VARIABLES

```
B = 11.424;
p=-2.75;
d=-2.75;
u_0=[0 0 0];
du_0=[0 0 0];
m=3849000;
A = [337.4 -2.3596 -1564.5;
     -2.3596 6176 4414.5;
     -1564.5 4414.5 3633000];
I=2908160664;
Pos = [-30 -16 5 26 40];
Setting = [0 1 1 1 0]; % 0 is sway correcting, 1 is surge correcting
n= length(Pos);
```

PREPARING VECTORS

```
U = zeros(length(T),3);
dU = zeros(length(T),3);
error_x = zeros(length(T),n);
error_y = zeros(length(T),n);
x_extra = zeros(length(T),n);
y_extra = zeros(length(T),n);
error = zeros(length(T),n);
d_error = zeros(length(T),n);
F_unit = zeros(length(T),n);
angle_unit = zeros(length(T),n);
F_x = zeros(length(T),n);
F_y = zeros(length(T),n);
M = zeros(length(T),n);
Fext = zeros(length(T),3);
F_xtotal = zeros(length(T),1);
F_ytotal = zeros(length(T),1);
M_total = zeros(length(T),1);
```

EXTERNAL FORCE

```
% Importing data
run('ImpData.m');

% Filters
run('Filter.m');
```

```

% Correction factor
run('CorFact.m');

% Interpolation
tstart = 150; % time the external force starts

for i=(tstart/T_step)+1:(tstart+length(Run110_F_27600_0(:,1))-1)/T_step;
Fext(i,1) = interp1(Run110_F_27600_0(:,1),Run110_F_27600_0(:,2),T(i)-tstart)*1000;
Fext(i,2) = interp1(Run110_F_27600_0(:,1),Run110_F_27600_0(:,3),T(i)-tstart)*1000;
Fext(i,3) = interp1(Run110_F_27600_0(:,1),Run110_F_27600_0(:,7),T(i)-tstart)*1000;
end

```

CALCULATIONS

```

% For each time step:
for i=1:length(T)

    if i==1 || i==2
    else
        % For each unit:
        for j=1:n
            % error by yaw
            x_extra(i,j) = Pos(j)*cos(U(i-2,3))-Pos(j)+(B/2)*sin(U(i-2,3));
            y_extra(i,j) = Pos(j)*sin(U(i-2,3))+(B/2)-(B/2)*cos(U(i-2,3));

            %error x
            error_x(i,j) = U(i-2,1)+x_extra(i,j);
            % error y
            error_y(i,j) = U(i-2,2)+y_extra(i,j);

            if Setting(j) == 1 % in case of surge correcting unit
            % error unit
                error(i,j) = error_x(i,j);
                Fmax = 100000;
            else % in case of sway correcting unit
                error(i,j) = error_y(i,j);
                Fmax = 200000;
            end

            % derivative of total error
            d_error(i,j) = (error(i,j) - error(i-1,j))/T_step;

            % total force
            F_unit(i,j) = Fmax*(p*error(i,j)+d*d_error(i,j));
            if F_unit(i,j) <= -Fmax
                F_unit(i,j) = -Fmax;
            elseif F_unit(i,j) >= Fmax
                F_unit(i,j) = Fmax;
            end

            % x force and y force
            if Setting(j)
                F_x(i,j) = F_unit(i,j);
                F_y(i,j) = 0;
            else

```

```

        F_y(i,j) = F_unit(i,j);
        F_x(i,j) = 0;
    end
    % moment
    M(i,j) = F_y(i,j)*(Pos(j)+x_extra(i,j))+F_x(i,j)*(0.5*B-y_extra(i,j));
end

%F_xtotal
F_xtotal(i) = sum(F_x(i,:)) + Fext(i,1);
%F_ytotal
F_ytotal(i) = sum(F_y(i,:)) + Fext(i,2);
%M_total
M_total(i) = sum(M(i,:)) + Fext(i,3);
end

if i==1 % First time step, use initial values for displacement and velocity
    [t,y] = ode45(@(t,y) MydiffthreeDOFadd(t,y,m, I, F_xtotal(i), F_ytotal(i), M_total(i),
A), [T(i),T(i+1)], [u_0(1) du_0(1) u_0(2) du_0(2) u_0(3) du_0(3)]);
elseif i==length(T) % Last time step, use time length of one more time step
    [t,y] = ode45(@(t,y) MydiffthreeDOFadd(t,y,m,I, F_xtotal(i), F_ytotal(i), M_total(i),
A), [T(i),T(i)+T_step], [U(i-1,1) dU(i-1,1) U(i-1,2) dU(i-1,2) U(i-1,3) dU(i-1,3)]);
else % Every other timestep, use time length form this time step until the next, use
previous outcomes for displacement and velocity
    [t,y] = ode45(@(t,y) MydiffthreeDOFadd(t,y,m,I, F_xtotal(i), F_ytotal(i), M_total(i),
A), [T(i),T(i+1)], [U(i-1,1) dU(i-1,1) U(i-1,2) dU(i-1,2) U(i-1,3) dU(i-1,3)]);
end
U(i,1) = y(end,1); % displacement
U(i,2) = y(end,3);
U(i,3) = y(end,5);

dU(i,1) = y(end,2); % velocity
dU(i,2) = y(end,4);
dU(i,3) = y(end,6);

end

```

FIGURES

```

% limits
for i=1:length(T)
    limitSurge(i,:) = [0.4 -0.4];
    limitSway(i,:) = [0.4 -0.4];
    limitYaw(i,:) = [0.25 -0.25];
end

% rad --> degree
U(:,3) = radtodeg(U(:,3));
dU(:,3) = radtodeg(dU(:,3));

figure
hold on
subplot(2,1,1)
hold on
plot(T,Fext(:,1:2));
title('External force', 'FontSize', 24);
xlabel('Time (s)', 'FontSize', 22);

```

```

ylabel('Fext (N)', 'FontSize', 22);
legend('Surge','Sway');
set(gca,'fontsize',22)

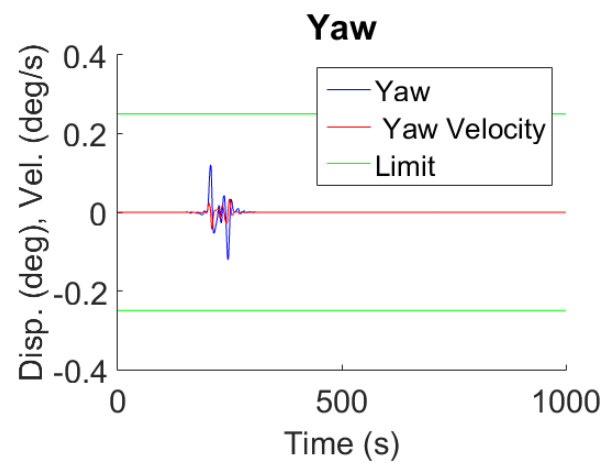
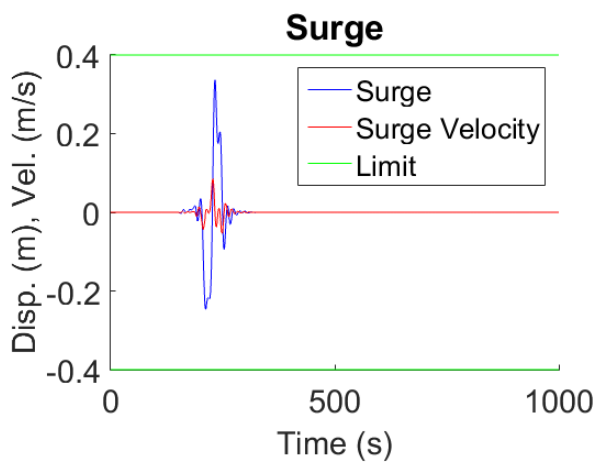
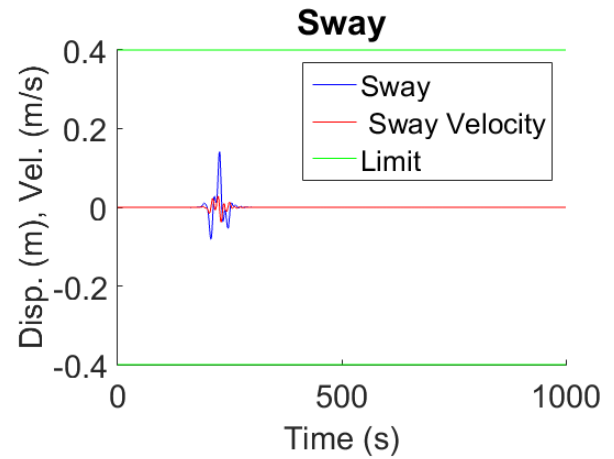
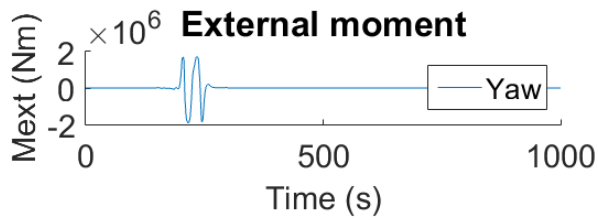
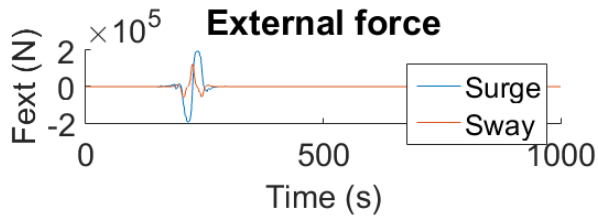
subplot(2,1,2)
hold on
plot(T,Fext(:,3));
title('External moment', 'FontSize', 24);
xlabel('Time (s)', 'FontSize', 22);
ylabel('Mext (Nm)', 'FontSize', 22);
legend('Yaw');
set(gca,'fontsize',22)

figure
hold on
plot(T,U(:,1), 'b');
plot(T,du(:,1), 'r');
plot(T,limitsurge, 'g');
title('Surge', 'FontSize', 24);
xlabel('Time (s)', 'FontSize', 22);
ylabel('Disp. (m), vel. (m/s)', 'FontSize', 22);
legend('Surge','Surge velocity', 'Limit');
set(gca,'fontsize',22)

figure
hold on
plot(T,U(:,2), 'b');
plot(T,du(:,2), 'r');
plot(T,limitsway, 'g');
title('Sway', 'FontSize', 24);
xlabel('Time (s)', 'FontSize', 22);
ylabel('Disp. (m), vel. (m/s)', 'FontSize', 22);
legend('Sway',' Sway velocity', 'Limit');
set(gca,'fontsize',22)

figure
hold on
plot(T,U(:,3), 'b');
plot(T,du(:,3), 'r');
plot(T,limityaw, 'g');
title('Yaw', 'FontSize', 24);
xlabel('Time (s)', 'FontSize', 22);
ylabel('Disp. (deg), vel. (deg/s)', 'FontSize', 22);
legend('Yaw',' Yaw velocity', 'Limit');
set(gca,'fontsize',22)

```



DIFFERENTIAL FUNCTION

```
function dy = MydiffthreeDOFadd(t,y, m, I, F_x, F_y, M, A)
```

```
dy(1,1)= y(2);
dy(2,1)= (F_x-A(1,2)*y(3)-A(1,3)*y(5))/(m+A(1,1));
dy(3,1)= y(4);
dy(4,1)= (F_y-A(2,1)*y(1)-A(2,3)*y(5))/(m+A(2,2));
dy(5,1)= y(6);
dy(6,1)= (M-A(3,1)*y(1)-A(3,2)*y(3))/(I+A(3,3));
```

```
end
```

Published with MATLAB® R2015a

APPENDIX M. DELFRAC OUTPUT

DATE : 09-SEP-15

TIME : 10:42:00

Key_ship

HYDROMECHANIC DATA

FREQUENCY 1.0000E-01 WATERDEPTH 6.0000E+00 VOLUME 3.8492E+03

WAVENUMBER 1.3048E-02

SPRING COEFFICIENTS

BODY IB= 1 BODY JB= 1

0.000E+00	0.000E+00	0.000E+00	0.000E+00	0.000E+00	0.000E+00
0.000E+00	0.000E+00	0.000E+00	0.000E+00	0.000E+00	0.000E+00
0.000E+00	0.000E+00	1.197E+04	-1.596E+00	2.379E+04	0.000E+00
0.000E+00	0.000E+00	-1.596E+00	1.198E+05	2.158E+02	0.000E+00
0.000E+00	0.000E+00	2.379E+04	2.158E+02	1.135E+07	0.000E+00
0.000E+00	0.000E+00	0.000E+00	0.000E+00	0.000E+00	0.000E+00

BODY IB= 1 BODY JB= 2

0.000E+00	0.000E+00	0.000E+00	0.000E+00	0.000E+00	0.000E+00
0.000E+00	0.000E+00	0.000E+00	0.000E+00	0.000E+00	0.000E+00
0.000E+00	0.000E+00	0.000E+00	0.000E+00	0.000E+00	0.000E+00
0.000E+00	0.000E+00	0.000E+00	0.000E+00	0.000E+00	0.000E+00
0.000E+00	0.000E+00	0.000E+00	0.000E+00	0.000E+00	0.000E+00
0.000E+00	0.000E+00	0.000E+00	0.000E+00	0.000E+00	0.000E+00

DAMPING COEFFICIENTS

BODY IB= 1 BODY JB= 1

5.962E+00	-6.850E-02	3.563E-01	-1.287E-01	1.751E+03	-6.172E+00
1.350E-02	2.542E+01	-4.758E+01	-7.325E+01	-7.067E+01	6.533E+00
-1.902E+00	-6.168E+01	5.131E+03	1.524E+02	1.027E+04	1.463E+02
-1.670E-01	-7.126E+01	1.357E+02	2.054E+02	1.662E+02	-1.322E+01
1.790E+03	-1.190E+02	1.036E+04	1.951E+02	5.474E+05	-1.472E+03
-9.070E+00	7.389E+00	2.726E+01	-1.609E+01	-2.513E+03	4.772E+02

BODY IB= 1 BODY JB= 2

5.933E+00	-8.663E-02	2.465E-01	3.389E-01	1.740E+03	1.141E+01
-5.590E-02	2.528E+01	3.740E+01	-7.291E+01	4.295E+01	9.011E+00
-2.327E+00	-2.451E+01	4.986E+03	1.006E+02	9.942E+03	1.623E+02
-2.882E-02	-7.087E+01	-1.025E+02	2.044E+02	-1.706E+02	-2.064E+01
1.779E+03	-5.587E+01	1.011E+04	2.485E+02	5.435E+05	3.840E+03
-1.442E+01	7.698E+00	4.877E+01	-1.731E+01	-4.203E+03	4.373E+02

ADDED MASS COEFFICIENTS

BODY IB= 1 BODY JB= 1

3.374E+02 -4.068E+00 2.131E+02 -1.565E+01 8.655E+04 -1.498E+03
-6.512E-01 6.176E+03 9.740E+02 -1.485E+04 -9.352E+02 4.418E+03
1.966E+02 8.408E+02 5.647E+04 -1.581E+03 9.373E+04 1.583E+03
-1.331E+01 -1.442E+04 -1.571E+03 5.976E+04 -2.125E+03 1.885E+04
8.862E+04 -2.099E+03 9.484E+04 -2.515E+03 3.515E+07 -8.838E+05
-1.631E+03 4.411E+03 5.245E+02 1.782E+04 -9.353E+05 3.633E+06

BODY IB= 1 BODY JB= 2

2.172E+02 -7.584E-01 1.465E+02 9.897E+01 6.379E+04 7.984E+03
-4.438E+00 -1.435E+03 7.416E+03 2.496E+03 3.817E+03 -1.939E+03
1.343E+02 -7.362E+03 3.803E+04 2.119E+04 7.164E+04 1.125E+03
-8.455E+01 2.319E+03 -2.036E+04 -6.087E+03 -4.115E+04 -2.228E+03
6.542E+04 -4.468E+03 7.225E+04 4.394E+04 2.407E+07 3.783E+06
-8.129E+03 -2.015E+03 -6.933E+02 -2.237E+03 -3.780E+06 -1.265E+06

NATURAL FREQUENCIES

0.000E+00 0.000E+00 4.454E-01 9.327E-01 5.461E-01 0.000E+00

WAVE DIRECTION 0.0

AMPLITUDE OF WAVE FORCES

5.045E+02 5.616E+01 1.037E+04 1.592E+02 1.564E+05 7.575E+02

PHASE ANGLE OF WAVE FORCES

8.810E+01 1.817E+02 5.575E+00 3.580E+02 8.162E+01 2.711E+02

AMPLITUDE OF MOTIONS

1.232E+01 4.757E-01 9.106E-01 3.832E-02 7.436E-01 5.988E-01

PHASE ANGLE OF MOTIONS

2.685E+02 3.575E+02 1.230E+00 3.518E+02 8.990E+01 9.454E+01

TOTAL MEAN FORCES

MODE FI FII FIII FIV TOTAL

1	0.000E+00	1.305E+00	-1.267E+00	-1.703E-02	2.127E-02
2	0.000E+00	-4.801E+00	6.476E-01	2.475E+00	-1.678E+00
3	0.000E+00	-5.530E+02	9.197E+02	-3.082E+00	3.636E+02
4	0.000E+00	1.692E+01	-3.902E+00	-7.999E-08	1.302E+01
5	0.000E+00	-4.240E+02	1.076E+03	-2.190E-02	6.520E+02
6	0.000E+00	-3.749E+01	2.538E+01	1.740E-02	-1.210E+01

APPENDIX N. ANSYS SCRIPT FILE

```
!  
! ansys script file for the plate model  
!  
finish  
/clear  
/filename,panelShalimar  
/title,panelShalimar  
!/uis,msgpop,3 !suppress modelling warning messages  
!=====
```

!preprocessing
!=====

```
/prep7  
!-----  
! define panel geometry parameters  
!-----  
!Length and width panel  
lsp=1250.0  
bpl=500.0  
!plate thickness  
tpl=9
```

!height and thickness web plate
hsw=150
tsw=8

!Width and thickness flange
bsf=100
tsf=8

!properties of HP140x8
zhp=81.8
A=1380
Iyy=2060000
Iyz=0
Izz=100000
Iw=23000
J=10000
CGy=0.0
CGz=81.8
SHy=0.0
SHz=81.8
TKz=140
TKy=27

!emod and poisson ratio
emod=210000
nxy=0.3

!*ask,es,element size,lsp/12.0

*ask,ns,number elements,40.0
es=lsp/ns

```
!-----  
!element type
```

```

!-----
et,1,shell181
keyopt,1,1,0    !bending and membrane stiffness
keyopt,1,3,2    !full integration with incompatible modes
keyopt,1,8,1    !store data for top and bottom of all layers
et,2,beam188

!-----
! select and define beam element section
!-----

ey = 0.0 !element offset in y-direction relative to origin 'o'
ez = 0.5*tpl+(140-zhp) !element offset in z-direction relative to origin 'o'

beff = 500

sectype,1,beam,ASEC,HP,1    !define section type 1: beam element, User defined type, name "HP", cross-
section mesh refinement level
secoffset,user,ey,ez
secdata,A,Iyy,Iyz,Izz,Iw,J,CGy,(140-CGz),SHy,(140-SHz),TKz,TKy

!-----
!define shell element sections
!-----
sectype,2,shell,,plate,0    !define section type 1: shell element, name "plate"
secdata,tpl,1,,3            !thickness 'tpl', number of integration points: 3
secoffset,mid,              !offset: mid,bot,top,user
seccontrol,0,0,0,0,1,1,1

sectype,3,shell,,web,0      !define section type 1: shell element, name "web"
secdata,tsw,1,,3            !thickness 'tsw', number of integration points: 3
secoffset,mid,              !offset: mid,bot,top,user
seccontrol,0,0,0,0,1,1,1

sectype,4,shell,,flange,0  !define section type 1: shell element, name "flange"
secdata,tsf,1,,3            !thickness 'tsf', number of integration points: 3
secoffset,mid,              !offset: mid,bot,top,user
seccontrol,0,0,0,0,1,1,1

!-----
!define material
!-----
mp,ex,1,emod
mp,nuxy,1,nxy
!-----
! set view
!-----
/view,all,1,1,1
/vup,all,Z
!-----
!panel keypoints
!-----
k, 1,0.0,-bpl/2,0.0
k, 2,0.0, 0.0,0.0
k, 3,0.0, bpl/2,0.0
k, 4,lsp,-bpl/2,0.0
k, 5,lsp, 0.0,0.0
k, 6,lsp, bpl/2,0.0

```

```

k, 7,bsf/2,-bpl/2.0,-hsw-tpl/2.0-tsf/2.0
k, 8,0.0,-bpl/2,-hsw-tpl/2.0-tsf/2.0
k, 9,-bsf/2, -bpl/2.0,-hsw-tpl/2.0-tsf/2.0
k,10,bsf/2,bpl/2.0,-hsw-tpl/2.0-tsf/2.0
k,11,0.0, bpl/2,-hsw-tpl/2.0-tsf/2.0
k,12,-bsf/2, bpl/2.0,-hsw-tpl/2.0-tsf/2.0
!-----
!panel areas
!-----
a,1,4,5,2
a,2,5,6,3
a,8,1,3,11
a,7,10,11,8
a,8,11,12,9
!-----
!boundary conditions on lines
!-----
lsel,all
lsel,s,loc,x,-1.0,1.0
dl,all,,uy
dl,all,,uz
lsel,all
lsel,s,loc,x,lsp-1.0,lsp+1.0
dl,all,,uz
dl,all,,ux
lsel,all
lsel,s,loc,y,-bpl/2.0-1.0,-bpl/2.0+1.0
dl,all,,uy
dl,all,,rotx
dl,all,,rotz
lsel,all
lsel,s,loc,y,bpl/2.0-1.0,bpl/2.0+1.0
dl,all,,uy
dl,all,,rotx
dl,all,,rotz
lsel,all
!----
!mesh
!----
esize,es
allsel
secnum,1      !activate section type 1
mat,1
lmesh,3
secnum,2      !activate section type 2
mat,1
amesh,1,2
secnum,3      !activate section type 3
mat,1
amesh,3
secnum,4      !activate section type 4
mat,1
amesh,4,5
!-----
!loads
!-----

```

```
sfa,1,1,pres,0.1
sfa,2,1,pres,0.1
!-----
!merge nodes and keypoints if coincident
!-----
nummrg,node,lsp/10000.
nummrg,kp,lsp/10000.

/eshape,1 !plot elements
eplo,all
!=====
!solve
!=====
/solu
solve
!=====
!post-processing
!=====
/post1
plesol,s,x,0,1
```

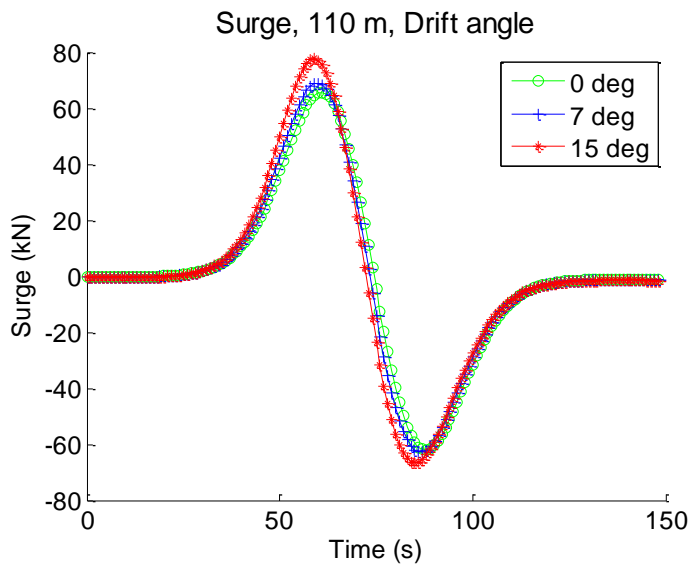


Figure O.1 Surge force for different drift angles. (110 m vessel passing, 88.2 m passing distance)

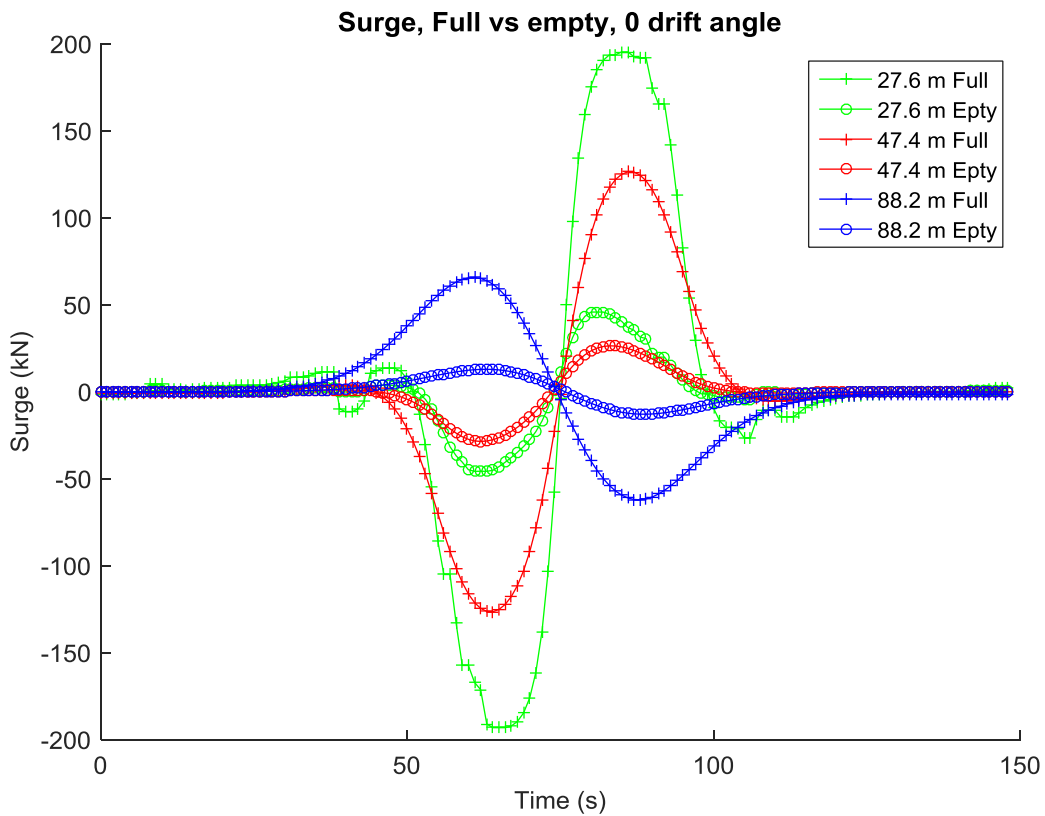


Figure O.2 Surge force for different loading conditions (110 m vessel passing, 88.2 m passing distance)

APPENDIX P. REACTION FORCES OF MOORMASTER™ UNITS

The figures show the forces exerted by the MoorMaster™ units on the hull of the moored vessel. All figures show one line for the most aft unit and one line for the most forward unit, which are configured to work in sway direction. The three groups of two units that are configured to work in surge direction, are represented by one line. Each pair of units exerts this force.

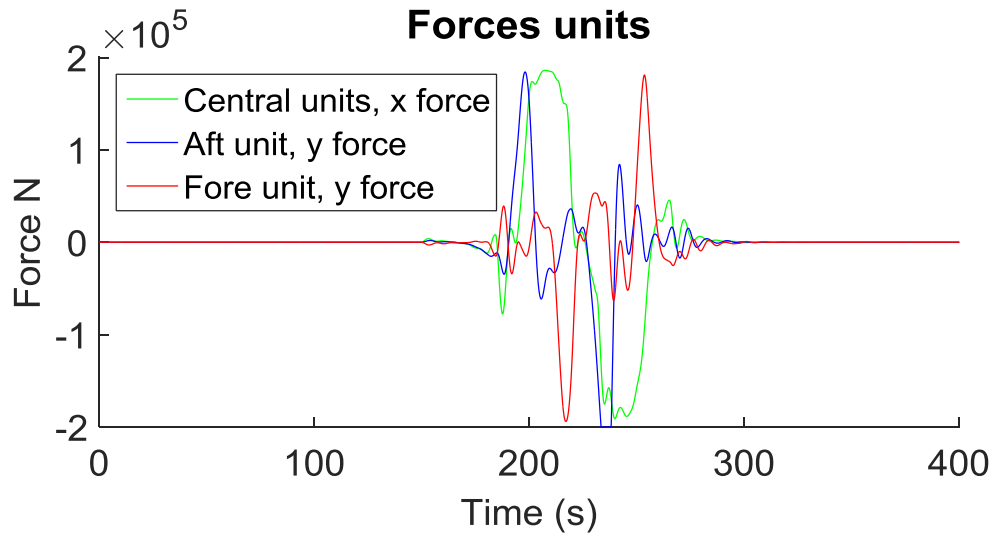


Figure P.1 Forces of units caused by 200m 4 barge convoy at 18 km/h, at a passing distance of 33.35m, P=-5, D=-3

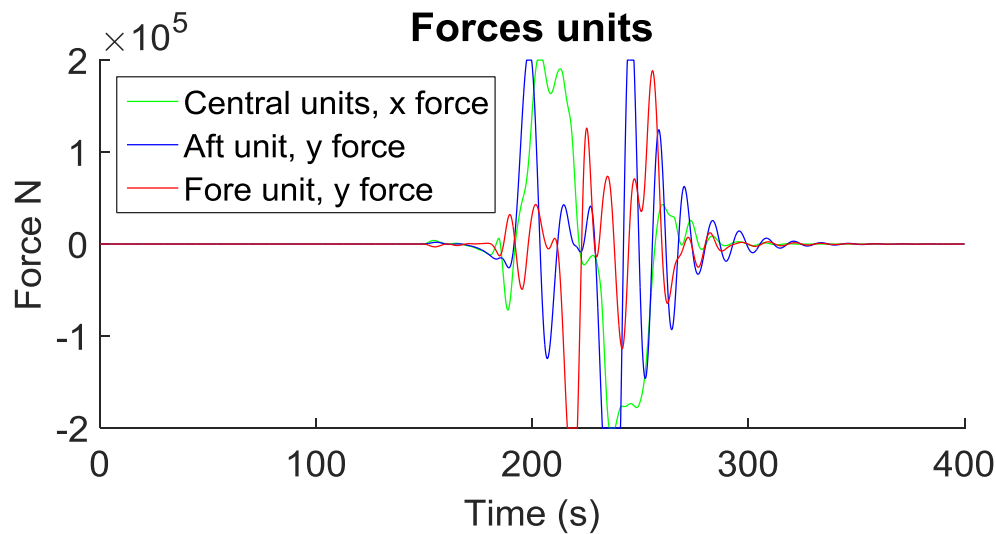


Figure P.2 Forces of units caused by 200m 4 barge convoy at 18 km/h, at a passing distance of 33.35m, P=-2.5, D=-1.5

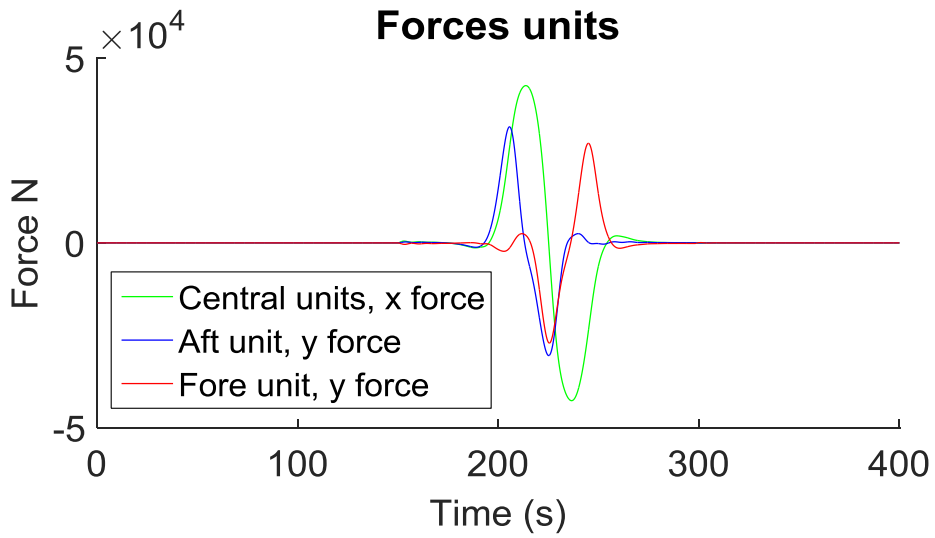


Figure P.3 Forces of units caused by 110m Large Rhine vessel at 18 km/h, at a passing distance of 47.40m, P=-5, D=-3

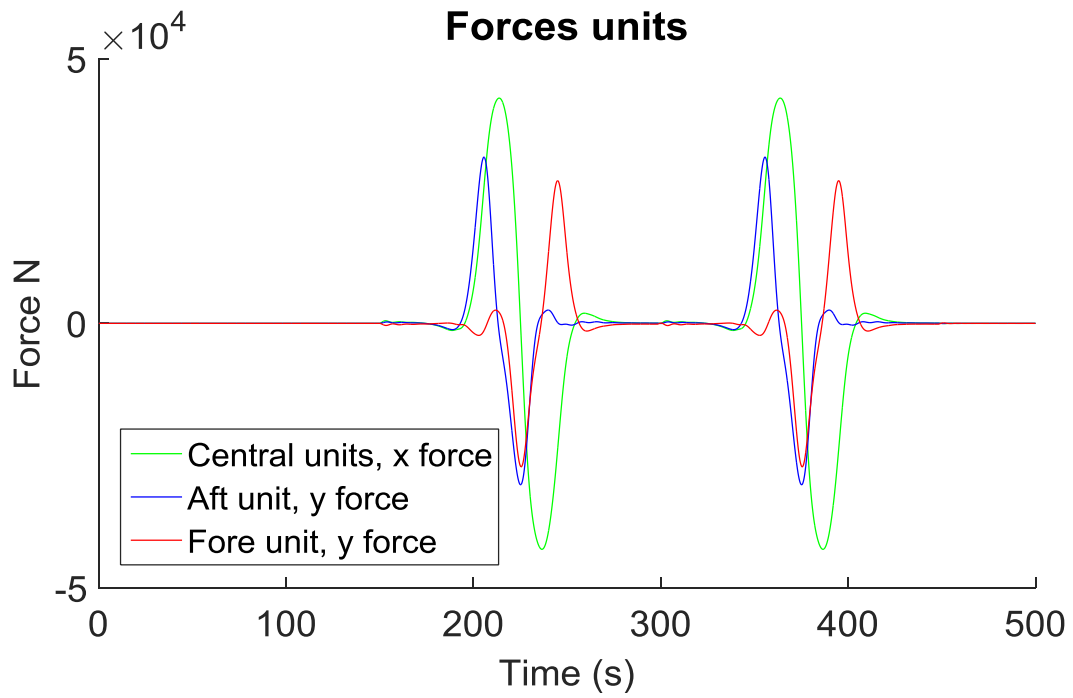


Figure P.4 Forces of units caused by 2 Large Rhine vessels passing 5 seconds after each other, at 18 km/h, at a passing distance of 47.40m, P=-5, D=-3

LOWER PD SETTING

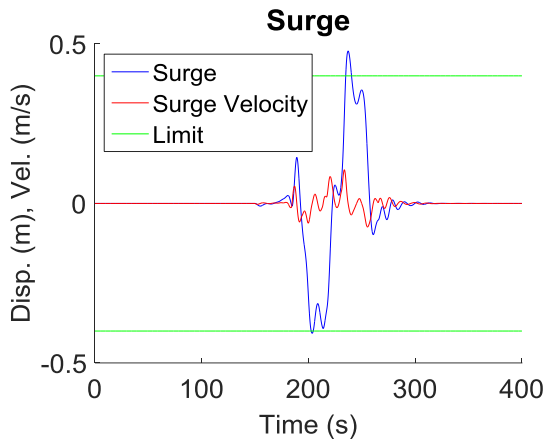


Figure Q.1 Resulting surge motions caused by 200m 4 barge convoy at 18 km/h, at a passing distance of 33.35m, $P=-2.5$, $D=-1.5$

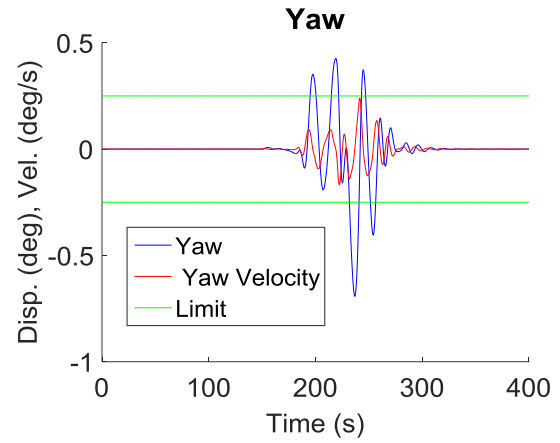


Figure Q.3 Resulting yaw motions caused by 200m 4 barge convoy at 18 km/h, at a passing distance of 33.35m, $P=-2.5$, $D=-1.5$

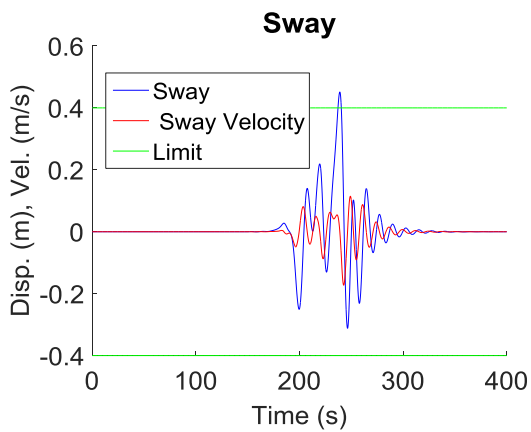


Figure Q.2 Resulting sway motions caused by 200m 4 barge convoy at 18 km/h, at a passing distance of 33.35m, $P=-2.5$, $D=-1.5$

110M LARGE RHINE VESSEL, 47.40 M

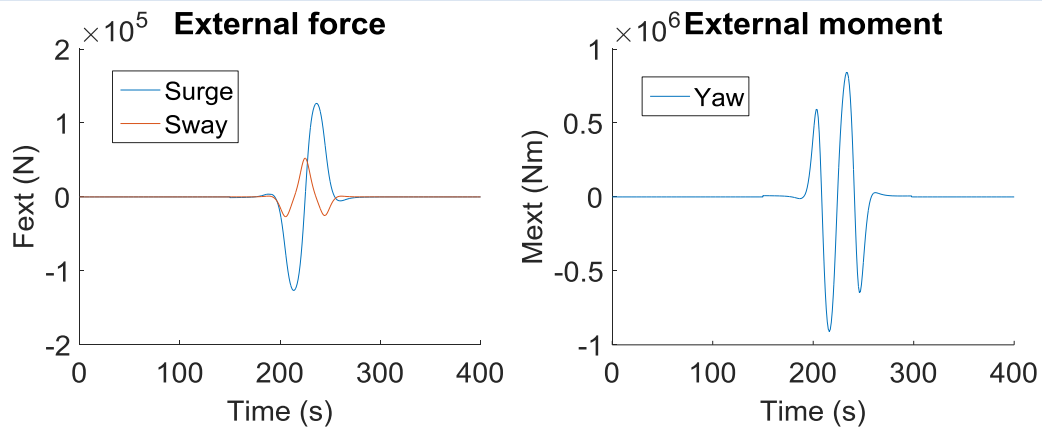


Figure Q.4 External forces and moment caused by 110m Large Rhine vessel at 18 km/h, at a passing distance of 47.40m, P=-5, D=-3

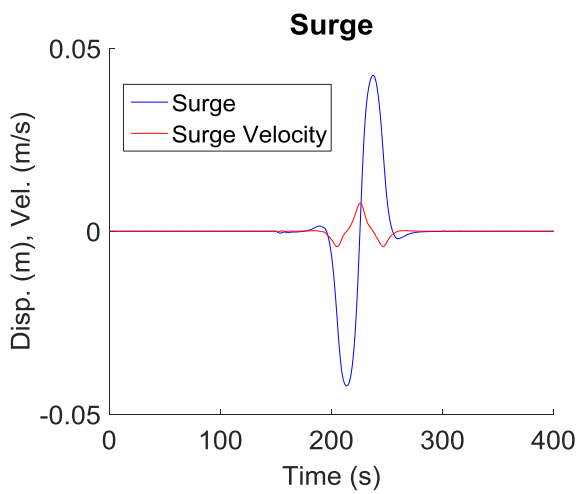


Figure Q.5 Resulting surge motion caused by 110m Large Rhine vessel at 18 km/h, at a passing distance of 47.40m, P=-5, D=-3

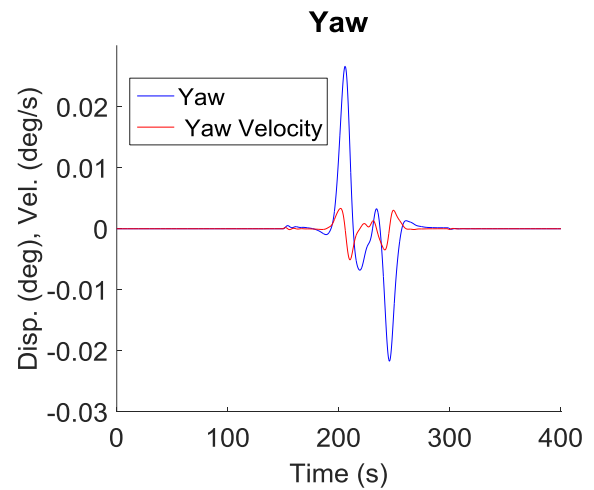


Figure Q.7 Resulting yaw motion caused by 110m Large Rhine vessel at 18 km/h, at a passing distance of 47.40m, P=-5, D=-3

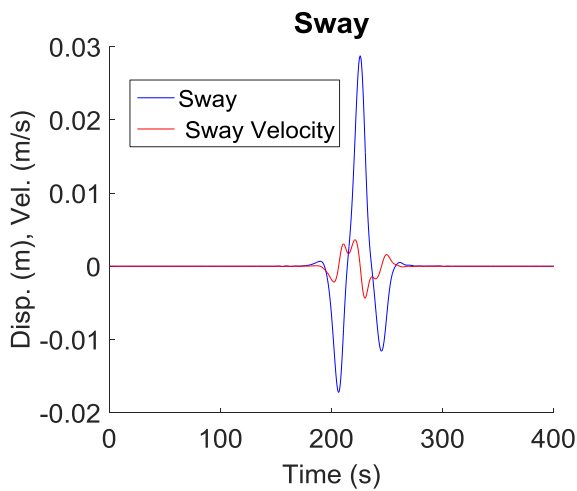


Figure Q.6 Resulting sway motion caused by 110m Large Rhine vessel at 18 km/h, at a passing distance of 47.40m, P=-5, D=-3

TWO TIMES 110M LARGE RHINE VESSEL, 47.40 M

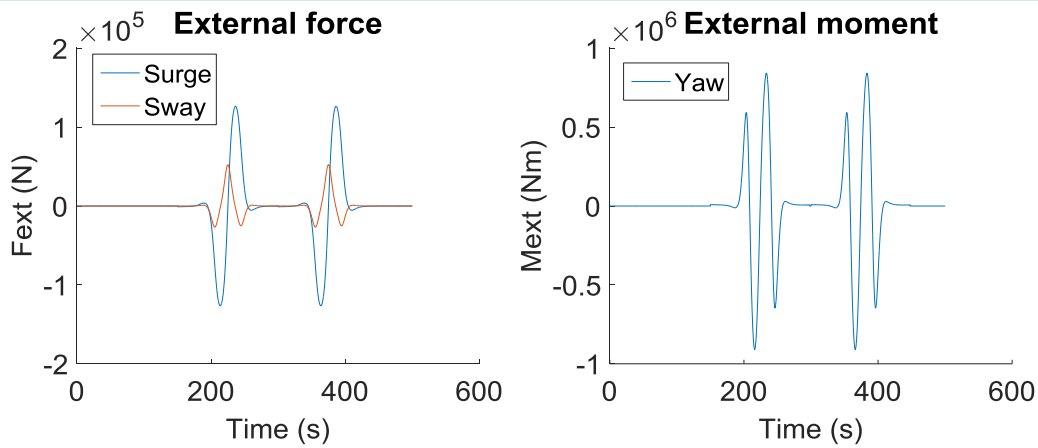


Figure Q.8 External forces and moment caused by 2 Large Rhine vessels passing 5 seconds after each other, at 18 km/h, at a passing distance of 47.40m, P=-5, D=-3

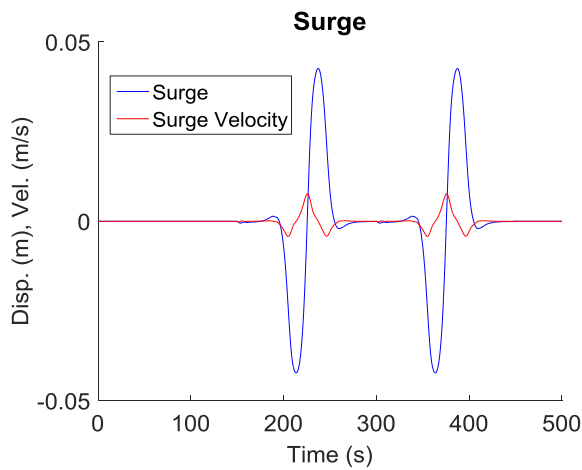


Figure Q.9 Resulting surge motion caused by 2 Large Rhine vessels passing 5 seconds after each other, at 18 km/h, at a passing distance of 47.40m, P=-5, D=-3

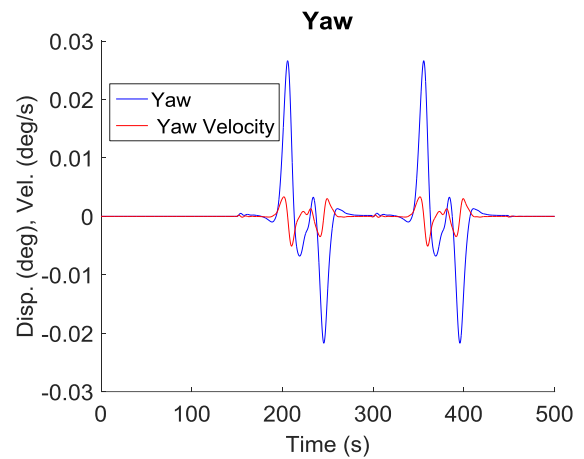


Figure Q.11 Resulting yaw motion caused by 2 Large Rhine vessels passing 5 seconds after each other, at 18 km/h, at a passing distance of 47.40m, P=-5, D=-3

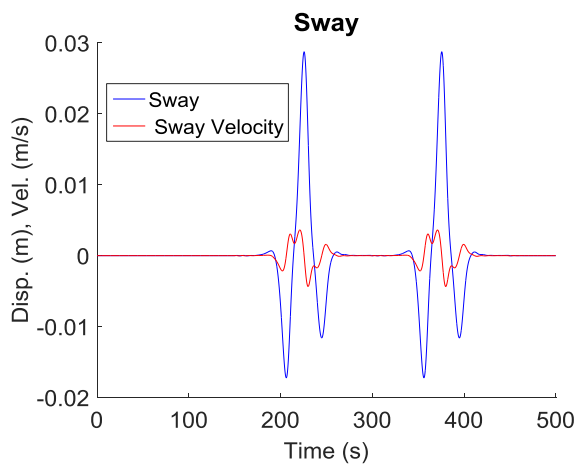


Figure Q.10 Resulting sway motion caused by 2 Large Rhine vessels passing 5 seconds after each other, at 18 km/h, at a passing distance of 47.40m, P=-5, D=-3

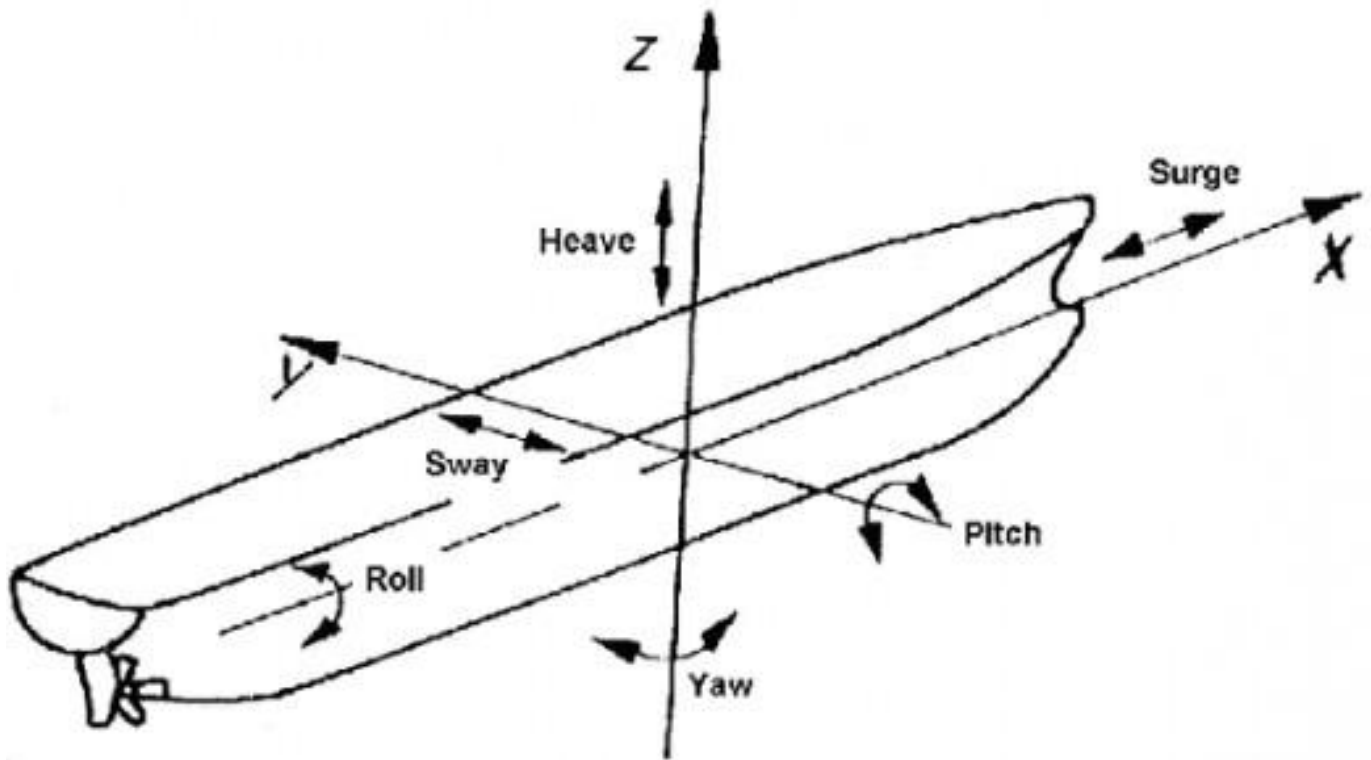


Figure R.1 Ship motions